HOW QUANTITATIVE CLINICAL PHARMACOLOGY CAN BRING VALUE TO THE PATIENT

By

NAVEEN MANGAL

A DISSERTATION PRESENTED TO THE GRADUATE SCHOOL
OF THE UNIVERSITY OF FLORIDA IN PARTIAL FULFILLMENT
OF THE REQUIREMENTS FOR THE DEGREE OF
DOCTOR OF PHILOSOPHY

UNIVERSITY OF FLORIDA

2017

To my parents, Pradeep Mangal and Saroj Agarwal and my wife, Diksha Sahai

ACKNOWLEDGMENTS

I would like to express my gratitude to my dissertation supervisor, Dr. Stephan Schmidt, who gave me the opportunity to pursue a PhD under his excellent mentorship. Dr. Schmidt's expertise in pharmacometrics and systems pharmacology, understanding and patience have greatly helped me to pursue the Ph.D. degree. He is a great mentor to work with. He has always supported me in my tough times and motivated me to come back harder. Due to his understanding and support, I was able to work on some of the very interesting and important research projects in the center. Also, I was able to get first-hand experience in pharmaceutical industry as I was permitted to pursue two summer internships in 2015 (GlaxoSmithKline) and 2016 (AbbVie). I would also like to thank my committee members Dr. Peter W. Stacpoole, Dr. Margaret O. James, Dr. Lawrence Lesko and Dr. Hartmut Derendorf who were always available to provide their valuable feedback on my research. Also, I would like to express my deep appreciation to Dr. Kevin Freise and Dr. Ahmed Hamed Salem who provided me an excellent mentorship during internship at AbbVie Inc. I would also like to thank Pinnacle Laboratory Services (Ocala, FL) and Florida High Tech Corridor Council for their funding to oxycodone project. Finally, I would like to thank Dr. Carolina Miranda De Silva for her contribution to the oxycodone project as well as all past and present colleagues at the center who have always motivated and supported me during the PhD.

TABLE OF CONTENTS

page

LIST OF TABLES

LIST OF FIGURES

Abstract of Dissertation Presented to the Graduate School
of the University of Florida in Partial Fulfillment of the
Requirements for the Degree of Doctor of Philosophy

HOW QUANTITATIVE CLINICAL PHARMACOLOGY CAN BRING VALUE TO THE PATIENT

By

Naveen Mangal

December 2017

Chair: Stephan Schmidt
Major: Pharmaceutical Sciences

The quantitative clinical pharmacology- based tools such as population (Pop) pharmacokinetic (PK) / pharmacodynamic (PD), physiology-based PK/PD modeling and simulation are being increasingly used to support all phases of drug development (discovery, pre-clinical, clinical) including post-marketing analysis. In our work, we utilized these tools to improve patient care in 3 different therapeutic areas. In first study, our aim was to provide dosing recommendations for dichloroacetate (DCA) for the treatment of congenital lactic acidosis (CLA), a rare disease in children. A Pop-PK model was developed and qualified using the PK information from adults which was extrapolated to pediatrics using allometry and physiology-based scaling. The model was applied to predict optimal DCA doses in children. Doses of 12.6 mg/kg and 10.6 mg/kg were optimal for the treatment of normal metabolizers and slow metabolizers, respectively. In second study, we provided dosing recommendations for optimization of voriconazole therapy in invasive fungal infections. We conducted a clinical study to prospectively evaluate the impact of *CYP2C19* genotype, drug-drug interactions, race, and gender on the PK of voriconazole. A Pop-PK/PD model was developed using the clinical trial and MIC distribution data for *Candida* and *Aspergillus spp*. *CYP2C19*

polymorphisms and pantoprazole were significant factors influencing the PK of voriconazole. A standard voriconazole dose of 200 mg was optimal for the treatment of *Candida spp.* infections while doses ranging from 300-600 mg were proposed for treatment of *Aspergillus spp.* infections, depending on the clinical phenotype of the patient and type of *Aspergillus* infection. In third study, the aim was to optimize oxycodone therapy for the management of chronic pain. We developed a PBPK model for oxycodone and its metabolites using *in vitro* enzyme kinetics and published as well as in-house PK data. The model was applied to predict the effect of polymorphisms and drug-drug interactions on PK of oxycodone. We found that there is a pronounced impact of germline mutations in *CYP2D6* as well as *UGT2B7* and drug-drug-interactions resulting in up to a 15-fold increase in steady-state exposure. In summary, we have successfully applied QCP tools to influence decision making in drug development and improve patient care in clinic.

CHAPTER 1
INTRODUCTION AND BACKGROUND

Traditional Drug Development and Quantitative Clinical Pharmacology-based Approaches

During traditional drug development process, clinical trials are designed to select a safe and efficacious dose[1]. However, the population(s) studied in drug development trials are typically smaller and more homogenous compared to the target patient population. As a consequence, the dose selected during these trials may not be always equally effective in all patients. For example, inter-individual differences in the patient's pharmacokinetics (e.g. as the result of genetic polymorphisms in metabolizing enzymes or organ impairment) and/or pharmacodynamics (e.g. under or over-expression of a receptor) can result in inter-individual differences in treatment response which may not have been studied in the clinical trial due to difficulties in enrolling such patients[2]. In these cases, it becomes imperative to delineate the sources of variability leading to inter-individual differences in therapeutic outcome in order to tailor therapy to an individual patient. One of the ways to identify these sources of variability would be to perform multiple clinical studies with diverse groups of patients under all possible scenarios. However, the time and money required for developing a new drug is already as high as $ 1.5 billion[3], conducting multiple studies may not be the most efficient way of identifying sources of variance. It can also extend the time needed for a new drug to reach to the caregivers and the patients. Moreover, conducting studies in some group of patients may not be even feasible. For example, therapeutic concentrations of a drug which is partly excreted in urine and metabolized by CYP2C19 enzyme would depend on the renal function (mild/moderate/severe insufficiency) and CYP2C19 metabolic status (Extensive/Poor metabolizer/Ultra-rapid metabolizer) of a patient. In practice,

conducting a study in patients with CYP2C19 poor metabolizer status and severe renal insufficiency can be risky for a pharmaceutical company. However, these patients do exist and need care in clinic. In these cases, it will be best to utilize approaches which can leverage prior information and can predict the clinical outcome of unstudied situations or identify the most important clinical studies to conduct.

Quantitative clinical pharmacology-based approaches, such as Pharmacokinetic/Pharmacodynamic (PK/PD) or Physiologically-Based Pharmacokinetic (PBPK) modeling and simulation (M&S), are now widely used to inform decisions related to drug development[4-6]. In recent past, M&S based approaches had a big impact on FDA approval and labelling decisions. In 2011, FDA conducted a review[7] to determine the number of submissions with pharmacometric analysis (submitted 2000-2008) and impact of those analyses on regulatory approval, labeling decisions and trial design decisions. Out of 198 submissions, M&S was critical in approval decisions for 126 (64%) submissions[7]. Similarly, M&S was responsible for facilitating labeling related decisions for 133 (67%) submissions. FDA also reviewed 52 submissions for pediatric indications during 2000-2008[7]. Out of 52 submissions, doses for pediatrics for 38 submissions were determined based on either exposure-response analysis in pediatrics (41%), matching of drug exposure in adults and pediatrics (37%) or a combination of both (11%)[7]. These survey results highlight the growing importance of M&S approaches in regulatory decision making related to drug approval in adults and pediatrics.

M&S approaches can not only use the existing clinical data while making a recommendation but earlier data from previous studies can also be incorporated to

leverage all the information about a new medical entity (NME), following "Learn, Confirm and Apply" paradigm[8]. These approaches have the potential to better characterize Dose-Exposure-Response relationship of different compounds, which can be harnessed to individualize patient therapy. Figure 1-1 shows a schematic of development and application of modeling and simulation based approaches. Selection of the modeling approach is usually governed by the clinical question at hand as well as the data (*in vitro*, pre-clinical or clinical) which is available to inform the model. Once identified, data from the single/multiple studies can be integrated into a single, unifying mathematical or statistical model. The developed model is then externally qualified by overlaying the model predictions with observations obtained from another dataset which was not used for model development. External qualification, although highly desirable, may or may not be possible depending on the availability of dataset. Once a reasonable confidence is established in such a model, it can be used to predict the effect of various intrinsic (age, race, disease, genetics) and extrinsic factors (diet, smoking, drug-drug interactions) on the PK/PD of drug and ultimately the therapeutic outcome. A clinician or a caregiver would feel more confident while considering the modeling based recommendations if he/she is presented with the magnitude of the effect as well as uncertainty around that effect. These modeling and simulation approaches can provide both estimates (e.g. mean/median along with 95% prediction interval), making it easy to perform a benefit-risk analysis of a particular recommendation in light of uncertainty.

Clinical Applications of Modeling and Simulation

In our research, we utilized both PK/PD and PBPK-based approaches to answer clinically relevant questions pertaining to the therapy of 3 different compounds: (1) Dose prediction in children- A case study of dicloroacetate for the treatment of congenital

lactic acidosis in children; 2) Dose optimization of voriconazole for the treatment of invasive fungal infections in adults); 3) Optimization of oxycodone therapy for chronic pain management. Some brief introduction about these three different clinical applications are shown below:

Dose Prediction in Children- A Case Study of Dichloroacetate for the Treatment of Congenital Lactic Acidosis

The establishment of drug dosing in children is often hindered by the lack of actual pediatric efficacy and safety data. To overcome this limitation, scaling approaches are frequently employed to leverage adult clinical information for informing pediatric dosing. In Chapter 2, we provided a comprehensive overview of the different scaling approaches used in pediatric pharmacotherapy as well as their proper implementation in drug development and clinical use. We started out with a brief overview of the current regulatory requirements in pediatric drug development, followed by a review of the most commonly employed scaling approaches in increasing order of complexity ranging from simple body weight-based dosing to physiologically-based pharmacokinetic (PBPK) modeling approaches. Each of the presented approaches has advantages and limitations, which were highlighted throughout the course of the review by the use of clinically-relevant examples. The choice of approach employed consequently depends on the clinical question at hand and the availability of sufficient clinical data. The main effort while establishing and qualifying these scaling approaches should be directed towards the development of safe and effective dosing regimens in children rather than identifying the best model, i.e. models should be fit for purpose. Details are presented in Chapter 2.

In Chapter 3, we applied the scaling approaches discussed in Chapter 2 to provide optimal dosing recommendations for dichloroacetate for the treatment of congenital lactic acidosis in children. Dichloroacetate (DCA) is an investigational drug used to treat congenital lactic acidosis (CLA) and other mitochondrial disorders. Response to DCA therapy in young children may be sub-optimal following body weight-based dosing. This is due to auto-inhibition of its metabolism, age dependent changes in pharmacokinetics and polymorphisms in glutathione transferase zeta1 (GSTZ1), its primary metabolizing enzyme. According to US Food and Drug administration (FDA), doses for children can be determined by extrapolating from adult data, if it is reasonable to assume that the disease progression, response to the intervention and exposure-response relationship is similar in pediatrics and adults. In such a case, a sponsor is usually required to conduct only a PK study to select a dose to achieve similar exposure ("full extrapolation") or similar target PD effect ("partial extrapolation") as attained in adults. For DCA, studies have shown that steady state trough concentrations of 5-25 mg/L are correlated with the clinical efficacy of DCA in adults as well in children. Consequently, a full extrapolation approach coupled with existing exposure-response information in children was used to inform dosing in children. This approach also allowed us to better understand the determinants of DCA plasma clearance, separate system-specific from drug-specific parameters and explore the potential reasons for the age-dependent kinetics observed in earlier studies.

This was achieved by developing a semi-mechanistic pharmacokinetic-enzyme turnover model in a step-wise approach: (i) a population pharmacokinetic (PopPK) model for adults was developed, (ii) the adult model was scaled to children using

allometry and physiology-based scaling, and (iii) the scaled model was externally qualified, updated with clinical data. The developed model was applied in clinical trial simulations to predict optimal doses for children based on identified covariates. Details are presented in Chapter 3.

Dose Optimization of Voriconazole for the Treatment of Invasive Fungal Infections

Invasive Fungal Infection (IFIs) represents one of the most detrimental complications of immunosuppression in the settings of bone marrow transplant, solid organ transplant and receipt of induction chemotherapy for hematologic malignancies [9]. Based on epidemiological studies, mortality rates can reach 80% to 100% if the condition is left untreated [10].Given the poor prognosis of IFIs, early diagnosis and prompt treatment with effective systemic antifungal agents are central to good patient outcomes.

Voriconazole is a second generation azole antifungal agent, currently recommended by Infectious Disease Society of America (IDSA) as the standard of care for the treatment of IFIs [11]. Efficacy of VCZ is dependent on the attaining steady state trough plasma concentration (2-6 mg/L). It undergoes extensive hepatic metabolism which is accountable for 98% of the overall elimination, primarily via CYP2C19, with the remaining 2% excreted unchanged via the kidneys [12]. CYP2C19 is known to undergo polymorphisms resulting into 4 different clinical phenotypes of voriconazole – Extensive metabolizers (EM:*1/*1), Intermediate metabolizers (IM:*1/*2, *2/*17), Poor metabolizers (PM: *2/*2) and Ultra-rapid metabolizers (UM:*1/*17, *17/*17).

Voriconazole is currently dosed according to a fixed weight-based dosing regimen in IFIs patients. The main shortcoming of this dosing strategy is the wide inter-

individual variability in drug exposure, where trough plasma concentrations ranging from as low as 0.2 mg/L to as high as 15 mg/L have been observed in patients treated with standard dose of voriconazole [13]. Consequently, therapeutic drug monitoring (TDM) is used as a tool to monitor drug exposure and maintain steady state troughs within the therapeutic range (2-6 mg/L). Voriconazole underexposure (trough ≤2 mg/L), has been found to be associated with high rates of treatment failure (54%), thereby portending greater mortality risks. On the other hand, a trough ≥2 mg/L resulted in treatment success rates of at least 85% [14]. Multiple linear regression analysis [15] revealed that approximately 50% of the variance can be solely explained by polymorphisms in *CYP2C19* gene. However, there is limited evidence [16] indicating the need for dose adjustment based on *CYP2C19* polymorphisms alone. Moreover, effect of other potential PK-related sources of variability such as age, race, gender and concomitant medications has not been studied so far. From a pharmacodynamics point of view, variability in minimum inhibitory concentration (MIC) values amongst different strains of *Candida* and *Aspergillus* fungi can also contribute to the overall variability in therapeutic outcome along with any PK-related variability.

The objective of our research was to optimize the clinical therapy of voriconazole in adult patients, by providing dosing recommendations. In order to achieve that, we first conducted a clinical study to prospectively investigate the impact of *CYP2C19* polymorphisms along with various other intrinsic and extrinsic factors (age, race, gender, co-medications) on voriconazole pharmacokinetics, following TDM based approach. A population PK model was then developed using the obtained clinical data. The model was applied to predict the probability of target attainment for different fungal

species and phenotypes of voriconazole. A benefit-risk analysis was then conducted to identify optimal voriconazole doses for different phenotypes. Details are presented in Chapter 4.

Optimization of Oxycodone Therapy for Chronic Pain Management

Chronic pain is the most common cause of long-term disability. In US, it is the most common reason Americans access the health care system. Estimates indicate that approximately 30-60 million Americans suffer from a type of pain annually[17,18]. For management of chronic pain, several categories of medications are used. Most common agents include Nonsteroidal Anti-inflammatory Drugs (e.g. acetaminophen), Antidepressants (e.g. amitriptyline, desipramine), anticonvulsants (e.g. phenobarbital, valproic acid), muscle relaxants (e.g. baclofen, chlorzoxazone) and opioids (e.g. oxycodone, morphine). However, opioids are most commonly used agents for pain management. According to an estimate, 259 million prescriptions including opioids for pain management were wrote in 2012, enough for every adult American to have a bottle of pills[19]. Oxycodone alone accounts for 60% of opioid use for chronic pain management. Oxycodone gets metabolized by multiple CYP450 enzymes (CYP3A4, CPY2D6) as well as phase-II enzyme (UGT2B7) into various metabolites such as oxymorphone, noroxycodone and noroxymorphone. However, oxymorphone is the major active metabolite, which is formed by CYP2D6-mediated metabolism of oxycodone. As we know, CYP2D6 and UGT2B7 enzymes are susceptible for polymorphisms which can result in different phenotypes in clinic. Also, drug-drug interactions (DDI) with strong CYP inducers or inhibitors can also result in phenoconversion of subjects. Due to polymorphisms and DDI, the concentrations of

oxymorphone can get affected, changing the benefit-risk profile of oxycodone therapy in chronic pain management.

The objective of this study was to investigate if urinary measurements are predictive of plasma exposure of oxycodone and its major metabolites. To do so, a PBPK/PGx model for oxycodone and its metabolites following intravenous and oral administration was developed using prior knowledge of the relevant metabolic pathways and formation of noroxycodone, oxymorphone and noroxymorphone. The model was informed using intravenous and oral data from the literature as well as the individual patient level data. The model was developed by mapping out the different metabolic pathways of oxycodone (i.e. CYP2D6, CYP3A4 and UGT2B7) in a stepwise manner. Once developed, the model was successfully qualified by overlaying model-based predictions with respective sets of observations, which were not used for model building. The developed model was also applied to predict the effect of germ-line mutations in CYP2D6 and UGT2B7 on the plasma and urine PK of oxycodone and its metabolites. Effect of drug-drug interactions with strong CYP2D6 inhibitors (e.g. paroxetine, quinidine), CYP3A4 inhibitors (e.g. ketoconazole) and CYP3A4 inducers (e.g. rifampin) were evaluated. Details are presented in Chapter 5.

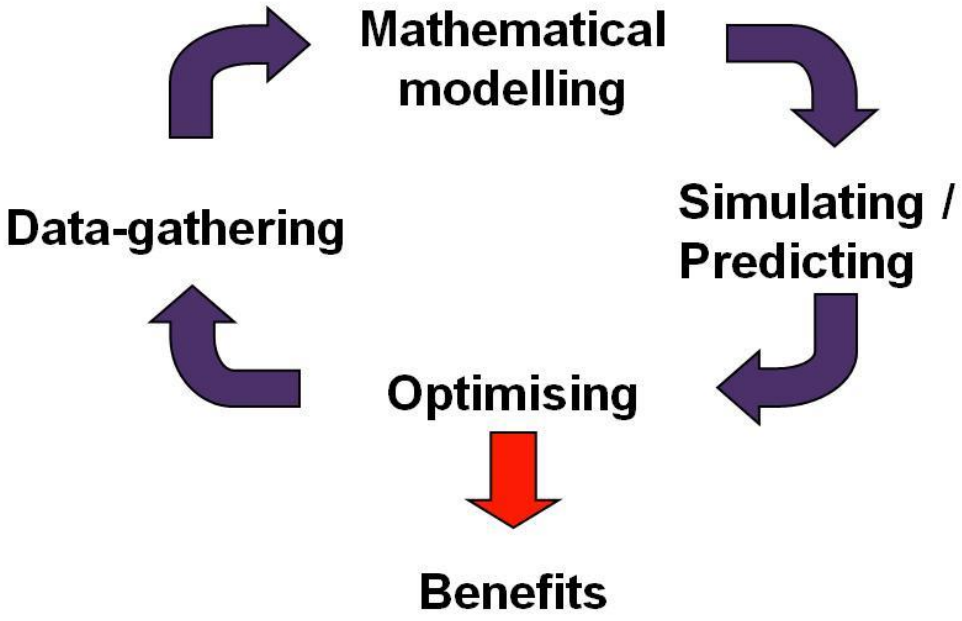

Figure 1-1. A Schematic workflow of development and application of modeling and simulation based approaches

CHAPTER 2
QUANTITATIVE CLINICAL PHARMACOLOGY FOR SIZE AND AGE SCALING IN PEDIATRIC DRUG DEVELOPMENT: A SYSTEMATIC REVIEW

Introduction

Pediatric clinical pharmacotherapy is an essential discipline that facilitates the development of drugs for children as well as the management of pharmacotherapy in children requiring medicine.[20] While many challenges in pediatric clinical pharmacology are similar to those in adults (e.g. disease progression, dose selection, therapeutic window), others are more specific to children and are driven to a large extent by the dynamics of the developing child, particularly by (patho)physiological changes from birth, which may impact the drugs' pharmacokinetics (PK) and pharmacodynamics (PD). Employed PK or PK/PD approaches consequently need to account for these changes when attempting to select an appropriate study design and/or dose or interpret PK/PD data based on sparse sampling. In addition, there is frequently limited or no information available on the efficacy and safety of drugs in children which makes this special patient population "Therapeutic Orphans".[21] Legislators around the globe have responded to this challenge over the past two decades by integrating pediatric drug development tighter into the overall development process in order to make new safe and effective drugs more readily available to children. In particular, Pediatric Exclusivity legislation under the Food and Drug Administration Modernization Act (FDAMA) in 1997 along with FDA's mandatory Pediatric Rule (1998) resulted in recommendations from the regulators, which provides sponsors with a six month pediatric marketing exclusivity.

This work has been published as an article cited as: Samant TS, Mangal N, Lukacova V, Schmidt S. "Quantitative Clinical Pharmacology for Size and Age Scaling in Pediatric Drug Development: A Systematic Review." The Journal of Clinical Pharmacology 2015, 55 (11): 1207 1217.

This led to an incremental increase in the number of clinical trials solely designed for children. Recommendations from the Best Pharmaceuticals for Children Act (BPCA) (2002) and Pediatric Research Equity Act (PREA) (2003) have also resulted in more than 500 pediatric labelling changes as of July, 2014.[22] Manufacturers in the United States are required by law since 2012 to submit a Pediatric Study Plan (PSP) no "later than 60 calendar days after the date of end-of-phase 2 meeting".[23] The European Medical Agency (EMA) requires a similar submission, referred to as pediatric investigation plan (PIP), to be completed by the end of Phase 1 clinical trials in adults.[24]

The successful implementation of PSPs is largely guided by the Pediatric Study Decision Tree[25] that was first proposed by FDA in 2003. The main purpose of this regulatory document is to guide sponsors through the pediatric development process and to make optimal use of adult PK information for dose finding in children and to reduce the number of clinical studies in this vulnerable patient population. Updated draft guidance was published in December 2014 and is now open for public review. This draft guidance also contains an updated decision tree (Figure 2-1) also referred to as Pediatric Study Planning & Extrapolation Algorithm. This decision tree distinguishes between three different approaches: 1) a PK only approach ("Full extrapolation"), 2) a PK and PD approach ("Partial extrapolation"), and 3) a PK and efficacy approach ("No extrapolation").[26] The "PK only approach" suggests the conduct of PK only studies in pediatrics if it is reasonable to assume that there is *i)* similar disease progression, *ii)* similar response to therapeutic intervention(s) and *iii)* similar exposure- response relationship between adults and children. The PK and PD approach can be used if disease and intervention are similar between adults and children but the exposure

response relationship is not. The PK and efficacy approach requires a full-scale safety and efficacy trial and is applied if the disease progression is different between adults and children or if the response is undefined with respect to adults.

Despite the continuous efforts by regulators to avoid off label use, about 50% to 75% drugs used in children have not been clinically studied to provide accurate labelling information in pediatrics.[27] Laughon *et al.*, for example, showed that only 1 out of the top 10 most commonly used drugs in intensive care settings is actually labeled for use in premature infants.[28] This is in line with a report from FDA that states that there is PK data in patients younger than 1 year for only 18 out of 161 products studied under FDA's Amendment Act (FDAAA) as of December 2012.[22] This is at least in part due to the fact that conventional dose finding approaches in adults are not applicable to children due to sample size limitations and/or ethical concerns. As a consequence, alternative dose finding approaches, such as extrapolation from adult dosing regimens to children by accounting for differences in body size, have become standard practice in pediatric drug development. The methods used for extrapolation range from simple age-, weight- or body surface area-based dosing approaches to complex mechanism- or physiologically-based pharmacokinetic-pharmacodynamic (PBPKPD) modeling approaches. The objective of this review is to: *i*) compare and contrast these different scaling approaches in an increasing order of complexity and *ii*) to showcase examples of how these approaches have helped to guide dose finding and optimization in children.

Use of Scaling Approaches for Prediction of Pharmacokinetics in Pediatrics from Adults

According to the FDA's Center for Drug Evaluation and Research (CDER) the pediatric population can be divided into 4 main subpopulations: 1) neonates (birth up to 1 month), 2) infants (1 month up to 2 years), 3) children (2 years up to 12 years), and 4) adolescents (12 years up to 16 years).[26] In order to select safe and effective doses for these different pediatric subpopulations, it is important to account for maturational changes in the patient's PK and/or PD from birth.

A.J. Clark[29] was one of the first to propose that the dose for children ($Dose_{pediatric}$) can be determined by multiplying the respective adult dose ($Dose_{Adult}$) with the body weight ratio of the pediatric target population ($BW_{pediatric}$) and adults (BW_{adults}) as shown in Equation 2-1. Body weight is consequently used in this approach to account for differences in body size between adults and children.

$$Dose_{pediatric} = \left(\frac{BW_{pediatric}}{BW_{Adult}}\right) * Dose_{Adult} \quad (2\text{-}1)$$

However, this relationship assumes that there is a linear relation between body weight and dose, which typically does not hold true across the entire age spectrum.[30] It could also be shown that direct weight-based extrapolation of adult doses to children can lead to lack of either efficacy or safety due to inappropriate dosing. Inappropriate drug exposure can be result of either under- or over-dosing. For example, gentamicin was shown to be under-dosed with more frequent dosing interval in neonates using body weight - and surface area-adjusted doses.[31] On the other hand, chloramphenicol, a broad spectrum antibiotic, was over-dosed in neonates and pediatrics after a weight-based linear extrapolation of the adult dose, which resulted in increased mortality rate compared to the placebo group.[32] These differences in mortality were later attributed to

reduced glucuronidation in newborns and infants, which poses a problem because glucuronidation is the primary metabolic pathway for chloramphenicol. Penicillin/sulfisoxazole-induced kernicterus is another example for drug-induced adverse events in children, particularly in premature and full term newborn infants. Simple weight based dose adjustment and, thus, failure to account for the immaturity of glucuronidation in neonates resulted in increased mortality due to increased bilirubin levels in their basal ganglions.[33] As a consequence, other approaches that account for non-linear changes in metabolism from birth have been employed for scaling adult doses to children.

Moore[34] proposed that the rate of drug metabolism depends on the basal metabolic rate (BMR) of the organism, which can be measured in terms of heat loss. Body surface area (BSA), which is proportional to heat loss from the body[35,36,37] is frequently used as a surrogate for metabolic rate. In addition, it was found that many physiological parameters, such as organ size, blood flow, tissue volume, correlate better with BSA than body weight.[38] It was consequently suggested that BSA should be used instead of body weight for selecting starting doses in children as shown in Equation 2-2

$$\text{Dose}_{\text{Pediatric}} = \left(\frac{BSA_{Pediatric}}{BSA_{Adult}}\right) * Dose_{Adult} \quad (2\text{-}2)$$

Where $BSA_{\text{Pediatrics}}$ represents the body surface area of the pediatric target population and BSA_{Adult} represents the body surface area of the respective adult population.

It should be noted that BSA in and by itself is a non-linear expression, which uses a combination of height, weight and different exponents as shown in Equation 2-3. It should further be noted that there are different formulas available for computing BSA

and Equation 2-3 represents one of the most commonly used relationships proposed by DuBois and DuBois Equation.[39]

$$BSA\ (m^2) = 0.2047 * Height\ (m)^{0.725} * Weight\ (kg^{0.425} \quad (2\text{-}3)$$

In 1932, Max Kleiber[40] proposed the famous "Power Law", which relates the basal metabolic rate of an organism (BMR) to the animal's mass using a fixed exponent of 3/4th (Equation 2-4).

$$BMR\ \alpha\ M^{3/4} \quad (2\text{-}4)$$

The law is based on the fact that the metabolic capacity of an animal is primarily governed by the relationship between resting and maximum metabolism. Maximum oxygen consumption (VO_{2max}), which is similar in organisms of different sizes, is used as a surrogate for this relationship and can be best expressed by a power function with a fixed exponent of ¾ as shown in Figure 2-2.[41]

"Allometric Scaling", the most widely used pediatric scaling approach, was derived from this power law. It proposes that the PK parameter of interest (Y) can be retrieved from the corresponding adult value (a) by multiplication with the normalized body weight to the power of the allometric exponent b as shown in Equation 2-5.

$$Y = a \times BW^b \quad (2\text{-}5)$$

Equation 2-5 typically uses a fixed allometric coefficient of: 0.75 for CL, 1 for volume of distribution, and -0.25 for time-dependent variables, such as rate constants. Although this approach is typically superior to body-weight or BSA-based scaling approaches, it is important to realize that it may or may not hold for pediatric subgroups at the lower extreme of the age spectrum, particularly for those under the age of 1 year. This is due to the fact that additional maturational processes, such as changes in

enzyme expression levels, closure of tight junctions or brain weight, do not necessarily correlate with body size across the entire age spectrum.

This limitation can be addressed by including time-dependent functions, such as a maturation function (MF) or an organ function (OF), in Equation 2-6 that account for changes from birth.[42] The inclusion of MF and OF into the general allometric scaling function can minimize its tendency to over-predict clearance, especially in very young children.

$$CL_{pediatric} = \left(\frac{BW_{pediatric}}{BW_{Adult}}\right)^{0.75} * CL_{Adult} * MF * OF \quad (2\text{-}6)$$

It should be noted that MF is a continuous, asymptotic function that reaches the adult value (MF=1) at some finite point in development.[42] OF, on the other hand, is reflective of the health status of an organ. It is set to 1 for healthy subjects, but can reach higher or lower values under diseased conditions. For instance, it can be substantially lower than 1 for a subject with renal impairment depending on severity of the disease. It is important to note that both of these functions have limited predictive performance since they are data driven and empirical in nature.

It should further be noted that most of the scaling approaches assume linear PK, and that the drug is primarily cleared from the central compartment. However, this does not hold true for all drugs, particularly for protein therapeutics which can undergo target-mediated drug disposition (TMDD) and or substantial drug clearance in tissues. As a consequence, body weight-based allometric scaling may be sufficient to predict pediatric doses for therapeutic proteins, such as monoclonal antibodies (mAb) that show linear clearance[43,44] but may not be appropriate to use for mAbs exhibiting TMDD depending on the therapeutic concentration range, nature and location of the target.[45]

Although allometric scaling approaches have been widely applied to characterize maturational changes in clearance from birth, not much attention has been paid to non-linear changes in volume of distribution (V_d). The volume of distribution of a drug depends on both drug-specific (e.g. pKa, logP, molecular weight) and system-specific properties (e.g. organ volume and composition, blood flow, transporter expression levels).[46] It is the combination of drug- and system-specific properties that determines how fast and to what extent a drug will distribute throughout the body. While drug-specific parameters are invariant with time, system-specific properties can undergo age-related changes.[47] Total body water as a percentage of body weight is higher in preterm and term neonates ranging from 87% and 75% respectively. There are rapid changes in water content as the percentage falls to 60 % by age 1 year and to 55 % in adults.[48] Similarly, the extracellular water content is higher in neonates (45%) and decreases to about 20% in adults.[49] This can substantially impact the V_d for hydrophilic drugs, such as gentamicin, for which it is higher in neonates than in adults.[50,51] Reduced plasma protein binding in infants and neonates can also result in a higher V_d of drugs compared to adults.[52] The central nervous system (CNS) volume reaches 80-90% of the adult volume by ages 4-6 years but is not correlated with BSA.[49] In addition, the blood-brain barrier is more permeable in newborns than in older children[49], which in combination with the relatively larger brain volume can have implications on drug distribution into the brain. All of these physiological differences between adults and children contribute to changes in V_d and may not be sufficiently accounted for using simple allometric scaling approaches. Therefore, maturational changes impacting V_d warrant closer evaluation.

There are many examples for the successful application of between species scaling of PK using allometric scaling approaches.[53,54,55,56] However, there are also examples, particularly for within species scaling, where allometric scaling approaches have met variable success. For example, Momper *et al.*[57] showed that the absolute % prediction error was relatively small and ranged from 0.6 - 36 % when using a fixed exponent of 0.75 for 27 drugs (19 oral, 8 IV products) to scale from adults to adolescents. The authors concluded that "allometric scaling may be a useful tool to avoid unnecessary dedicated PK studies in the adolescent population during pediatric drug development". Hamberg *et al.*[58] proposed a mechanism- based adult PK/PD model for warfarin and bridged to children using allometric scaling. Overall, it was shown that the bridged model predicted INR response reasonably well in 64 warfarin- treated children (median age 4.3 years). However, there was a tendency to over-predict INR in children ≤ 2yrs of age. Mahmood *et al.*[59] compared 4 different scaling approaches, namely simple allometry, scaling based on maximum lifespan potential (MLP), MLP coupled with a correction factor (for prediction of pediatric clearance from rat, dog and human data), and a fixed exponent of 0.75 (for prediction of pediatric clearance from adult human data only) for 28 different drugs. It was shown that scaling based on the fixed coefficient of 0.75 over-predicted pediatric clearances by at least 100% for 49 out of 125 observations (39.2 %) for all the drugs from neonates to adolescents. It is also worthwhile noting that most of these over-predictions were made for premature neonates or children <1 year of age (42 observations out of 71 observations = 59.1%). Johnson *et al.*[30] compared 3 different scaling approaches BW, BSA, $BW^{0.75}$ to predict maintenance doses across the pediatric age band from equivalent adult doses for 30

different drugs and compared them with doses observed by British National Formulary for Children 2006 (BNFc). It was concluded that no single method reliably predicts pediatric doses across the entire age range and all of these scaling approaches should be treated as "last resort" for the dose prediction in children. Mahmood[60] showed that in children < 5 years of age, use of fixed allometric coefficient of 0.75 resulted in higher prediction errors as compared to children > 5 years of age. Hence an age-dependent exponent model was proposed with variable exponents for scaling of clearance for different age groups of children. The author concluded that although this method performed better, it is unsuitable for use in clinical settings for dose adjustment due to inaccurate individual predictions.

All the above summarized case studies suggest that different scaling approaches including allometric scaling may be able to predict PK reasonably well in older children above the age of 2- 3 years but it faces limitations with making predictions with same accuracy and precision in premature neonates and children with predictions progressively worsening below the age of 1 year. Although this may not hold true universally, it has been observed in majority of the cases studied so far. The reason for this anomaly goes back to the assumptions of conventional scaling approaches. They assume that there is a monotonic relation between body functions such clearance and size of an organism (Figure 2-3 A, B). Consequently, this monotonic relation is used for allometric scaling based on body size alone rather than a combination of body size and function. Clearly, these allometric approaches do not accurately account for the changes associated with the developing physiology of a child and changes in the metabolizing enzyme expression and activity levels in the eliminating organs which are

the primary drivers of clearance i.e. exposure ($AUC_{0\text{-}infinity}$). Edginton *et al.*[61] showed that there was a significant overlap between PBPK and allometric predictions above the age of 4 years (Figure 2-4 A, B). However PBPK predictions were relatively more accurate before 4 years. As the enzyme expression levels and activity of enzymes starts approaching adult values, allometry and other scaling approaches usually start making better predictions which are closer to the observed values in children. To improve on the predictions below the age of 2-3 years and to characterize the non-monotonic changes in clearance (Figure 2-3 C), a more mechanistic and physiological approach is required which considers the underlying developing physiology from pediatrics to adults.[62]

Use of PBPK in Scaling of Pharmacokinetics from Adults to Pediatrics

In recent years, the use of PBPK modeling for predicting the PK of drugs in children has increasingly gained interest although there are few examples used for dose selection in regulatory submissions. Many investigators have developed pediatric PBPK models based on adult PK data and scaled them to children by incorporating information on the changes in the underlying physiology, such as ontogeny of relevant metabolic enzymes, renal function, or organ development. This has been of interest to regulatory agencies in US and Europe who now also encourage the use of PBPK models in pediatric drug development in order to enable the science to evolve.[23]

PBPK models typically consist of three distinct parts: 1) drug-specific parameters, 2) system-specific parameters and 3) trial design parameters (also called intrinsic and extrinsic factors) as shown in Figure 2-5. Drug-specific parameters characterize the physicochemical properties of the drug (e.g. pKa, molecular weight, logP) and can often be predicted on the basis of *in vitro* bioassays. Biological system-specific parameters describe the physiological functions and can differ between and within species. Finally,

trial design parameters determine the impact of the intrinsic (e.g. demographics, disease states, genetic constitution) and extrinsic factors (e.g. diet, smoking, drug-drug interactions) on the drug's PK.

The development and application of PBPK models is not a new concept given that they have been used in environmental toxicology for decades.[63,25] However, it took until the early 2000s for the models to be used also for applications in children. For example, Pelekis *et al*, used qualified PBPK models and simplified their structure in order to translate chemical exposure to tissue concentrations in both adults and children. The investigators concluded that the results from conventional PK approaches and PBPK models were very similar but emphasized that PBPK approaches provide a more scientific and physiologically meaningful framework for accounting for changes in the parameters evaluated.[64] Around the same time, Price *et al.* employed a PBPK modeling approach for chemical risk assessment in adults and children.[65] In recent years, many attempts have been made to optimize pediatric PBPK models by incorporating enzyme ontogeny, maturation of absorption mechanisms, and other routes of drug disposition, such as renal elimination. Ginsberg, 2004, developed PBPK models for caffeine and theophylline (CYP1A2 substrates)[66] to assess the risk for children arising from these drugs as part of their daily environment, such as breast milk and water. Both adults and neonates were used for the model development by scaling up *in vitro* metabolic parameters to whole liver *in vivo* parameters and incorporating the ontogeny in the development of CYP1A2 enzymes. The developed and qualified PBPK model could effectively simulate the differences in clearance and half-life of caffeine and theophylline in adults and neonates. It was also able to predict the faster clearance of

theophylline as compared to caffeine in neonates, which was primarily attributed to the back conversion of theophylline to caffeine that occurs only in neonates but not in adults. Parrott *et al.*, showed the utility of successfully predicting age dependent PK from neonates to adults by establishing a model for the intravenous and orally administered oseltamivir and its active metabolite, oseltamivir carboxylate.[67] A PBPK model for acetaminophen, which is metabolized by multiple phase I and phase II pathways, was able to successfully predict the clinical PK data from neonates to adults.[68] Another exhaustive study facilitated the prediction of distribution as well as clearance of 11 widely used drugs (midazolam, caffeine, diclofenac, omeprazole, cisapride, carbamazepine, theophylline, phenytoin, s-warfarin, gentamycin and vancomycin) for IV and oral dosing while accounting for the enzyme ontogeny and physiological changes in children (at all age groups) and adults.[69] The authors illustrated the usefulness of PBPK modeling over allometry in better prediction of PK for children <2 years of age.[69] For midazolam and theophylline, PBPK models effectively captured the ontogeny of enzymes and other clearance mechanisms by a good overlay of observed data for changes in volume of distribution, clearance and terminal half-life from neonates to adults.[70]

PBPK modeling is an emerging tool for integrating available knowledge into a physiologically relevant mechanistic model which can be applied to guide pediatric drug development and dose finding. Regulatory agencies are willing to engage with industry and academia to improve the usefulness and shortcomings of pediatric PBPK modeling. There is a growing plethora of knowledge on the various transporters and receptors for drug safety and efficacy. As the field continues to grow and information on new drug

disposition pathways becomes available, these factors can be incorporated into various PBPK models to better account for drug disposition and PK. Given the physiologically based nature of the model incorporation of transporter and receptor ontogeny can be achieved in a much more meaningful way as compared to conventional scaling models.

PBPK models have demonstrated their utility in the area of small molecules as well as for large molecules, such as monoclonal antibodies.[71,72,73] While conventional allometric approaches may be sufficient to predict the PK of antibodies with linear kinetics in children, they may face limitations for antibodies exhibiting non-linear kinetics.[45] The physiological changes in children influencing the disposition kinetics of large molecules is subject to ongoing research but pediatric PBPK models exploring large molecule disposition have not yet been proposed in the literature to the best of our knowledge.

While the development and qualification of PBPK models has gained quite a bit of momentum in recent years, a second clinically very important population, i.e. the elderly, has been neglected thus far. This is likely to change in the next few years as the world's geriatric population is projected to cross a mark of 2 billion by 2050[74] and optimal geriatric dosing will be of high importance to ensure safe, effective and affordable drug therapy. PBPK models may be an effective approach to do so, as much of the lessons learned for pediatrics can be translated into the geriatrics arena. In addition, the modular setup of PBPK models, in combination with advancements in characterizing the clinically important factors impacting drug absorption, PBPK models may serve as the scientific basis for establishing bioequivalence between brand and generic drug products. This may become particularly important for complex drug

formulations or parenteral administration routes as outlined in a recent publication from the Office of Generic Drugs at FDA.[75]

Given the complex nature of PBPK models, it is important to achieve a general consensus on how to establish and qualify them according to best practices.[23,76] PBPK models are usually qualified by overlaying the model predictions with observations from an external dataset that is not used for model building. Given that no actual estimation step is performed, respective PBPK qualification criteria are typically less stringent than those used in conventional PK/PD modeling approaches. PBPK models are typically found acceptable within the PBPK/PD community if the visual predictive check shows less than a two-fold difference between observed and simulated area under the concentration-time curve (AUC) and maximum plasma concentrations (C_{max}) values. The establishment and qualification of pediatric PBPK models is frequently limited by the lack of rich clinical data and insufficient knowledge of ontogeny and systems properties in pediatrics, which can pose a problem when attempting to accurately characterize AUC and C_{max}. Although this may pose a challenge for stringent model qualification of pediatric PBPK models, their physiological basis is thought to yield a better predictive performance for scenarios at the extremes of the available data/populations (e.g. for pre-term neonates) or even for unstudied scenarios compared to conventional PK/PD models, which are typically data-centric and descriptive in nature. However, many PBPK models still use generic variance estimates on their physiological input parameter, which may or may not accurately reflect reality. Going forward it will consequently be important to more accurately characterize parameter variance in order to obtain unbiased PBPK model predictions, particularly for respective

prediction intervals. Figure 2-6 provides an example of a schematic workflow for how to establish and qualify pediatric PBPK models.[68] This workflow can be used as a scientific rationale for bridging *in vitro* information to children using adult PK data as an intermediate qualification step. This approach consequently delineates critical model building and qualification steps and is intended to increase the confidence in pediatric PK predictions, particularly in the absence of actual clinical data in children. To gain confidence in the developed PBPK models, they need to be characterized on the basis of: a) "biological basis of the model structure and parameters", b) "comparison of model simulations with experimental data" and c) "reliability of model predictions of dose metrics relevant to the risk assessment (model testing, uncertainty and sensitivity analysis)".[12] This three-pronged approach for qualifying the PBPK would enable simulations to be translated into effective predictions for dose extrapolations. The International Workshop on Uncertainty and Variability in PBPK Models, held 31 Oct – 2 Nov 2006 identified changes to the practice and implementation of PBPK models and divided the research priorities into short term and long term needs.[77] The short term needs specified integration of statistical and deterministic models, enhanced use of sensitivity analysis and greater reproducibility of documentation. The long term needs included methodological improvements in statistical models, better means of evaluating alternate models, review by the scientific community, PBPK model building across different chemicals and appropriate training material. These needs are a quintessential example for development of strong diverse PBPK models. Also, most of the models which have been developed for adult and pediatric PBPK are retrospective models while its main application lies in developing prospective models. These prospective

models would help simulate PK profiles and enable clinicians to develop and recommend appropriate sampling times and better dosing recommendations. PBPK models can become an important tool for answering clinically relevant questions and decision making in pediatrics.

Conclusions

In summary, although the application of quantitative analysis techniques has substantially improved pediatric pharmacotherapy over the last decades, there is still a high degree of uncertainty and off-label drug use in pediatrics due to the lack of respective pediatric dosing recommendations. All of the employed techniques for dose finding and optimization in children have advantages and limitations. In order to overcome these limitations, employed scaling approaches need to sufficiently reflect physiological reality and be able to address the clinical question at hand, i.e. be fit for purpose. While relatively simple (allometric) scaling approaches are in many cases sufficient to predict pediatric dosing regimens down to the age of about two to three years, more complex approaches, such as PBPK modeling, may be needed to accurately reflect physiological reality in younger age groups, such as in neonates and in preterm neonates. This need arises from rapid changes in the underlying (patho)physiology after birth, which may or may not be accurately reflected by changes in body mass only. The choice of which approach to use in order to establish pediatric dosing regimens is also influenced by the number of clear case examples available in the literature and the level of transparency in the employed approach. The latter can be a particular challenge for PBPK models as the frequent unavailability of: *i*) source code and *ii*) consistent model parameterizations leads to skepticism around model predictions amongst members of the clinical pharmacology community. Irrespective of the approach

chosen, the successful establishment of optimal pediatric dosing regimens is reliant upon an appropriate characterization and implementation of the relevant (patho)physiological processes into the employed quantitative decision support tool, i.e. the model.

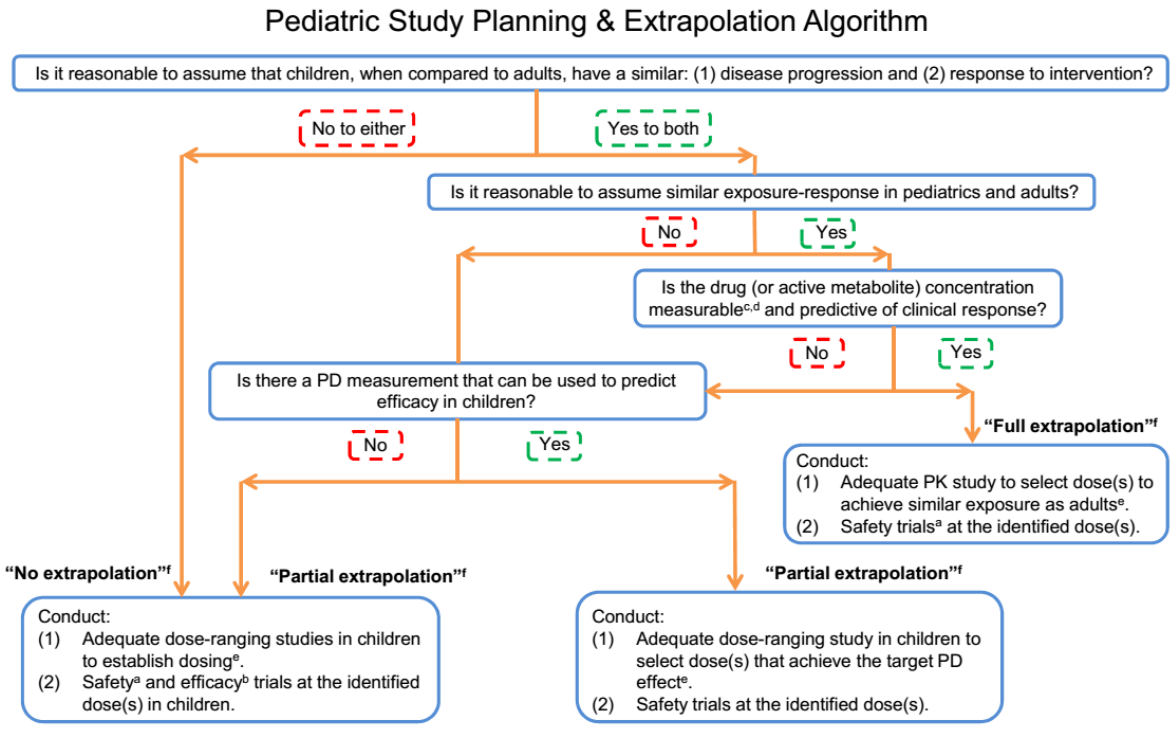

Footnotes:

a. For locally active drugs, includes plasma PK at the identified dose(s) as a part of safety assessment.
b. For partial extrapolation, one efficacy trial may be sufficient.
c. For drugs that are systematically active, the relevant measure is systemic concentration.
d. For drugs that are locally active (eg., intra-luminal or mucosal site of action), the relevant measure is systematic concentration only if it can be reasonably assumed that systemic concentrations are a reflection of the concentrations at the relevant biospace (eg., skin, intestinal mucosa, nasal passages, lung).
e. When appropriate, use of modeling and simulation of dose selection (supplemented by pediatric clinical data when necessary) and/or trial simulation is recommended.
f. For a discussion of no, partial and full extrapolation, see Dunne J, Rodriguez WJ, Murphy MD, et al. "Extrapolation of adult data and other data in pediatric drug-development programs." Pediatrics. 2011 Nov; 128 (5): e1242-9

Figure 2-1. FDA's decision tree to guide clinical study designs in pediatrics utilizing the adult clinical trial data[25]

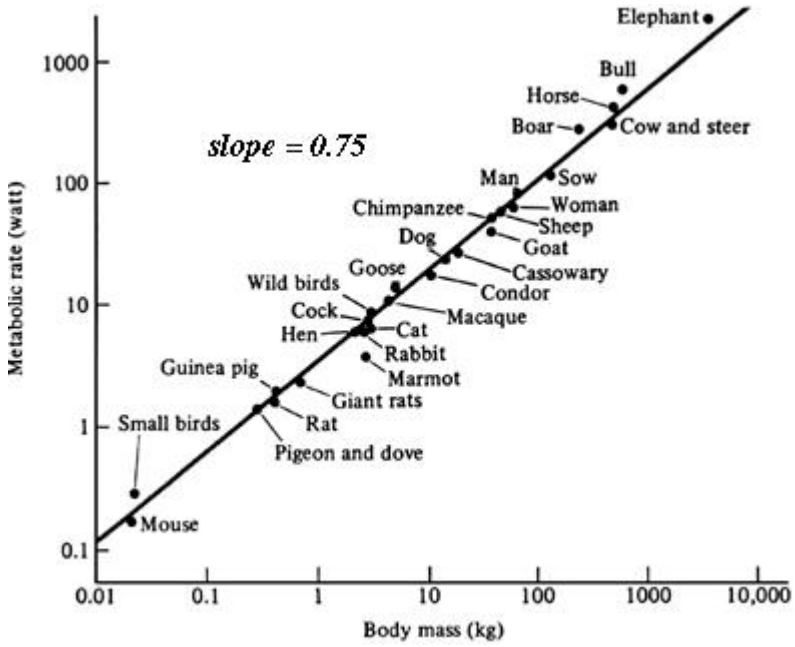

Figure 2-2. Allometric scaling relating metabolic rate (watt) to body mass (kg) for species of different sizes[40]

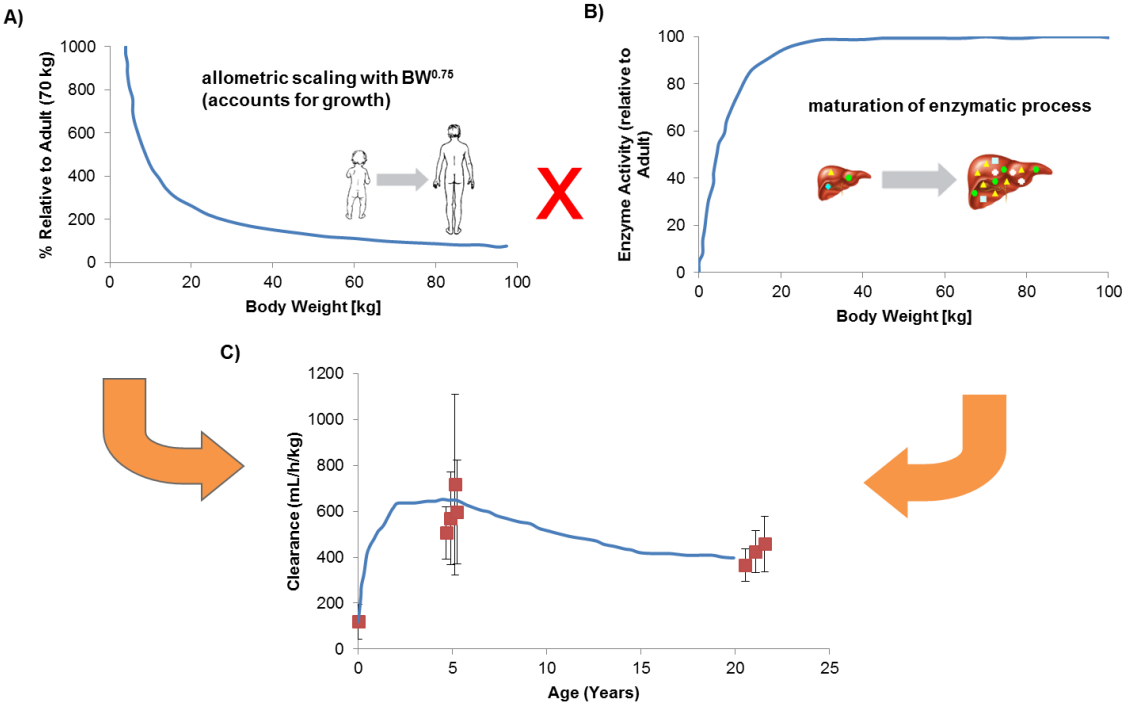

Figure 2-3. Change in clearance with body weight or age. A) Monotonic changes in clearance with body weight. B) Monotonic change in enzymatic activity with body weight. C) Non-monotonic change in clearance as a function of body weight and maturation of enzymatic process (Figure 2-3C adapted from Bjorkman, 2005)[70]

A)

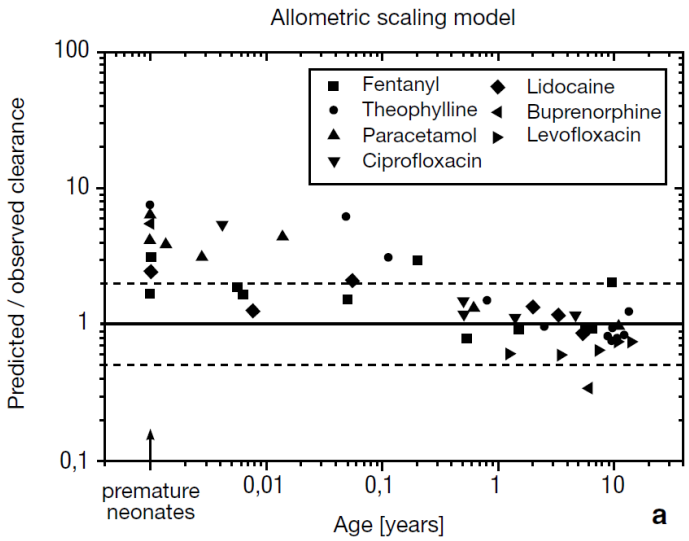

B)

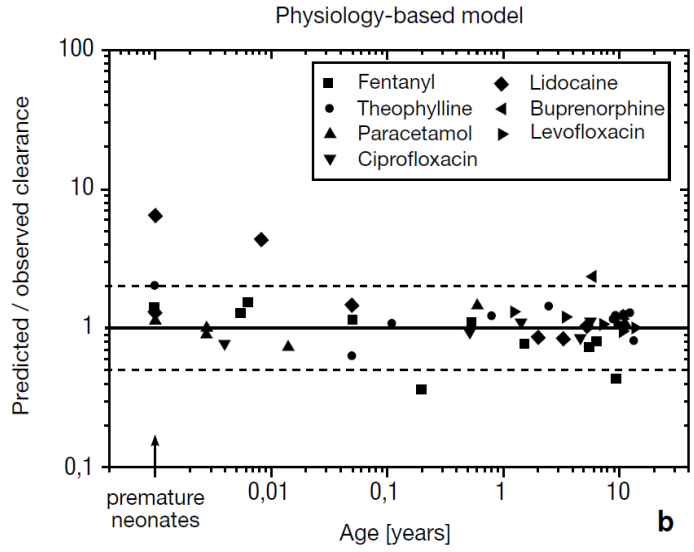

Figure 2-4. Comparing clearance predictions obtained from different methods for 7 different compounds. A) Allometry approach. B) Physiology-based modeling approach[61]

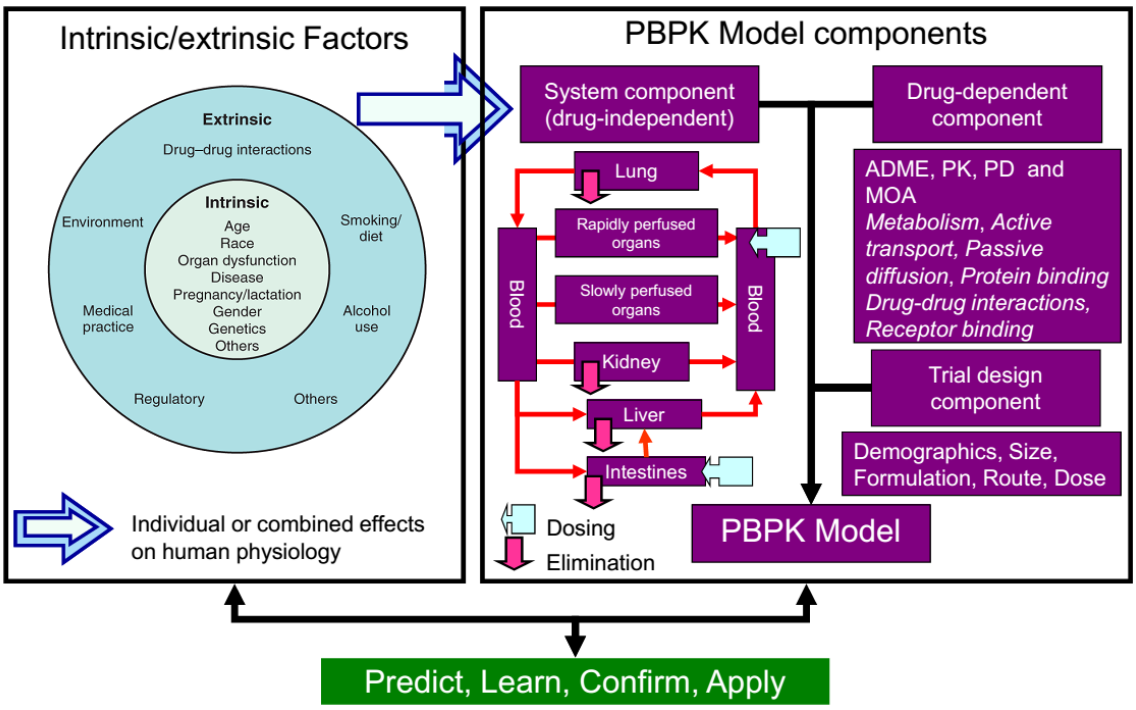

Figure 2-5. Flowchart describing the applications of PBPK modeling and simulation to evaluate the effect of various extrinsic and intrinsic factors on drug exposure and response. Adapted from Zhao, et al. 2011[23]

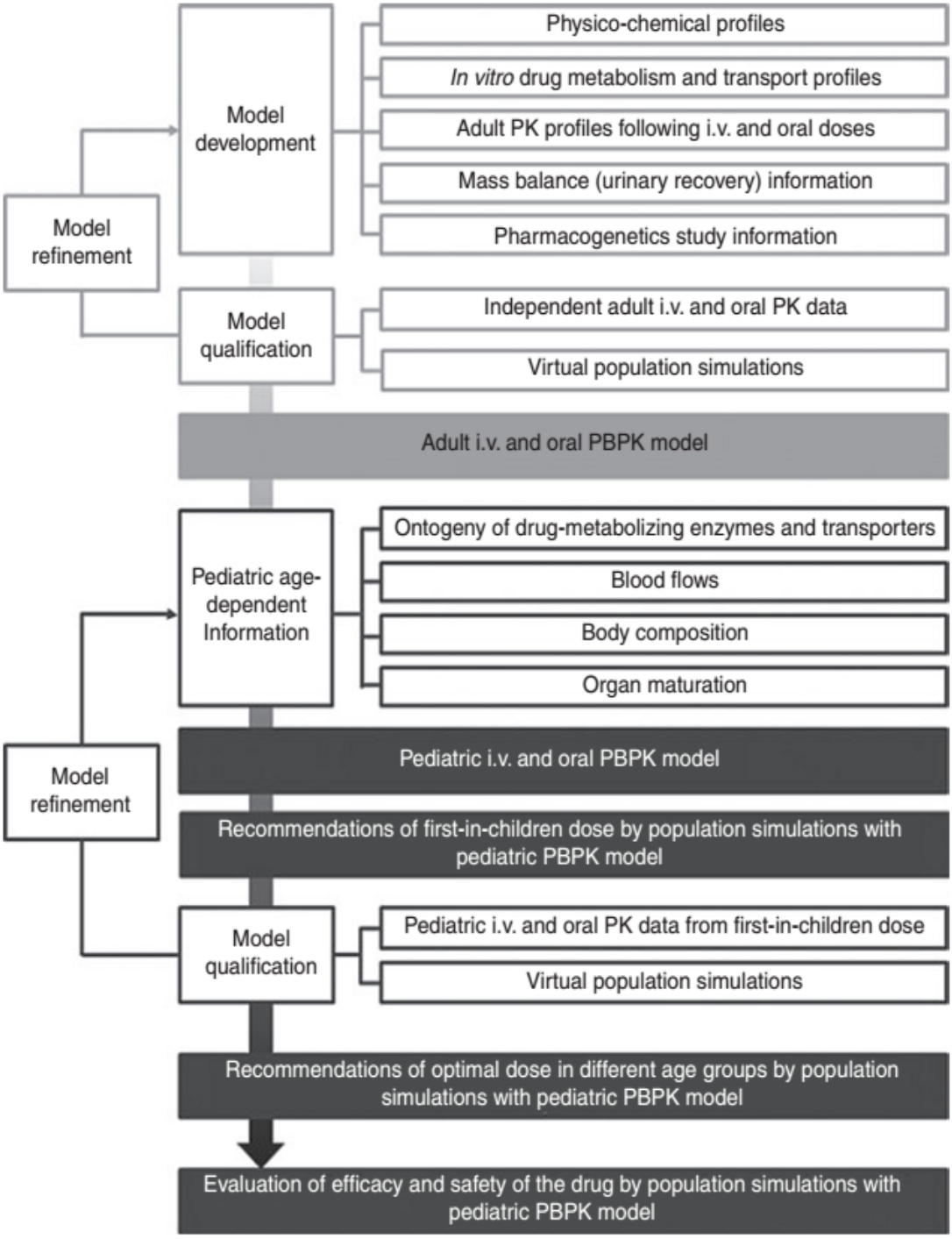

Figure 2-6. Flowchart of step-wise building of pediatric PBPK models[68]

CHAPTER 3
MODEL INFORMED DOSE OPTIMZATION OF DICHLOROACETATE FOR THE TREATMENT OF CONGENITAL LACTIC ACIDOSIS IN CHILDREN

Introduction

Congenital Lactic Acidosis (CLA) is a rare genetic disorder that consists of a group of inborn errors of mitochondrial metabolism, characterized by abnormal accumulation of lactate in body fluids and tissues. CLA is primarily caused by mutations in nuclear or mitochondrial DNA that encode genes of the pyruvate dehydrogenase complex (PDC) or enzymes in respiratory chain[78]. Signs of disease often occur very early in life and include lactic acidosis and progressive neurological and neuromuscular degeneration[79]. Currently, there are no FDA-approved therapies for these life-threatening diseases.

Dichloroacetate (DCA) is an investigational drug effective in reducing blood and CSF lactate concentrations in patients with CLA, including PDC deficiency. The PDC megacomplex is a gatekeeper enzyme linking cytoplasmic glycolysis with the mitochondrial tricarboxylic acid cycle and oxidative phosphorylation. PDC undergoes reversible phosphorylation in humans by pyruvate dehydrogenase kinase (PDK), which inhibits the enzyme, and pyruvate dehydrogenase phosphatase, which restores PDC catalytic activity[80-82]. DCA activates PDC by directly inhibiting PDK and by decreasing PDC enzyme turnover, thereby facilitating oxidative removal of lactate[83,84].

This work has been accepted for publication in Journal of Clinical Pharmacology cited as, Mangal N., James MO, Stacpoole PW, Schmidt S. "Model informed dose optimization of dichloroacetate for the treatment of congenital lactic acidosis in children" J Clin Pharmacol. 2017 Sep 15. doi: 10.1002/jcph.1009. [Epub ahead of print]).

Despite its efficacy, optimal dosing of DCA has been challenging in both adults and children because both populations are treated according to a fixed weight-based dosing regimen[85,86]. The major limitation of this approach is that it does not consider the effects of well-known pharmacological variables that can influence DCA's kinetics and biotransformation. For example, it has been shown that the half-life of DCA increases after repeated administration in adults and children. This phenomenon is attributable to the drug's mechanism-based inhibition of glutathione transferase zeta 1 (*GSTZ1*), which dechlorinates DCA to glyoxylate[87]. This auto-inhibition of DCA's biotransformation pathway makes it difficult to predict changes in plasma drug clearance and, consequently, dose, during treatment. Moreover, plasma half-life increased approximately 10-fold after 6 months of daily administration in adults, whereas half-life increased only about 2.5-fold in children, suggesting that age-dependent changes may play a role in the metabolism of DCA[87]. Finally, it is known that *GSTZ1* is polymorphic[88,89], resulting in the expression of 5 major haplotypes: EGT (wild-type, 45-55% of the population), KGT (25-35% of population), EGM (10-20% of population), KRT (1-10% of population) and KGM (<1% of population).[90] Subjects who have at least one EGT allele (EGT carriers) clear the drug from plasma faster than those who do not possess EGT allele(s) [91,92] (EGT noncarriers).

In light of these challenges, the objective of this study was to develop a population pharmacokinetic (PopPK) model for DCA to predict optimal DCA dosing regimens in children. This was achieved in a stepwise manner: (i) A PopPK model for DCA in healthy adults was developed, (ii) The developed model was then scaled to children, using data from a randomized controlled trial of DCA in children with CLA and

(iii) The scaled model was further refined, updated and optimal doses for children are recommended.

Materials and Methods

Data for Model Development

Data for building the model was collected from prior studies of DCA in adults[91] and children[86] that investigated the effect of single and repeated doses on its pharmacokinetics and the influence of *GSTZ1* polymorphisms thereon. All studies were conducted in the Clinical Research Center in Shands Hospital at the University of Florida after approval by the university's Institutional Review Board. Informed consent was obtained from all the participants or parent/guardian prior to subject enrollment.

Adult data

The demographic characteristics of the adult population[91] are presented in Table 3-1. Briefly, 12 participants (5 males), aged 26±4.5 years were genotyped for *GSTZ1* haplotype status and were administered an oral dose of 25 mg/kg/day DCA for 5 consecutive days. 1, 2, -^{13}C DCA was administered on day 1 and day 5, while 1, 2 -^{12}C-DCA was administered on days 2-4. Plasma kinetics were investigated on days 1 and 5 and DCA concentrations were measured by gas chromatography-mass spectrometry.

Seven subjects possessed the EGT allelic variant of *GSTZ1* (EGT carriers) and five of them lacked this variant (EGT noncarriers). Four EGT carriers were homozygous while 3 were heterozygous (1-EGT/KGT, 2-EGT/KRT). Subject 12 was excluded from the analysis as the subject possessed an extremely rare non-synonymous[91] SNP in addition to rare KGM allelic variant of *GSTZ1*.

Data in children

The demographic characteristics of the pediatric population[86] are presented in Table 3-1. Forty-three children with CLA, aged 0.9-19 years at entry, were enrolled. All patients were genotyped for *GSTZ1* haplotype status and received placebo for 6 months. Thereafter, patients were randomized to receive either placebo (n=22) or DCA (n=21) for an additional 6 months. After this initial 12-month period, all patients were treated with open label DCA for a minimum of 12 additional months. DCA kinetics was evaluated following administration of 12.5 mg/kg of 1, 2-^{13}C-DCA on day 1 and thereafter every 6 months for up to 60 months. During these 6 month intervals, patients were administered 12.5 mg/kg of 1, 2-^{12}C-DCA every 12 hours. Of the 21 patients in the original DCA group, 5 patients did not complete the study due to disease-related death (3) or dropout (2). Hence, data from 16 children (11 EGT carriers and 5 EGT noncarriers), aged 5.9 ± 4.9 years at entry, were included and analyzed via non-linear mixed effect modeling approach.

Modeling and Simulation

A stepwise approach for modeling and simulation was adopted (Figure 3-1). First, an *in vitro-in vivo* correlation (IVIVC) of GSTZ1 enzyme kinetic data was performed. Using these IVIVC vales, clinical data and GSTZ1 enzyme turn over[93], a PopPK model for adults was developed. Second, the adult PopPK model was scaled to the children and the model predictions were externally qualified with the observed DCA concentrations measured in children and model parameterization was further updated if needed. Finally, clinical trial simulations were run to predict optimal doses for children.

Development of adult PopPK model

Structural model. A PopPK model was developed in NONMEM v.7.3 (Icon Development Solutions, Dublin, Ireland) using plasma concentration-time data obtained from healthy adult volunteers[91]. One-compartment and two-compartment models were explored as structural models. Non-linear biotransformation of DCA by GSTZ1 enzyme [94] was characterized by considering Michelis-Menten[95] kinetics using maximal velocity (V_{max}) and Michaelis constant (K_m) parameters. Adult human *in vitro* estimates for V_{max} and K_m were obtained from the literature[96] and scaled to corresponding *in vivo* values by accounting for GSTZ1 protein expression and the estimated liver weight of adults according to Equation 3-1 and Equation 3-2.

$$V_{max,in\ vivo} = V_{max,in\ vitro} * CPPGL * Liver\ weight \quad (3\text{-}1)$$

$$K_{m,in\ vivo} = K_{m,in\ vitro} \quad (3\text{-}2)$$

CPPGL = Cytosolic protein per gram of liver = 71 mg/g of liver[97] ;

Liver weight = 1500 g for an average 70-kg adult

After performing *IVIVC*, the calculated *in vivo* values for V_{max} and K_m were 4.6 mg/h/kg and 6.1 mg/L, respectively, which were fixed in the model. The turnover rate of free GSTZ1 enzyme was considered by accounting for natural synthesis (K_{syn}), a zero-order rate constant and degradation of the enzyme (K_{deg}), a first-order rate constant. Literature evidence[93] suggest that it takes approximately 2 months for GSTZ1 to recover to its baseline activity after inhibition by a single oral dose of DCA. This phenomenon corresponds to an estimated half-life of 0.0026 1/h (K_{deg}), which was fixed in the model. DCA-induced auto-inhibition of GSTZ1 was incorporated into the model using a function that characterizes the change in V_{max} by a first-order inactivation constant (K_{inac}).

Mathematically, this translates into the following set of differential Equations (Figure 3-3):

$$\frac{dV_{max}}{dt} = K_{syn} - K_{deg} * V_{max} - K_{inac} * \frac{V_{max} * C}{K_m + C} \quad (3\text{-}3)$$

With $V_{\max(0)} = V_{max0}$;

$V_{max0} = Starting\ maximal\ velocity\ of\ GSTZ1\ mediated\ metabolism$

$$V_{\max(t)} = V_{max0} + \int_o^t \frac{dV_{max}}{dt} \quad (3\text{-}4)$$

In this model, we are assuming that the system is at steady-state at baseline in the absence of DCA. However, when DCA is administered, a metabolite intermediate covalently binds to free GSTZ1, forming a complex that undergoes further transformation to ultimately release an inactive enzyme. This inhibitory effect is considered to be concentration-dependent, with greater extent of inhibition of GSTZ1 expected at higher concentrations of DCA. Consequently, the enzymatic activity of GSTZ1 enzyme decreases in a non-linear fashion (Equation 3-3). The residual activity at any time ($V_{max(t)}$) will depend on the duration of DCA exposure (t) and the starting GSTZ1 activity present in the population (V_{max0}) under study (Equation 3-4).

Variance model. Between subject variability (BSV) was assumed to be log-normally distributed, with a mean of zero and a variance of σ^2. Models using additive error, multiplicative error and a combination of both additive and multiplicative errors were tested to account for residual variability. Once a base model was identified, we tested the effect of covariates, such as *GSTZ1* genotype, on different model parameters by employing physiological plausibility and statistical criteria (forward inclusion: ΔOFV of 3.83 and backward exclusion: ΔOFV of 6.63). The robustness and reliability of the final model was tested based on goodness-of-fit (GOF) plots (e.g. Observations vs.

population predictions, observations vs. individual predictions, conditional weighted residuals vs. population predictions and conditional weighted residuals vs. time after last dose) and physiological meaningfulness of parameters (e.g. comparison of model-estimated parameters with other clinical studies or known information about DCA).

Development of PopPK model in children

The adult PopPK model was scaled to children using enzyme expression and activity levels[97] of GSTZ1 to scale enzymatic capacity (V_{max0}) and body weight-based scaling for central volume of distribution (V1). Other parameters, such as K_A, K_{deg} and K_{inac}, were assumed to be same between adults and children because studies to demonstrate otherwise have not been performed. These assumptions were tested quantitatively by performing model-based predictions of concentrations (median and 95% prediction intervals) in children that were overlaid with observed concentrations[86] in children. Finally, the developed PopPK model was further updated using the observed clinical data in children.

For the variance model, BSV was assumed to be log-normally distributed to identify random-effect parameters. For residual variability, a combined error model was used with both additive and proportional error components in it. The final model was identified based on goodness-of-fit plots, residual plots and physiological meaningfulness of parameter estimates.

Simulations for dose projection

Using the developed PopPK model for children, clinical trial simulations were performed and steady-state trough levels were determined for EGT carrier and EGT noncarrier children of different weights (10-60 kg). Optimal doses were then selected

based on matching of steady-state trough concentrations with the known therapeutic range of DCA (5-25 mg/L) in children[98].

Results

Data for Model Development

Adult data

Non-compartmental analysis obtained from this study[91] revealed that the plasma half-life of DCA after first dose was similar between adult EGT carriers and EGT noncarriers on day 1 (1.1± 0.5 vs 1.2 ± 0.5 h). However, the DCA half-life on day 5 was 4.5-fold lower in EGT carriers compared to EGT noncarriers (3.9 ± 1.4 vs 18.1 ± 12.1 h). These findings indicate that the half-life of DCA changes after repeated administration and that the magnitude of that change may be dependent on *GSTZ1* haplotype.

Data in children

Non-compartmental analysis of the data revealed that the half-life of DCA was higher after 6 months of exposure in both EGT carriers (5.2 ± 4.6 h) and EGT noncarriers (15.9 ± 13.1 h), compared to the DCA-naïve subjects (1.4 ± 0.4 h). After 6 months of exposure, the half-life of DCA did not change substantially until 30 months of DCA exposure in both EGT carriers and EGT noncarriers. However, in EGT carriers, there was an interesting trend of reduced plasma half-life 36 months onwards. Interestingly, it was found that the data beyond 30 months of exposure were only available in a set of twins who seem to have faster clearance compared to the rest of EGT carriers.

Modeling and Simulation

Development of adult PopPK model

A two-compartment body model (Figure 3-2) with non-linear clearance from the central compartment (V_{max}, K_m) was able to characterize the DCA PK in adults after its administration on day 1 and day 5 (Figure 3-3). However, there were slight under-predictions, mainly in the absorption phase, which can be attributed to high variability in the data. The auto-inhibitory effect of DCA on its metabolism explained the observed increase in half-life on day 5, compared to day 1, for both EGT and EGT noncarriers. *GSTZ1* genotype had a covariate effect on the clearance of DCA, because EGT noncarriers had an approximately 2-fold higher DCA-induced rate of enzyme inactivation (0.0715 1/h), compared to EGT carriers (0.0347 1/h) (Table 3-2). The total volume of distribution of DCA (V_1+V_2) was estimated to be 0.535 L/kg, which corresponds to a volume of distribution of 37.4 L in an average 70-kg adult. These data suggest that the drug was able to distribute completely in extracellular fluids along with some intracellular fluids in the body. The rate of absorption of DCA was estimated to be 0.83 1/h, which is in agreement with other clinical studies[99].

For the random effects model, between-subjects variability (BSV) was significant for $V_{max(0)}$ (24.1%), absorption rate constant (52%), V_1 (25.4%) and DCA-induced inactivation rate (20.2%). High BSV on K_A was consistent with the high variability of the data, particularly in the absorption phase. A combined error model (multiplicative + additive) was found appropriate to characterize the residual variability.

Development of a PopPK model in children

The developed adult PopPK model was successfully scaled and externally qualified in the pediatric population. There was a good agreement between the model

predictions and observations following a single dose of 1-2,-^{13}C DCA administered after 6, 12, 18, 24, 30, 36, 42, 48, 54 and 60 months of 1-2,-^{12}C DCA exposure in EGT carrier children (Figure 3-4A). However, the overlay between clinical observations and predictions in the terminal phase (clearance) was not as good beyond 30 months of exposure, because of an apparent trend for an increase in plasma clearance 36 months onwards (Figure 3-4A). Similarly, the model was able to predict the pharmacokinetics following a single dose of 1-2,-^{13}C DCA administered after 6,12,18,24, and 30 months of 1-2,-^{12}C DCA exposure in EGT noncarrier children (Figure 3-4B). However, the model predicted much lower concentrations in the absorption phase, which was particularly evident in EGT noncarriers.

The PopPK model developed on the basis of adult data was successfully fitted to the data in children (Figure 3-5) and model parameterization was updated (Table 3-2). Overall, the model captured the pediatric data well, with slight under-predictions in the absorption phase in some subjects. No trend was observed in CWRES vs PRED and CWRES vs TALD plots, indicating the suitability of the model (Figure 3-5). The model-estimated parameter values for starting metabolic capacity i.e. V_{max0}, total volume of distribution (V1+V2) and K_A were 1.95 mg/h/kg, 0.66 L/kg and 2.02 1/h, respectively. Furthermore, DCA-induced inactivation rate i.e. K_{inac} was estimated to be approximately 2-fold higher in EGT noncarrier (0.0024 1/h) compared to EGT carrier (0.0013 1/h) children.

For the random-effects model, BSV was found to be relatively high for the parameters, mainly for V_2 and CL_D. Similar to what was demonstrated in adults, a

combined error model (multiplicative + additive) was appropriate in children to characterize the residual variability.

Simulations for dose projection

Dose projections for EGT carrier and EGT noncarrier children are presented in Table 3-3. Clinical trial simulations revealed that the clearance of DCA becomes highly non-linear at doses > ~12.5 mg/kg in EGT carriers and > ~10.6 mg/kg in EGT noncarriers (Figure 3-6). In addition, a 12.5 mg/kg twice daily dose was sufficient to achieve target steady state trough concentrations (5-25 mg/L) in EGT carrier children. However, a 12.5 mg/kg dose would result in supra-therapeutic trough concentrations ranging from 44-179 mg/L in EGT noncarrier children, potentially resulting in toxicity issues with chronic exposure. Furthermore, we found that a 15% reduction in dose to 10.6 mg/kg twice daily would be optimal to achieve target steady state trough concentrations (5-25 mg/L) in EGT noncarrier children. The steady state concentrations were found to decrease non-linearly with the increasing body weight of children for both EGT carrier and EGT noncarrier children. However, this did not affect the optimal dose because the trough concentrations were still within the pre-defined therapeutic range (5-25 mg/L).

Discussion

In traditional drug development, doses for children are usually determined by extrapolating from adult data, if it is reasonable to assume that the disease progression, response to the intervention and exposure-response relationship is similar in pediatrics and adults[29,100]. In such a case, a sponsor is usually required to conduct only a PK study to select a dose to achieve similar exposure ("full extrapolation") or similar target PD effect ("partial extrapolation") as attained in adults[29,100]. For DCA, studies have

shown that steady state trough concentrations of 5-25 mg/L are correlated with the clinical efficacy of DCA in adults[101] as well in children[98]. Consequently, a full extrapolation approach coupled with existing exposure-response information in children was used to inform dosing in children. This approach also allowed us to better understand the determinants of DCA plasma clearance, separate system-specific from drug-specific parameters and explore the potential reasons for the age-dependent kinetics observed in earlier studies.

In the adult PK study[91], it was shown that the EGT carriers and noncarriers had similar half-lives after the first dose, whereas the magnitude of the increase in half-life after repeated dosing was smaller in EGT carriers (3.5-fold) than for EGT noncarriers (15-fold). This observation indicated that the clearance of DCA is a composite phenomenon, governed by three main factors: 1) the turnover rate of GSTZ1; 2) the initial GSTZ1 enzymatic capacity of the population; and 3) the DCA-induced inactivation rate of the protein[102]. We assumed the turnover rate of GSTZ1 enzyme to be same for both EGT and EGT noncarrier adults, although this assumption has not been tested experimentally. The base model accounting for natural enzyme turnover and the DCA-induced inactivation of GSTZ1 was able to explain the similar half-life estimates for EGT and EGT noncarriers on day 1. However, it failed to capture the observed differential increase in half-life due to auto-inhibition for EGT noncarriers (15-fold) and EGT carriers (3.5-fold) after 5 days of drug administration. Various possibilities were investigated to account for this interesting finding. One study[97] showed that the expression and *in vitro* enzymatic activity of GSTZ1 is similar between different GSTZ1 diplotypes. Moreover, if the enzymatic capacity was different between the 2 groups, the effect of having a lower

capacity should have resulted in lower clearance (higher half-life) estimates in EGT noncarriers after the first dose, which was not observed. The effect of DCA on GSTZ1 activity was manifested only after repeated drug administration, ruling out the possibility of different enzymatic capacity. The most likely scenario to explain this dissimilarity is that the interaction of GSTZ1 and DCA may be different between EGT carriers and noncarriers. Our results suggest that EGT noncarriers have a higher rate and extent of GSTZ1 enzyme inactivation by DCA, resulting in greater auto-inhibition and slower plasma clearance in EGT noncarriers. Because the auto-inhibition phenomenon is more likely to occur after repeated dosing, this would also explain the finding that there was no difference in half-life between EGT carriers and noncarriers after the first dose of DCA. This postulate is consistent with an *in vitro* study[103] that demonstrated that the magnitude of DCA-induced inactivation effect of *GSTZ1* is system-specific and differs between different *GSTZ1* haplotypes. Based on these findings, we hypothesize that auto-inhibition phenoconverts both EGT carriers and noncarriers into slow metabolizers after repeated DCA administration, a phenomenon known as “phenoconversion”, reported for many drugs[104-107] that are predominantly metabolized by phase I enzymes. However, the magnitude of phenoconversion is higher for EGT noncarriers, which converts them into ultra-slow metabolizers, compared to EGT carriers. Accordingly, a covariate effect of *GSTZ1* genotype on K_{inac} was able to explain the differential increase in half-life seen on day 5 of drug exposure between adult EGT carriers and EGT noncarriers.

Once developed, the PopPK model was successfully extrapolated to children using allometry and physiologically-based scaling of model parameters. The fact that

there were no significant differences in half-life[87] between adults (2.1 ± 1.5 h) and children (2.5 ± 0.4 h) after a single DCA administration indicated that the clearance of DCA is similar between these groups. This assumption is supported by an *in vitro* study[97] that showed that the age-related differences in *GSTZ1* enzyme expression and activity disappeared when activity was adjusted for expression by accounting for higher mass ratio of liver to body weight in children[108]. Hence, the body weight- based scaling of V_{max0} was justified in our model. In EGT carrier children, our model slightly under-predicted clearance, especially beyond 36 months of exposure. This was because data beyond 36 months of exposure were only available for a set of twins who seems to show faster clearance, compared to other EGT carriers. This could be an artifact, mainly because of lower sample size (N=2) after 36 months of exposure. It is also possible that, in addition to GSTZ1 genetics, there may be other yet unknown factors that can play significant roles in determining the clearance of DCA. There was also a slight mismatch between clinical observations and predictions in the absorption phase that was particularly evident in EGT noncarrier children, suggesting that the rate of absorption and/or rate of elimination may be different between adults and children. This hypothesis is supported by a much higher estimate of K_A in children compared to adults. Furthermore, the rates of DCA-induced GSTZ1 enzyme inhibition for EGT carrier and EGT noncarrier children were estimated to be 25-30 fold lower, compared to the adults indicating that the auto-inhibitory effect of DCA on GSTZ1 is much slower in children, compared to adults. This finding may explain the age dependency of DCA pharmacokinetics in children. In fact, studies[103,109] have shown that the physiological concentrations of chloride anions inhibit DCA-induced GSTZ1 inactivation and this

inhibitory effect is lower in adults compared to children. In other words, the reduced chloride-mediated inhibitory effect in adults is reflected in higher rate and extent of GSTZ1-inactivation, and hence more change in clearance after chronic DCA exposure, compared to what occurs in children. However, similar to the finding in adults, the magnitude of DCA-induced inactivation was estimated to be 2-fold higher in EGT noncarrier children, compared to EGT carrier children, which directly affects the clearance of DCA. This result suggests that dose adjustment may be needed in children, based on the presence of EGT allele. Abdelmalak *et al.*[98] showed that the steady-state DCA trough concentrations ranging from 5-25 mg/L were associated with clinical efficacy, viz. blood lactate-lowering, in children. However, concentrations above 50 mg/L were found to be associated with toxicity, as exhibited primarily as an asymptomatic, reversible peripheral neuropathy. Based on this targeted trough range, a 12.5 mg/kg twice daily dose was found optimal for EGT carrier children, while a 15% reduced dose i.e. 10.6 mg/kg twice daily dose was optimal for EGT noncarrier children. Although the trough concentrations were found to decrease non-linearly with increasing weight of children, it did not affect the respective optimal DCA doses for EGT carrier and EGT noncarrier children.

We acknowledge certain limitations to this study. Although, we were able to mechanistically quantify the differences in clearance between EGT carriers and EGT noncarriers, there still exists a large, unexplainable variability amongst EGT carrier or EGT noncarrier children. The availability of subjects with rare diseases who may be available for pharmacokinetic-pharmacodynamic assessment is limited; hence it becomes challenging to evaluate the impact of all potential covariates in such

populations. For example, in the set of twins we studied, we could not exclude the possibility that their DCA PK may have been influenced by unknown factors, in addition to GSTZ1 polymorphisms. Another limitation of this study was that the doses for children were projected on the basis of limited information[98], regarding the therapeutic range of plasma trough DCA levels (5-25 mg/L). Additional clinical studies are needed to confirm this range and/or better evaluate exposure-response relationship of DCA in children.

Conclusions

In summary, our mechanistic approach integrated information on DCA-induced GSTZ1 auto-inhibition, GSTZ1 enzyme turn over and the effect of *GSTZ1* polymorphisms into a mathematical relationship that accurately predicts PK in children following chronic exposure of DCA. The model also indicated that the observed phenotypic differences in clearance between EGT carriers and noncarriers after repeated dosing are attributable to GSTZ1 genotype-based phenoconversion. Moreover, children were found to exhibit a slower rate and extent of DCA-induced inactivation, compared to adults, which may explain the observed differences in clearance after repeated dosing between these populations. Based on clinical trial simulations, we propose that a 12.5 mg/kg and 10.6 mg/kg twice daily dose of DCA would be optimal for EGT carrier and EGT noncarrier children, respectively. Following these DCA doses, trough concentrations should be measured to ensure exposure within the targeted therapeutic range. These recommendations may be further optimized when pharmacodynamics information becomes available.

Table 3-1. Demographic characteristics of the adult[91] and pediatric population[86]

Subject	Age at Entry (yrs.)	Sex	Population	GSTZ1 genotype
EGT carrier adults				
1	24	F	Healthy	EGT/EGT
2	25	F	Healthy	EGT/EGT
3	24	M	Healthy	EGT/EGT
4	23	M	Healthy	EGT/EGT
5	26	F	Healthy	EGT/KGT
6	23	F	Healthy	EGT/KRT
7	25	F	Healthy	EGT/KRT
EGT noncarrier adults				
8	25	F	Healthy	KRT/KGT
9	37	M	Healthy	KGT/KGT
10	33	F	Healthy	KRT/KRT
11	21	M	Healthy	KRT/EGM
12*	26	M	Healthy	KGM/KGT
EGT carrier children				
1	3.7	F	PDHE1	(EGT/EGT)
2	3.7	F	PDHE1	(EGT/EGT)
3	6	M	MELAS	(EGT/EGT)
4	9.6	F	Complex I	(EGT/KGT)
5	1.5	M	Complex II	(EGT/KGT)
6	1.7	F	PDHE1	(EGT/KGT)
7	4.8	M	PDHE1	(EGT/KGT)
8	9.7	M	COX	(EGT/KGT)
9	13.1	M	MELAS	(EGT/KGT)
10	19.1	F	MELAS	(EGT/KGT)
11	1.8	F	Complex I	(EGT/KRT)
EGT noncarrier children				
12	2.7	M	PDHE1	(KGT/KGM)
13	1.2	M	OXPHOS	(EGM/EGM)
14	7.1	M	Complex I and IV	(KGT/KGT)
15	2.3	M	Complex II, III, IV	(KGT/EGM)
16	5.8	F	PDHE1	(KGT/KGT)

*This individual had a rare non-synonymous SNP in addition to rare KGM allele, excluded from the analysis

Notes:
MELAS- Mitochondrial Encephalomyopathy, lactic acidosis and stroke-like episodes;
Complex I, II, III, IV represents deficiencies in the respective complexes in the respiratory chain;
OXPHOS- Generalized reduction in respiratory chain enzyme activities;
PDHE1- Deficiency in E1 alpha subunit of pyruvate dehydrogenase (PDH) component of PDC
COX- Deficiency of Cytochrome C Oxidase

Table 3-2. Population pharmacokinetic model fitted and scaled parameters in adults and children

Parameters	Fitted adult parameters	Fitted adult parameters % BSV	Scaled children parameters	Fitted children parameters	Fitted children parameters % BSV
$V_{max(0)}$	322 mg/h Fix[96]	24.1	4.04 mg/h/kg	1.95 mg/h/kg	
K_m	6 mg/L Fix[96]		6 mg/L	6 mg/L Fix[96]	
K_{deg}	0.0026 1/h Fix[93]		0.0026 1/h	0.0026 1/h Fix[93]	
V_1	0.24 L/kg	25.4	0.24 L/kg	0.27 L/kg	25.7
V_2	0.29 L/kg		0.29 L/kg	0.39 L/kg	122.5
CL_D	3.78 L/h		3.78 L/h	0.91 L/h	143.2
K_A	0.83 1/h	52	0.83 1/h	2.02 1/h	46.4
$K_{inac(EGT\ carriers)}$	0.0347 1/h	20.2	0.0347 1/h	0.0013 1/h	69.4
$K_{inac(EGT\ noncarriers)}$	0.0715 1/h		0.0715 1/h	0.0024 1/h	
Residual Variability Estimates					
Proportional error	15.7 %		15.7 %	7.5 %	
Additive error	0.27 mg/L		0.27 mg/L	0.63 mg/L	

Table 3-3. Model informed dosing regimen of dichloroacetate for children

Recommended twice daily DCA dose (mg/kg)	
EGT carrier	EGT noncarrier
12.5	10.6

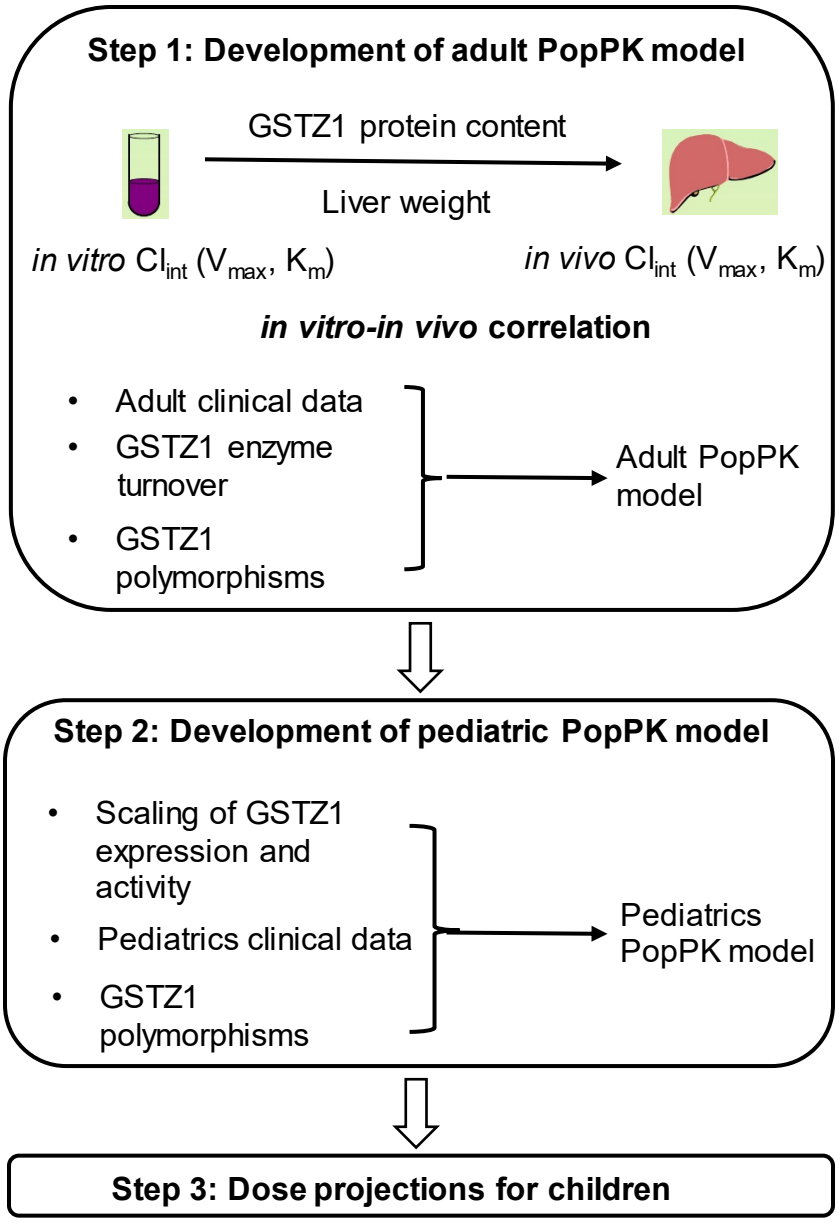

Figure 3-1. Stepwise workflow of the modeling and simulation approach

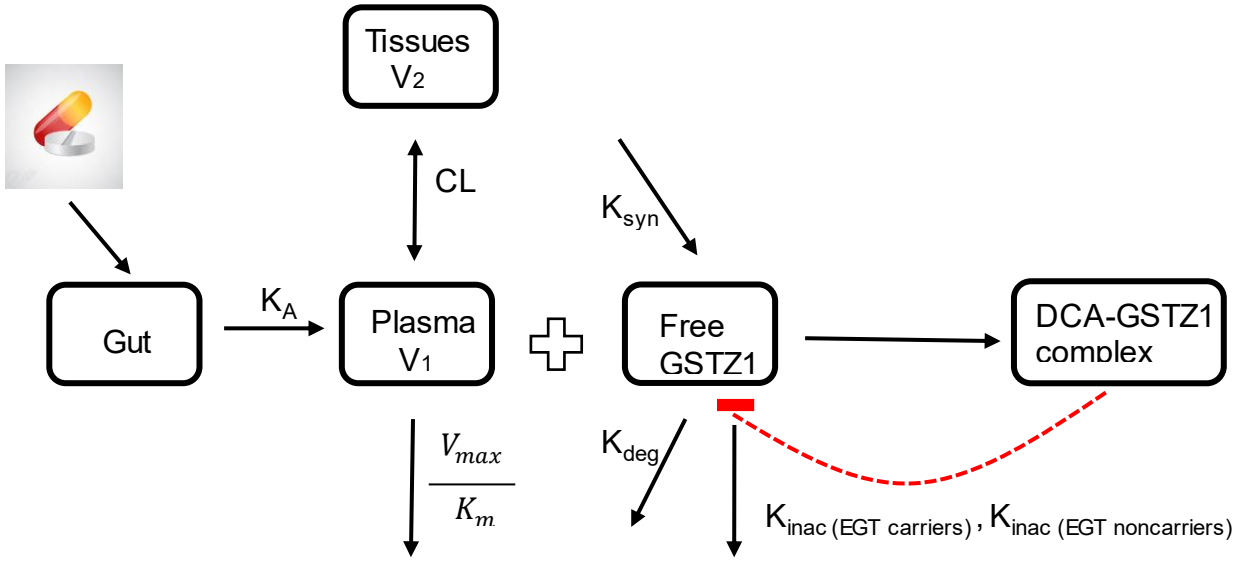

Figure 3-2. Schematic representation of the semi-mechanistic pharmacokinetic-enzyme turn over model for Dichloroacetate (DCA). K_{syn}, natural synthesis rate of GSTZ1 enzyme; K_{deg}, natural degradation rate of GSTZ1 enzyme; $K_{inac\ (EGT\ carriers)}$, DCA-induced GSTZ1-inactivation rate constant for EGT carriers; $K_{inac\ (EGT\ noncarriers)}$, DCA-induced GSTZ1-inactivation rate constant for EGT noncarriers; K_A, first-order absorption rate constant; CL_D, inter-compartmental clearance of DCA; V_{max}, maximum velocity of metabolism; K_m, affinity rate constant; V_1, volume of distribution of plasma compartment; V_2, volume of distribution of tissue compartment. DCA covalently binds to free GSTZ1 enzyme to form DCA-GSTZ1 complex which releases degraded GSTZ1 enzyme, resulting in auto-inhibition of DCA metabolism represented by dashed red line

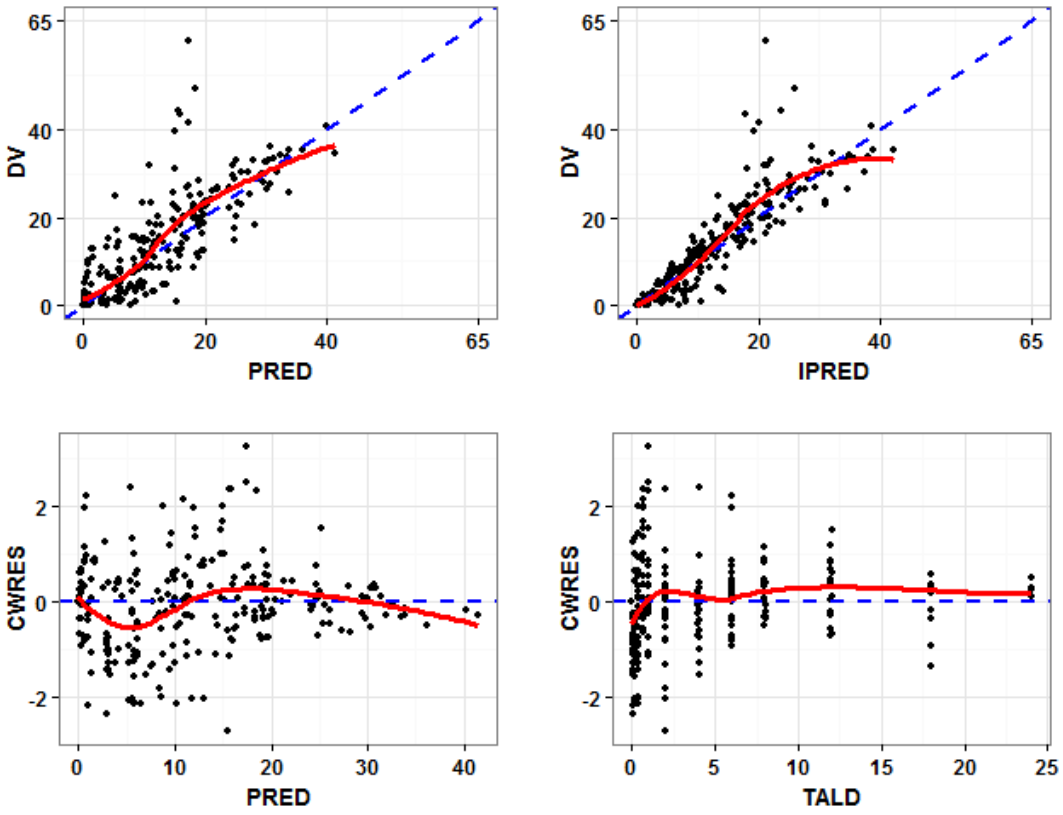

Figure 3-3. Goodness of fits plots for model fittings in EGT carrier and EGT noncarrier adults following a single oral dose of 1-2,-^{13}C DCA on day 1 and day 5. DV represent observed concentrations, PRED represent population predicted concentrations, IPRED represent individual predicted concentrations, CWRES represent conditional weighted residuals, TALD represents time after last dose, blue line represents unity line and red line represents trend line

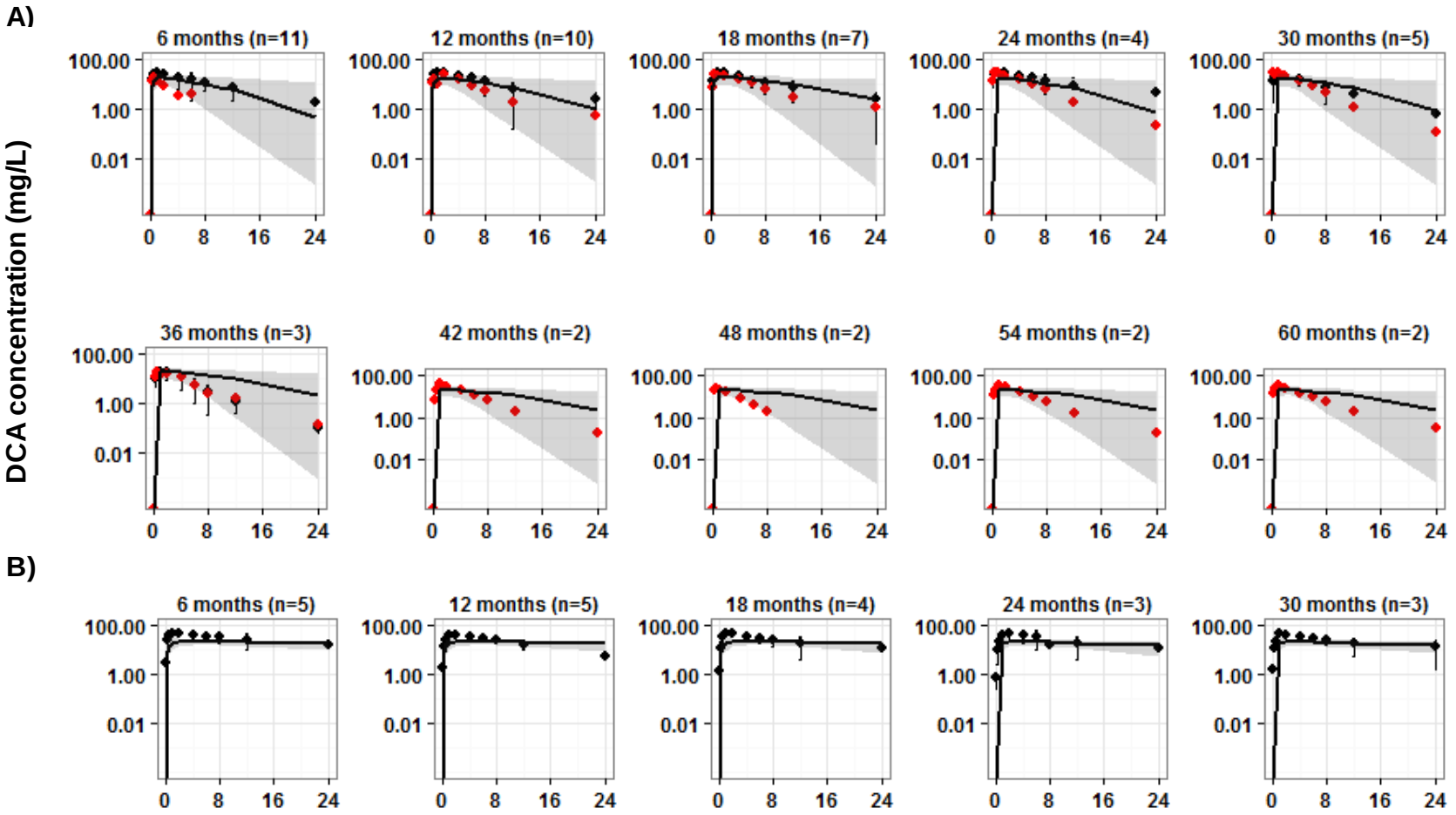

Figure 3-4. External model qualification in children. A) EGT carrier children and B) EGT noncarrier children following a single oral dose of 1-2,-13C DCA after 6, 12, 18, 24, 30, 36, 42, 48, 54 and 60 months of 1-2,-12C DCA exposure. Solid black diamonds represent observed mean DCA concentrations for all EGT carriers (including twins) along with standard deviation, solid red diamonds represent mean DCA concentrations for twins, black line represents predicted median concentration, grey bands represent 90% prediction interval and 'n' represent number of children from which the data was available (including twins)

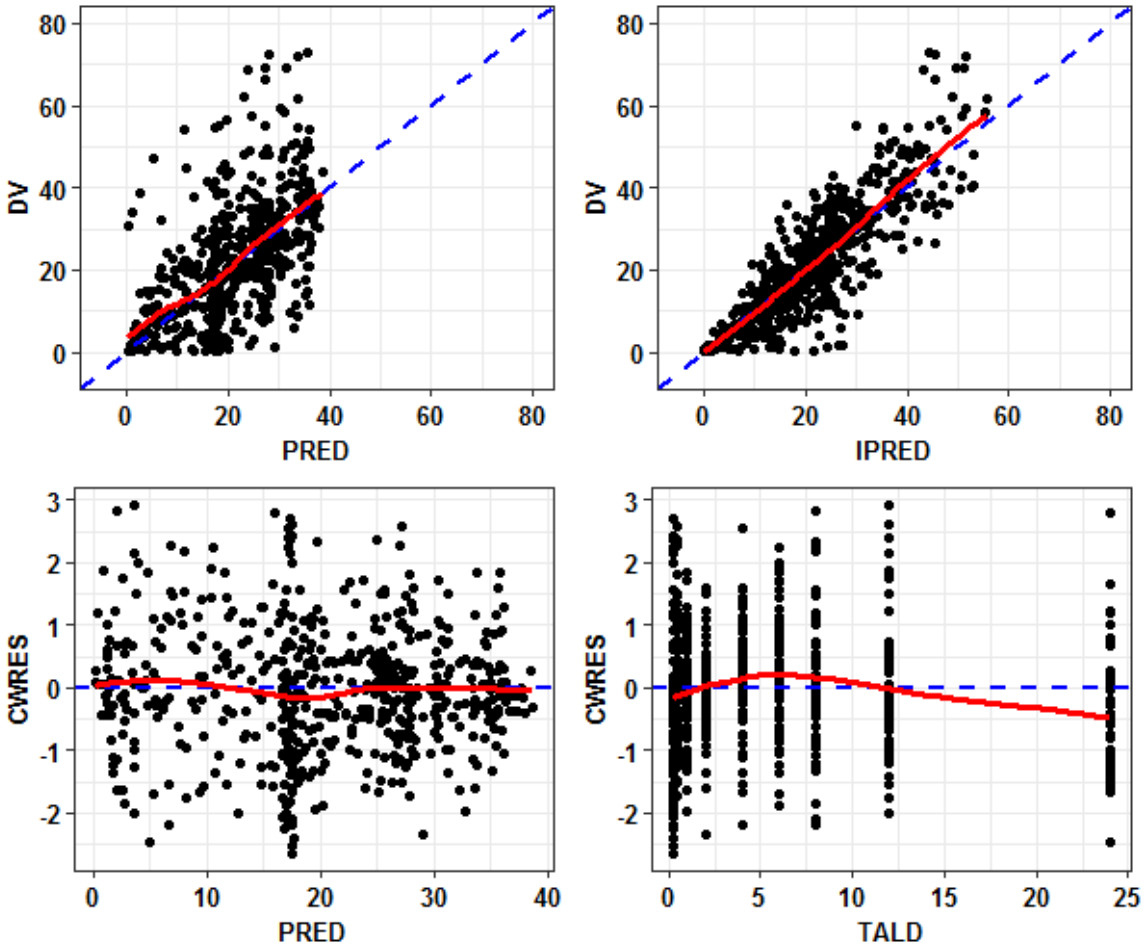

Figure 3-5. Goodness of fits plots for model fittings in EGT carrier and EGT noncarrier children following a single oral dose of 1-2, -^{13}C DCA after 6, 12, 18, 24, 30, 36, 42, 48, 54 and 60 months of 1-2, -^{12}C DCA exposure. DV represent observed concentrations, PRED represent population predicted concentrations, IPRED represent individual predicted concentrations, CWRES represent conditional weighted residuals, TALD represents time after last dose, blue line represents unity line and red line represents trend line

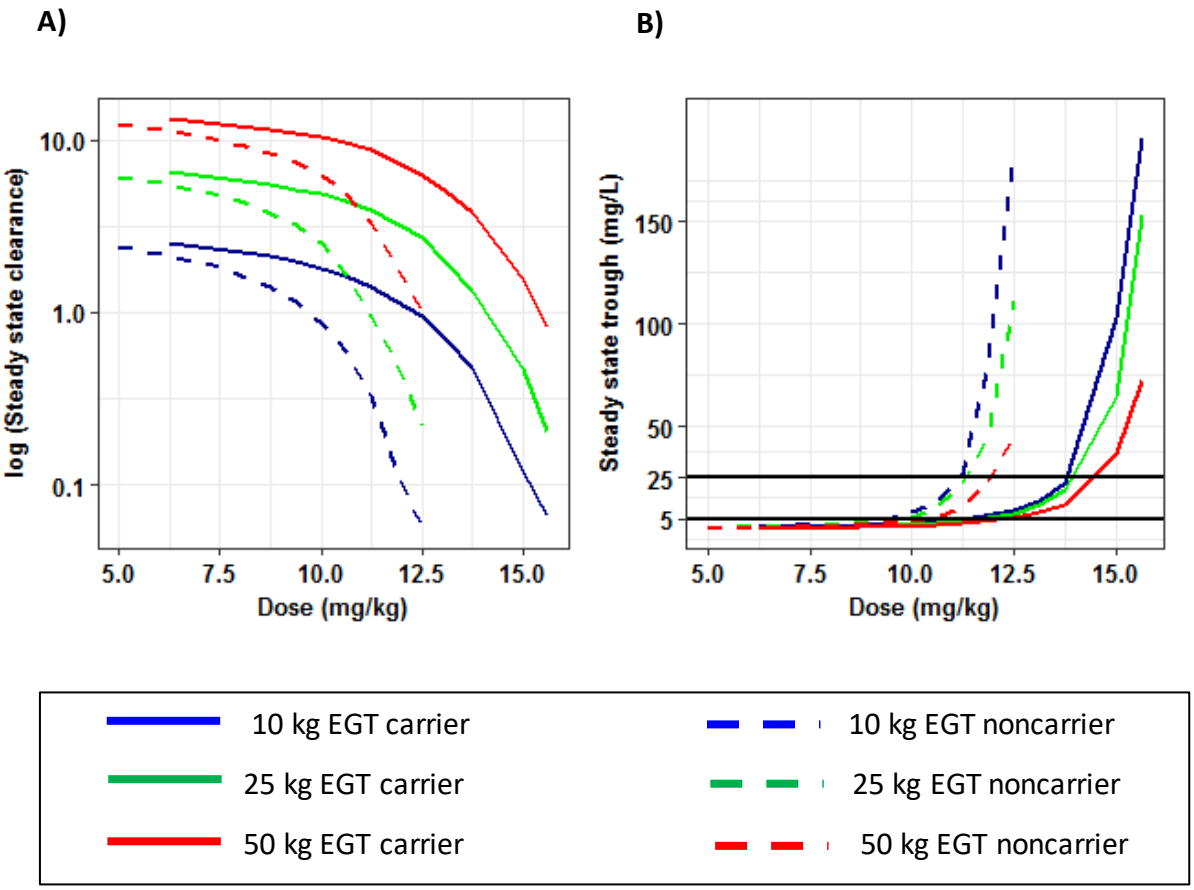

Figure 3-6. Model simulated relationships of clearance and trough concentrations with DCA dose. A) Clearance and B) Steady state trough concentrations for EGT carrier and EGT noncarrier children of different weights. Solid black lines represent the therapeutic range of DCA (5-25 mg/L) in panel B

CHAPTER 4
OPTIMIZATION OF VORICONAZOLE THERAPY FOR THE TREATMENT OF INVASIVE FUNGAL INFECTIONS IN ADULTS

Introduction

Invasive fungal infections (IFI) are common in immunocompromised patients, such as those with solid organ transplant/bone marrow transplant[9,10]. Voriconazole is a triazole, anti-fungal agent, used as a first-line of treatment for IFI, mainly caused by *Aspergillus* spp.[74] It is also effective against *Candida* spp., although it is not a first line agent for these fungal pathogens. According to the label, all patients are started on the standard dose of voriconazole (loading dose of 6 mg/kg intravenous (i.v.) infusion or 400 mg BID orally for 24 hour, followed by a 4 mg/kg i.v. or 200 mg BID oral maintenance dose)[110]. Voriconazole is metabolized non-linearly by CYP450 enzymes[12,111], mainly by CYP2C19 and it also shows a large inter-individual variability in its pharmacokinetics (PK). To ensure therapeutic concentrations are reached clinically, therapeutic drug monitoring (TDM) is widely used. Using TDM, steady state trough concentrations ($C_{trough,ss}$) are measured on day 5-7, doses are adjusted if the $C_{troug,ss}$ is not within the therapeutic range of voriconazole (2-6 mg/L). However, the delay in achieving therapeutic concentrations of voriconazole is associated with high fatality rates in critically ill patients[10]. Additionally, polymorphisms in CYP2C19 enzyme[112-114] affect the clearance of voriconazole, contributing to the large inter-individual variability observed in clinic. In healthy adults[113], *CYP2C19* polymorphisms can explain about 39% variability in clearance, following a single dose of voriconazole.

This work has been submitted for publication in Clinical Pharmacology and Therapeutics as, Mangal N, Hamadeh I, Arwood MJ, Cavallari LH, Samant TS, Klinker KP, Bulitta J, Schmidt S. “Optimization of voriconazole therapy for the treatment of invasive fungal infections in adults”.

In patients, we showed[115] that subjects with *1/*17 (Rapid metabolizers, RM) and *17/*17 (Ultra-rapid metabolizers, UM) *CYP2C19* allelic composition have, on an average, a higher prevalence of sub-therapeutic concentrations compared to *1/*1 (Normal metabolizers, NM) or *1/*2, *1/*3 (Intermediate metabolizers, IM) allelic composition at same mg/kg maintenance dose. Like *CYP2C19* polymorphisms, other variables such as drug-drug interactions, comorbidities, age, and weight can also affect voriconazole trough concentrations[116]. For instance, concomitant administration of rifampin, a CYP enzyme inducer, decreased the exposure (AUC) of voriconazole by 96%; hence contraindicated with voriconazole therapy[110]. It should be noted that, in isolation, PK is of limited meaningfulness. Hence, optimization of PK may not always translate in improved clinical outcome if the pharmacodynamics (PD) sources (e.g. MIC distributions) of variability are not evaluated. In light of these challenges, our objective was to quantitatively evaluate the effect of both PK-related- (e.g. *CYP2C19* polymorphism, drug-drug interactions, age, weight, sex, race) and PD-related- (e.g. MIC distributions of *Candida* spp. and *Aspergillus* spp.) sources of variability on the clinical outcome of voriconazole and provide dosing recommendations for voriconazole use in adults.

Materials and Methods

Patients and Data Collection

Previously, we conducted a clinical study[115] to prospectively evaluate the impact of *CYP2C19* polymorphisms on the PK of voriconazole in patients (N=81), following a standard TDM approach. Table 4-1 shows the demographics and clinical characteristics of the patient population. Majority of the patients were Caucasians (80.9%) and getting treated with pantoprazole concomitantly (70.6%). Steady state PK data was available in

68 patients (27 NM, 14 IM, 3 RM and 24 UM), excluding 1 NM patient with unphysiological peak concentration (due to a sampling error) i.e. $C_{peak,ss}$ (39 mg/L) and 1 poor metabolizer (*2/*2) patient. Exploratory analysis highlighted the significant inter-individual variability in $C_{trough,ss}$ (range=0.26-9.53 mg/L), indicating the involvement of potential covariates (Figure 4-1A). Median $C_{trough,ss}$ were lower in RM/UM group (median=1.9, 90% CI= 0.3-6.6 mg/L) compared to that of NM (median=4.6, 90% CI= 0.5-7.2 mg/L) and IM (median=4.7, 90% CI= 1.7-6.1 mg/L) group at the same mg/kg voriconazole dose (Figure 4-1B). Interestingly, there was a considerable overlap between 90% CI of RM/UM, NM and IM groups, indicating other potential sources of variability. Additionally, patients who were taking pantoprazole have higher median $C_{trough,ss}$ (median=4.5, 90% CI= 0.5-7.2 mg/L) in comparison to the patients who were not (median=1.9, 90% CI= 0.3-4.9 mg/L) (Figure 4-1C). This is consistent with the fact that pantoprazole competitively inhibits CYP2C19, resulting in higher concentrations of voriconazole.

Population Pharmacokinetic Analysis

$C_{peak,ss}$ and $C_{trough,ss}$ data obtained from the clinical study was evaluated using non-linear mixed effect modeling approach in NONMEM v.7.3. To identify a suitable structural model, one- and two- compartment models were tested using first-order conditional estimation method with interaction. Non-linear elimination of voriconazole was characterized by the Michaelis-Menten kinetic Equation as following:

$$CL = \frac{V_{max}}{K_m + C} \quad (4\text{-}1)$$

Where V_{max} (mg/h) represents maximal elimination capacity and K_m (mg/L) represents the concentration of voriconazole at which the elimination is half-maximal.

The value of K_m was fixed to 3.25 mg/L, based on an *in vitro* study[117] to provide stability to the model. This value is in agreement with the model-predicted value as reported by Dolton *et al.*[118]. Bioavailability of voriconazole is very high[116] (>=96%) and hence it was assumed to be 100% in this analysis. In the absence of rich pharmacokinetic information, characterization of absorption phase was unreliable. Hence, absorption rate constant was fixed to a value of 0.654 1/h, as reported by FDA in the briefing document[116] for voriconazole.

Inter-individual variability was assumed to be log-normally distributed and characterized using the following Equation:

$$P_{ij} = TV\left(P_j\right) \quad (4\text{-}2)$$

Where P_{ij} is the estimate of j^{th} pharmacokinetic parameter for i^{th} individual, TV (Pj) is the typical or mean value of j^{th} pharmacokinetic parameter for the population and n^{ij} is the random variable, distributed with mean of 0 and variance of ω^2 for the i^{th} individual and the j^{th} pharmacokinetic parameter.

To account for unexplained variability, various error models were tested including:

Additive error model: $C_{obs} = C_{pred} + \varepsilon$ (4-3)

Proportional error model: $C_{obs} = C_{pred} * (1 + \varepsilon)$ (4-4)

Combined error model: $C_{obs} = C_{pred} * (1 + \varepsilon) + \varepsilon_1$ (4-5)

Where ε and ε_1 are normal random variables with means of 0 and variances of σ^2 and σ_1^2, respectively.

Effect of categorical covariates such as race, sex, *CYP2C19* genotype, comorbidities was tested as a % change in V_{max} relative to that of other respective

groups. Pantoprazole is a competitive inhibitor of CYP2C19, hence its effect was estimated as a % change in K_m for pantoprazole-group relative to that of non-pantoprazole group. Effect of continuous covariates such as age and weight on V_{max} was also evaluated. A covariate effect was considered significant if it met all the following conditions: (i) Objective function value (OFV) decreased by 3.83 units for forward inclusion or 6.63 units for backward elimination of a parameter, (ii) improvement in goodness of fit plots and (iii) physiological and clinical relevance of the covariate.

Model fitting was evaluated by plotting goodness of fit plots including observed vs. population predictions, observed vs individual predictions, weighted residuals vs population predictions and weighted residuals vs. time after last dose plots. To test the robustness and reliability of the estimated parameters, bootstrapping with resampling was performed with a sample of 2000. Non-parametric statistics (median and 95% confidence interval [CI]) of pharmacokinetic parameters were compared with the point estimates obtained from the final model.

Population Pharmacokinetic-Pharmacodynamics Analysis

In NONMEM v.7.3, developed PopPK model was linked to MIC distribution data to perform 2000 Monte Carlo Simulations (MCS)[119] following standard dosing regimen of voriconazole (400 mg BID orally for 24 hours, 200 mg BID orally thereafter). $C_{trough,ss}$ were determined for all the subjects and probability of target attainment (PTA) were calculated for different pre-clinical and clinical PK/PD indices of efficacy for voriconazole (i) PTA1-Probability of achieving $C_{trough,ss}$ >2 mg/L (clinical)[115], the most commonly used index (ii) PTA2-Probability of achieving $fAUC_{24}$/MIC ≥25 (pre-clinical)[120], (iii) PTA2-Probability of achieving $C_{trough,ss}$/MIC >2 (clinical)[121]. Details on calculation of these probabilities are presented below:

$$PTA1 = \frac{Number\ of\ subjects\ achieving\ \ C_{trough,ss} > 2}{2000}\ X\ 100 \quad (4\text{-}6)$$

$$PTA2 = \frac{Number\ of\ subjects\ achieving\ fAUC_{24}/MIC \geq 25}{2000}\ X\ 100 \quad (4\text{-}7)$$

$$PTA3 = \frac{Number\ of\ subjects\ achieving\ C_{trough,ss}/MIC > 2}{2000}\ X\ 100 \quad (4\text{-}8)$$

The results of MCS were also expressed in terms of Cumulative Fraction of Response (CFR) which is defined as "the expected population probability of target attainment for a specific drug dose and a specific population of microorganisms"[122], calculated according to the following Equation 4-9:

$$\text{CFR (\%)} = \sum_i^n PTA_i * N_i \quad (4\text{-}9)$$

Where PTA_i is the probability of target attainment at MIC of '*i*' and N_i is the fraction of isolate susceptible at MIC of '*i*'.

In our study[115], data on susceptibility of fungal isolates were not available. Hence, MIC distributions for 4 *Aspergillus* spp. (*A. fumigatus, A. niger, A. terreus, A. flavus*) and 11 *Candida* spp. (*C. albicans, C. dubliniensis, C. famata, C. glabrata, C. guilliermondii, C. kefyr, C. krusei, C. lusitaniae, C. parapsilosis, C. pintolopesii, C. tropicalis*) were obtained from European Committee on Antimicrobial Susceptibility Testing (EUCAST)[35] database (Figure 4-2).

PTA and CFR were calculated following the standard maintenance dose of voriconazole (200 mg BID orally) as well as higher maintenance doses of voriconazole i.e. 250, 300, 350, 400, 450, 500, 600 mg BID orally. Probabilities of adverse events such as visual adverse event (VAE) and liver function abnormalities (aspartate transaminase (AST) elevation, alkaline phosphatase (ALP) elevation and bilirubin elevation) were calculated for different voriconazole doses using published

relationships[123]. Optimal doses of voriconazole were selected using a benefit-risk analysis of probabilities of efficacy and adverse events.

Results

Population Pharmacokinetic Analysis

A one-compartment body model with first-order absorption and Michaelis-Menten elimination adequately described the clinical data. Individual predicted voriconazole concentrations were in good agreement with the observed concentrations (Figure 4-3). However, there was a wider spread of population predictions and observations, consistent with the high inter-individual variability associated with the voriconazole use. Involvement of other covariates outside of those measured and tested in this dataset is plausible. Plots of conditional weighted residual and population predictions, conditional weighted residual and time after dose indicated the normal distribution of residuals and most of the values were within 2 standard deviations (Figure 4-3). A two-compartment model did not improve the goodness of fit plots significantly. Inter-individual variability was found significant for V_{max} (56.4%). Given the sparsity of the data, an additional inter-individual variability parameter on V_2 was not supported. A proportional error model was found appropriate to characterize the unexplained variability. Covariate analysis indicated that CYP2C19 phenotype and pantoprazole-use significantly affect the clearance of voriconazole. NM and IM were not found to be statistically significant from each other while V_{max} in RM/UM was estimated to be 29% higher than that of NM/IM (Table 4-2). Similarly, K_m for the pantoprazole group was estimated to be 79% higher compared to that of non-pantoprazole group. Both of these covariates resulted in assignment of patients into 4 different phenotypes-NM/IM non-pantoprazole, NM/IM pantoprazole, RM/UM non-pantoprazole and RM/UM pantoprazole. Other covariates,

such as age, weight, sex, comorbidities, were not found to be significant. The volume of distribution of voriconazole was estimated to be 291 L (Table 4-2), which is in agreement with the value of 4 L/kg reported by FDA in the briefing document[116] on voriconazole. All of the parameters were estimated with a reasonable precision, considering the sparsity of the analyzed data.

Bootstrap analysis showed that 80% of the runs were successfully converged for the final model. The point estimates of the final model were similar to the mean values obtained from bootstrapping method and all of them fell within the 95% CI (Table 4-2). However, the CI were wide for V_2 (4-fold) and pantoprazole effect on K_m (13-fold) consistent with the high % relative standard error (RSE) associated with these parameters (Table 4-2).

Population Pharmacokinetic-Pharmacodynamics Analysis

Following a standard dose of 200 mg BID oral voriconazole, both pre-clinical ($fAUC_{24}$/MIC ≥25) (Figure 4-4A) and clinical ($C_{trough,ss}$/MIC >2) (Figure 4-4B) PK/PD index of efficacy yield similar PTA for all the phenotypes of voriconazole. Below MIC of 0.12 mg/L, all phenotypes (NM/IM non-pantoprazole, NM/IM pantoprazole, RM/UM non-pantoprazole and RM/UM pantoprazole) are expected to show ≥90% PTA, with insignificant differences amongst them (Figure 4-4B). At MIC >0.12 mg/L, the PTA is lowest for RM/UM non-Pantoprazole (Figure 4-4B), while it is highest for NM/IM Pantoprazole. For instance, at a MIC of 1 mg/L, 23.3% RM/UM non-pantoprazole, 39.9% NM/IM non-Pantoprazole, 46.5% RM/UM Pantoprazole and 64.9% NM/IM pantoprazole patients will achieve the target (Figure 4-4B). Furthermore, PTA was lower in RM/UM compared to NM/IM patients in both pantoprazole and non-pantoprazole use groups. Pantoprazole improves the PTA by approximately 25%, for both RM/UM and

NM/IM patients. Overall, 43.6% patients will achieve the target following standard 200 mg BID oral dose of voriconazole at MIC of 1 mg/L, irrespective of the phenotype (Figure 4-4B). These probabilities are consistent with those predicted with PK/PD index of $C_{trough,ss}$>2 (Table 4-3).

Susceptibility of *Candida spp.* against voriconazole was higher than *Aspergillus spp.* as MIC distributions for *Candida spp.* were shifted to left (MIC<1 mg/L) compared to distributions of *Aspergillus spp.* (Figure 4-2). CFR was greater than 80% for most of the *Candida* spp. except *C. krusei* (Figure 4-5A) while it was approximately 40-70% for *Aspergillus* spp. (Figure 4-5B), following a standard 200 mg oral voriconazole dose. The phenotypic differences due to *CYP2C19* polymorphisms and pantoprazole-use were not pronounced in case of *Candida* spp. (Figure 4-5A), unlike *Aspergillus* spp. (Figure 4-5B). Irrespective of *Aspergillus spp.*, CFR was highest for NM/IM pantoprazole, followed by RM/UM pantoprazole, NM/IM non-pantoprazole and RM/UM non-pantoprazole phenotype (Figure 4-5B).

Supplementary Figure 4-6 shows the respective probabilities of efficacy (CFR) and safety (VAE) for all phenotypes and *Aspergillus* spp. with voriconazole dose. For *A. fumigatus*, the most frequent cause of *Aspergillus* spp. infections, 200 mg dose resulted in a delta of only 27.8%, 43.5%, 52.9% and 61.8% for RM/UM non-pantoprazole, NM/IM non-pantoprazole, RM/UM pantoprazole and NM/IM non-pantoprazole phenotypes, respectively (Figure 4-7). At proposed 500 mg, 400 mg, 400 mg and 300 mg doses (Figure 4-8), these deltas increase to 61.6%, 63.5%, 66.4% and 66.7% for RM/UM non-pantoprazole, NM/IM non-pantoprazole, RM/UM pantoprazole and NM/IM pantoprazole phenotypes, respectively (Figure 4-7). For harder to treat *A. terreus* infections, the

deltas increase from 5.8%, 19.7%, 25.2% and 39.9% to 51%, 52.5%, 56.2% and 58.2% at proposed 600 mg, 450 mg, 450 mg and 400 mg doses for RM/UM non-pantoprazole, NM/IM non-pantoprazole, RM/UM pantoprazole and NM/IM pantoprazole phenotypes, respectively (Figure 4-7 and Figure 4-8). Similar trends could be noticed for *A. niger* and *A. flavus* infections (Figure 4-7 and Figure 4-8). Other benefit-risk analysis revealed that the relationship of voriconazole dose with other AEs such as bilirubin elevation (Figure 4-9), AST or ALP elevation was shallow and did not affect the dose selection.

Based on our analysis, we have provided dosing recommendations for 2 main clinical scenarios: 1) Reactive dose adjustment for existing/suspected infection (Figure 4-10) and (2) Prospective dose optimization for subjects undergoing "high-risk procedures" such as organ transplant surgery (Figure 4-11). In other words, we have distinguished between intend-to-treat and intent-to-prevent scenarios. In scenario 1 (Figure 4-10), patients infected with *Candida* spp. and *Aspergillus* spp. infections should be started on a standard loading dose and the susceptibility of fungal isolates to voriconazole be tested. While label-recommended doses can be used prior to the availability of the susceptibility testing results, further dosing regimen should take the pathogen's susceptibility to voriconazole into consideration. For *Candida* spp. infections, the label-recommended maintenance dose of 200 mg voriconazole should be sufficient for all patients. In contrast, voriconazole doses need to be increased for patients with *Aspergillus* spp. infections. The magnitude of this increase depends on the *CYP2C19* genotype and co-administration of pantoprazole. TDM approach should be adopted when CYP2C19 genotype or susceptibility of infection is unknown. In scenario 2 (Figure 4-11), patients who are at risk for infections such as those undergoing liver/bone

marrow transplantation, should be genotyped for CYP2C19 *a priori*. If these patients are infected post-transplantation, the results from CYP2C19 genotyping can then be used to optimize steady state exposure of voriconazole early on, depending on the susceptibility of pathogen.

Discussion

According to the FDA-approved label[110] of voriconazole, a standard maintenance dose of 4 mg/kg i.v or 200 mg oral BID dose of voriconazole should be sufficient to achieve therapeutic concentrations. Although the label appreciates that patients with *2,*3 *CYP2C19* allelic variant have 4-fold higher exposure than the ones with wild-type *1 allele, no such information is shown for the patients harboring *17 *CYP2C19* allelic variant. Consequently, no specific dose adjustment for *CYP2C19* polymorphisms has been proposed. Clinical Phamacogenomics Implementation Consortium (CPIC) guidelines[124] for voriconazole acknowledge that the PTA at standard voriconazole dose is very small and therapy should be avoided in UM and RM patients. The risk of treatment failure due to sub-therapeutic levels or toxicities associated with elevated concentrations, is mitigated via TDM in clinical practice[125,126]. However, TDM-based dose optimization relies on the attainment of steady state PK of voriconazole which can take up to 5-7 days. This delay of 5-7 days in achieving therapeutic concentrations can be detrimental to critically ill patients[10]. To complement TDM approach, model-informed approaches[127-129] have been used to provide an estimate of starting maintenance dose to maximize the likelihood of steady state therapeutic concentrations. However, the effect of *CYP2C19* polymorphisms, mainly *17 allelic variant and pantoprazole use in light of PD-related sources of variability, on the maintenance dose have not been studied extensively. Moreover, studies have looked at the optimal dose from an efficacy

point of view; risks associated with dose escalation have not been considered quantitatively. In this study, we quantified both PK- (*CYP2C19* polymorphism, pantoprazole-use) and PD- (MIC distributions) related sources of variability and made clinical recommendations for the optimization of voriconazole therapy, considering benefits and risks associated with dose adjustment.

CYP2C19 genotype and pantoprazole use were significant covariates in the model. RM/UM were predicted to have 29% higher V_{max} compared to NM/IM phenotypes. No differentiation between RM and UM was possible due to very small number of patients in the UM group (N=4). Similarly, patients who were on pantoprazole were predicted to have 79% higher K_m compared to those who were not. Although there are studies[112,130,131] studying the impact of poor metabolizer CYP2C19 phenotype (*2, *3) on the pharmacokinetics of voriconazole, studies[15,16,118] focusing on RM/UM are limited. To the authors' knowledge, this is the first study which has quantified the changes in steady state clearance of voriconazole due to *17 *CYP2C19* genotype as well as pantoprazole use and translated those findings into an optimal dose recommendation. Pantoprazole is a weak inhibitor of CYP2C19 compared to other proton pump inhibitors (PPI) such as omeprazole *in vitro*[132]. However, *in vivo* studies[26,133,134] show that pantoprazole use can lead to a significant increase in $C_{trough,ss}$ of voriconazole. Moreover, benefit from TDM of voriconazole were greater in the patients who were co-treated with PPI at dosages≥40 mg intravenously[26]. These findings agree with our analysis which shows that pantoprazole use significantly increases the PTA in both NM/IM and RM/UM phenotypes.

For voriconazole, different PK/PD indices have been used as predictor of clinical efficacy. In a neutropenic murine model of disseminated candidiasis[120], *f*AUC$_{24}$/MIC correlated well with the clinical efficacy of voriconazole. However, the relationship of *f*AUC$_{24}$/MIC with efficacy has not been confirmed in human studies. In clinical practice, it is easier to measure $C_{trough,ss}$ than AUC and adjust the dose accordingly. Attainment of $C_{trough,ss}$ as low as 1 mg/L ($C_{trough,ss}$>1)[14] and as high as 2 mg/L ($C_{trough,ss}$>2)[135-137] has been found to correlate with clinical efficacy. Interestingly, an observational study[121] showed that consideration of MIC along with $C_{trough,ss}$ i.e. $C_{trough,ss}$/MIC>2 better correlates with efficacy and hence serves as a suitable PK/PD index of efficacy for voriconazole. In our analysis, we found that both *f*AUC$_{24}$/MIC and $C_{trough,ss}$/MIC>2 yield similar probability of target attainment (Figure 4-4A and Figure 4-4B). However, probabilities associated with $C_{trough,ss}$>2 index (Table 4-3) would not be same as those with *f*AUC$_{24}$/MIC and $C_{trough,ss}$/MIC>2 index except at MIC of 1 mg/L. Dose optimization based on $C_{trough,ss}$>2 may not be optimal for pathogens with MIC less than or greater than 1. Hence, the choice of using human-data driven and MIC-based PK/PD index i.e. $C_{trough,ss}$ /MIC>2 over animal model-derived index i.e. *f*AUC$_{24}$/MIC and non-MIC based index i.e. $C_{trough,ss}$ >2 for dose optimization is well justified.

Our analysis revealed that the CFR value for *Candida spp.* infections is ≥80% at a standard 200 mg voriconazole BID dose, indicating that 200 mg dose would be sufficient for all voriconazole phenotypes against these infections. Conversely, infections due to *Aspergillus spp.* are much harder to treat as their susceptibility towards voriconazole is comparatively less than *Candida spp.* Consequently, doses>200 mg were needed to achieve therapeutic concentrations in different voriconazole

phenotypes. However, voriconazole dose increase is significantly associated with adverse events such as VAE, followed by liver function test abnormalities (AST, ALP and bilirubin elevation) in patients[123]. These adverse events are transient and reversible[138,139] following discontinuation of voriconazole therapy. As expected, RM/UM non-pantoprazole patients were at most risk for therapeutic failure of voriconazole. A voriconazole dose of 500 mg BID provided an optimal trade-off between efficacy and safety for RM/UM non-pantoprazole patients, for treatment of *A. fumigatus* infections (Figure 4-7). However, for less sensitive *A.flavus*, *A. niger* and *A. terreus* infections, higher doses up to 600 mg were needed to maximize the overall benefit, for RM/UM non-pantoprazole patients. Dose adjustments in other phenotypes and *Aspergillus* spp. infections also resulted in optimization of overall benefit of therapy. At proposed doses, probability of bilirubin elevation only increases by 5% compared to the label-recommended 200 mg dose, not found to be critical for dose selection. Projected doses are in line with a retrospective study[140] which found that a 4 mg/kg (280 mg for a 70 kg adult) and 6.75 mg/kg (475 mg for a 70 kg adult) voriconazole dose was required to achieve target concentrations in CYP2C19 RM and UM phenotypes, respectively. Given the reversible nature of adverse events associated with voriconazole, as opposed to the detrimental effects of treatment failure, benefits associated with dose escalation may outweigh the risks in long term[141].

Conclusions

In conclusion, a standard dose of 200 mg voriconazole would be optimal for all phenotypic groups of patients in case of *Candida spp.* infections, however, dose should be adjusted based on patients' phenotype in case of *Aspergillus spp.* infections. It could be argued that TDM can also provide the same answer. Furthermore, an additional PK

sample on day 2-3 can also help in early dose adjustment, improving the utility of TDM. Hence, the utility of proposed approach lies more when *CYP2C19* genotype and MIC data can be readily available for the patients at the time of treatment. Also, *CYP2C19* genotyping should be performed *a priori* for organ transplant patients who are at risk for IFI, to avoid a genotype mismatch, post-transplantation. In the end, it cannot be a TDM vs genotype scenario, rather genotype should complement TDM in order to optimize the clinical outcome. Proposed approach allows clinicians to identify patients, at risk for efficacy and adjust dose based on *CYP2C19* genotype, pantoprazole-use and MIC, early in the time course of therapy. It also helps to identify the patients where frequent TDM may not be required as in case of *Candida spp.* infections, reducing the time and resources required for patient care.

Table 4-1. Demographics and clinical characteristics of patients included in the analysis. Table adapted from Hamadeh *et al*.[115]

Characteristic	Value* (n=68)
Age (years)	53.1 ± 17.9
Weight (kg)	68.9 ± 15
Male sex	41 (60.3)
Race	
Caucasian	55 (80.9)
African American	11 (16.2)
Asian	2 (2.9)
CYP2C19 phenotype	
Normal metabolizers	27 (39.7)
Intermediate metabolizers	14 (20.6)
Rapid Metabolizers	24 (35.3)
Ultra-rapid metabolizers	3 (4.4)
Concomitant medications	
Pantoprazole	48 (70.6)
Comorbidities	
Hematopoietic stem cell transplant	20 (29.4)
Hematologic malignancies	22 (32.4)
Solid organ transplant	12 (17.6)
Other	14 (20.6)

*Mean ± SD or Number (%)

Table 4-2. Population parameter estimates along with bootstrap intervals obtained from final population pharmacokinetic model

Parameters	Units	Pop. mean (% RSE)	Bootstrap median (95% PI)
$V_{max, EM/IM}$	mg/h	48.4 (17)	47.7 (30.9 - 60.1)
$V_{max, UM}$	mg/h	62.4 (12)	60.8 (46.6 - 78.5)
K_m	mg/L	3.35 Fix[117]	
Effect on K_m		0.79 (60)	0.8 (0.14 - 1.9)
V_2	L	291 (46)	271.3 (97 - 466.9)
K_A	1/h	0.654 Fix[116]	
	Between subject variability (BSV)		
$V_{max, EM/IM/UM}$	%	56.4 (41)	50.9 (17.6 - 91.9)
	Residual variability		
Proportional error	%	34.7 (17)	33.9 (23.3 - 54.1)

Table 4-3. Probability of target attainment for different phenotypes of voriconazole determined using Ctrough,ss>2 as the PK/PD index of efficacy, following standard dose of 200 mg BID voriconazole

Phenotype	PTA1 (%)
RM/UM non-pantoprazole	23.2
NM/IM non-pantoprazole	39.9
RM/UM pantoprazole	46.5
NM/IM pantoprazole	64.9
Overall	43.6

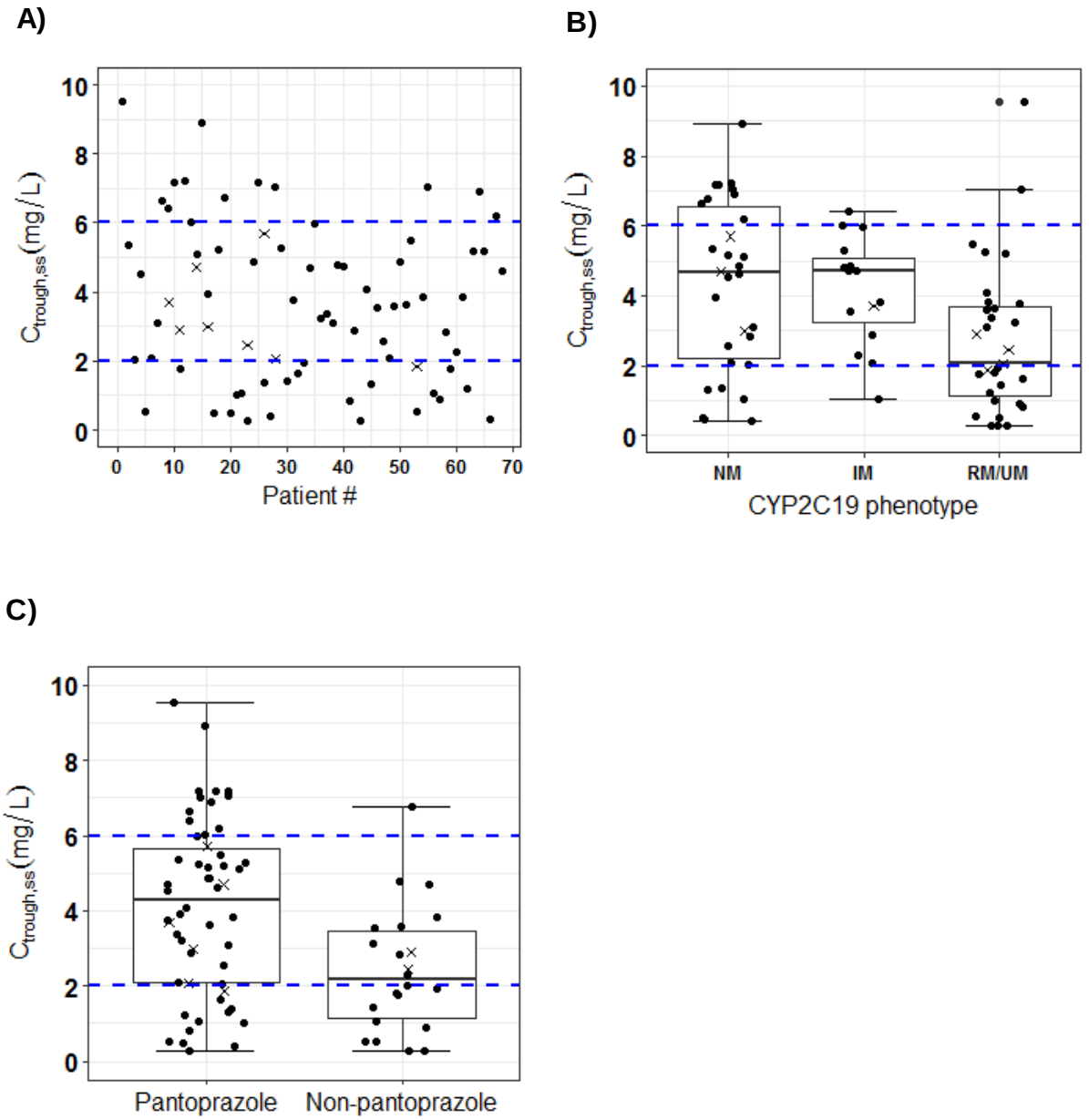

Figure 4-1. Voriconazole pharmacokinetic sources of variability. A) Steady state trough concentrations ($C_{trough,ss}$) in all the patients. B) $C_{trough,ss}$, stratified by CYP2C19 phenotype. C) $C_{trough,ss}$, stratified by pantoprazole use. Filled circles and cross symbols represents the $C_{trough,ss}$ obtained before and after the dose adjustment following TDM, respectively. Dashed blue line indicates the therapeutic range of voriconazole (2-6 mg/L)

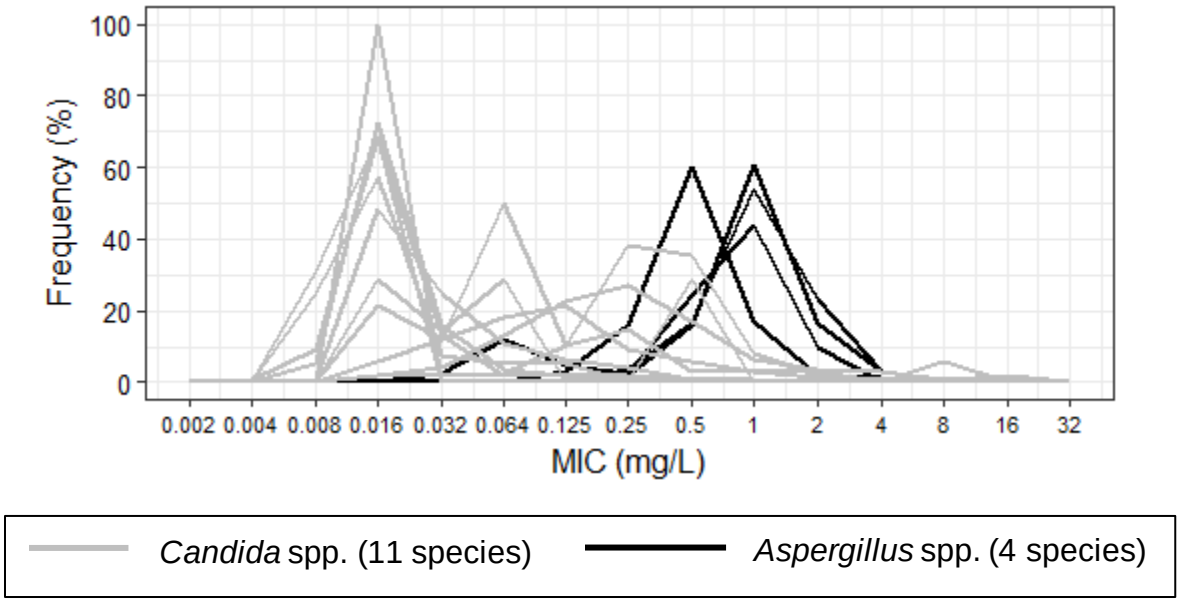

Figure 4-2. Voriconazole pharmacodynamic sources of variability: PD variability in MIC distributions of voriconazole against 4 *Aspergillus* spp. (*A. fumigatus, A. niger, A. terreus, A. flavus*, represented by black lines) and 11 *Candida* spp. (*C. albicans, C. dubliniensis, C. famata, C. glabrata, C. guilliermondii, C. kefyr, C. krusei, C. lusitaniae, C. parapsilosis, C. pintolopesii, C. tropicalis*, represented by grey lines) as obtained from EUCAST database

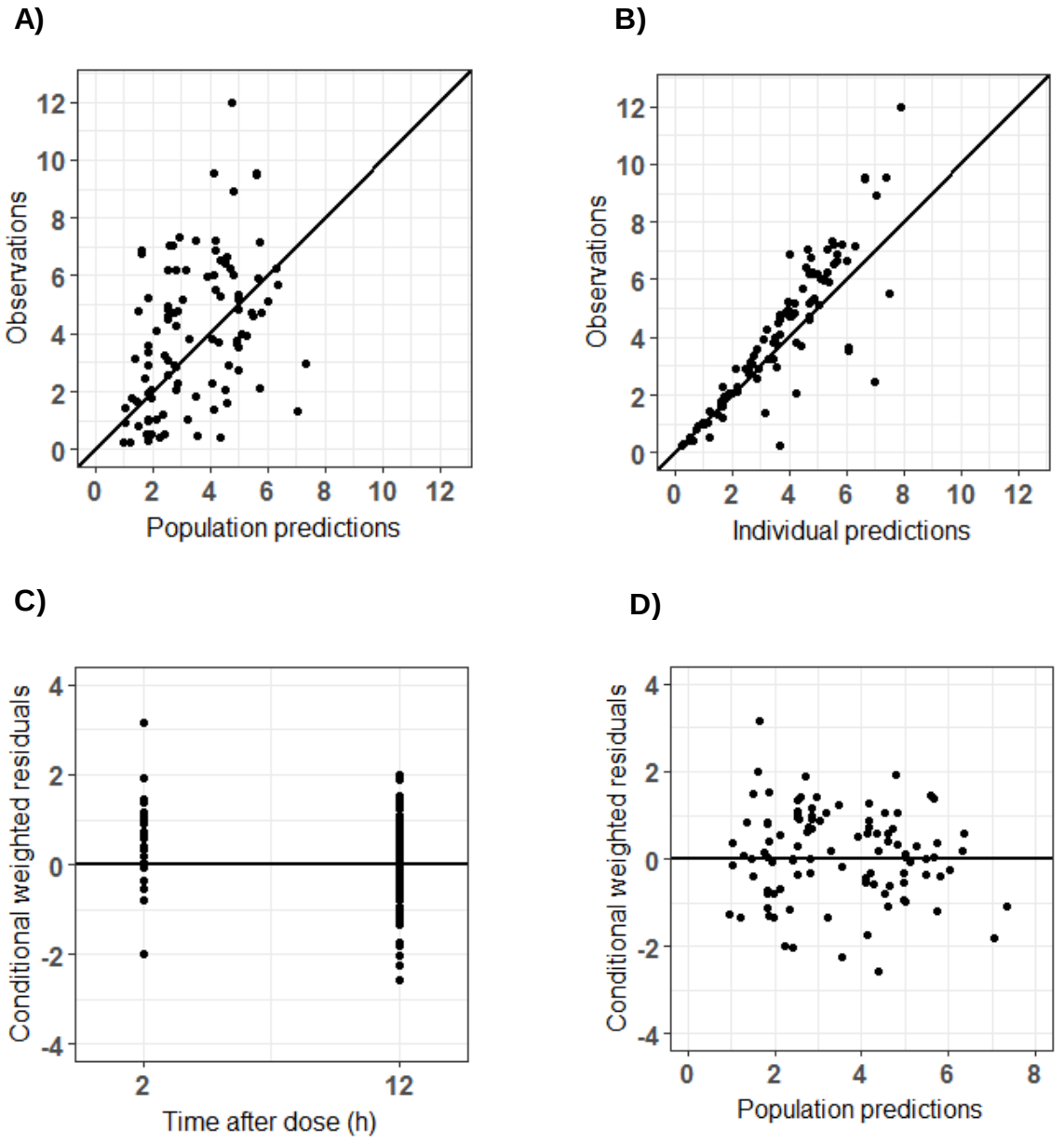

Figure 4-3. Goodness of fit plots for the final population pharmacokinetic model. A) Population predictions vs. observations. B) Individual predictions vs observations. C) Conditional weight residuals vs. population predictions. D) Conditional weighted residual vs. time after dose. Black line represents unity

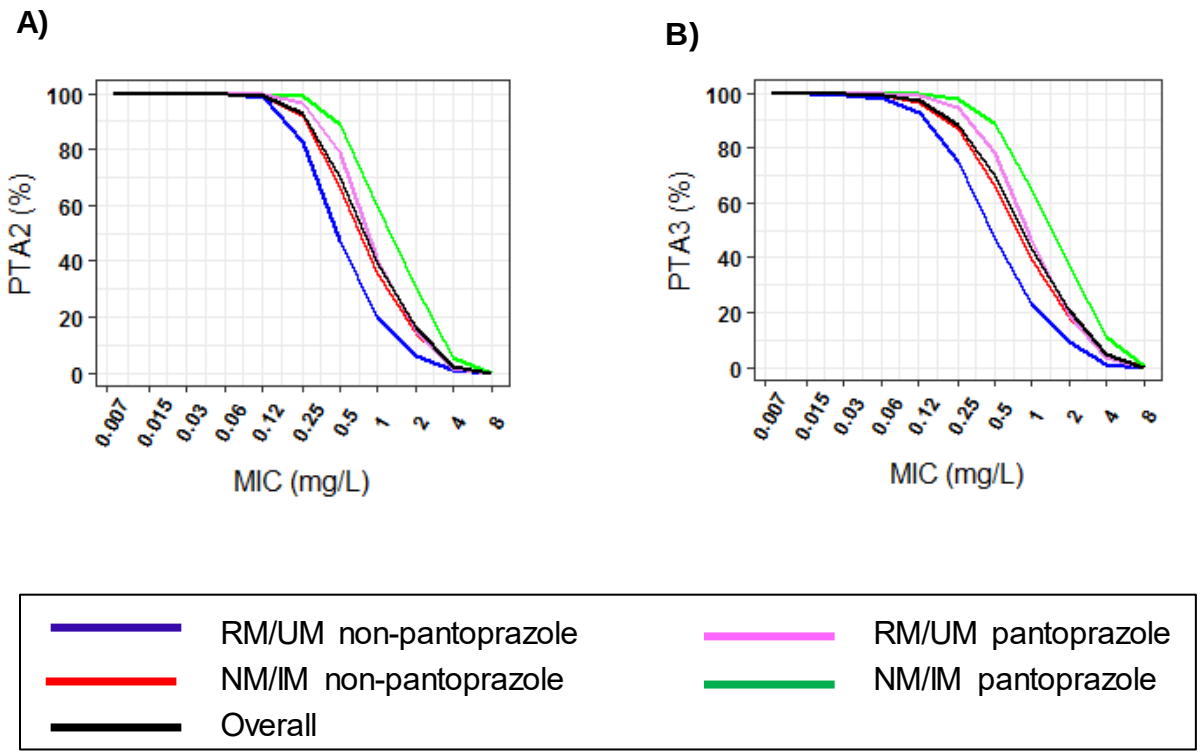

Figure 4-4. Probability of target attainment (PTA) following label-recommended dosing regimen of voriconazole (200 mg BID). A) PTA2-Probability of achieving *f*AUC24/MIC ≥25 (pre-clinical). B) PTA3-Probability of achieving $C_{trough,ss}$/MIC >2 (clinical)

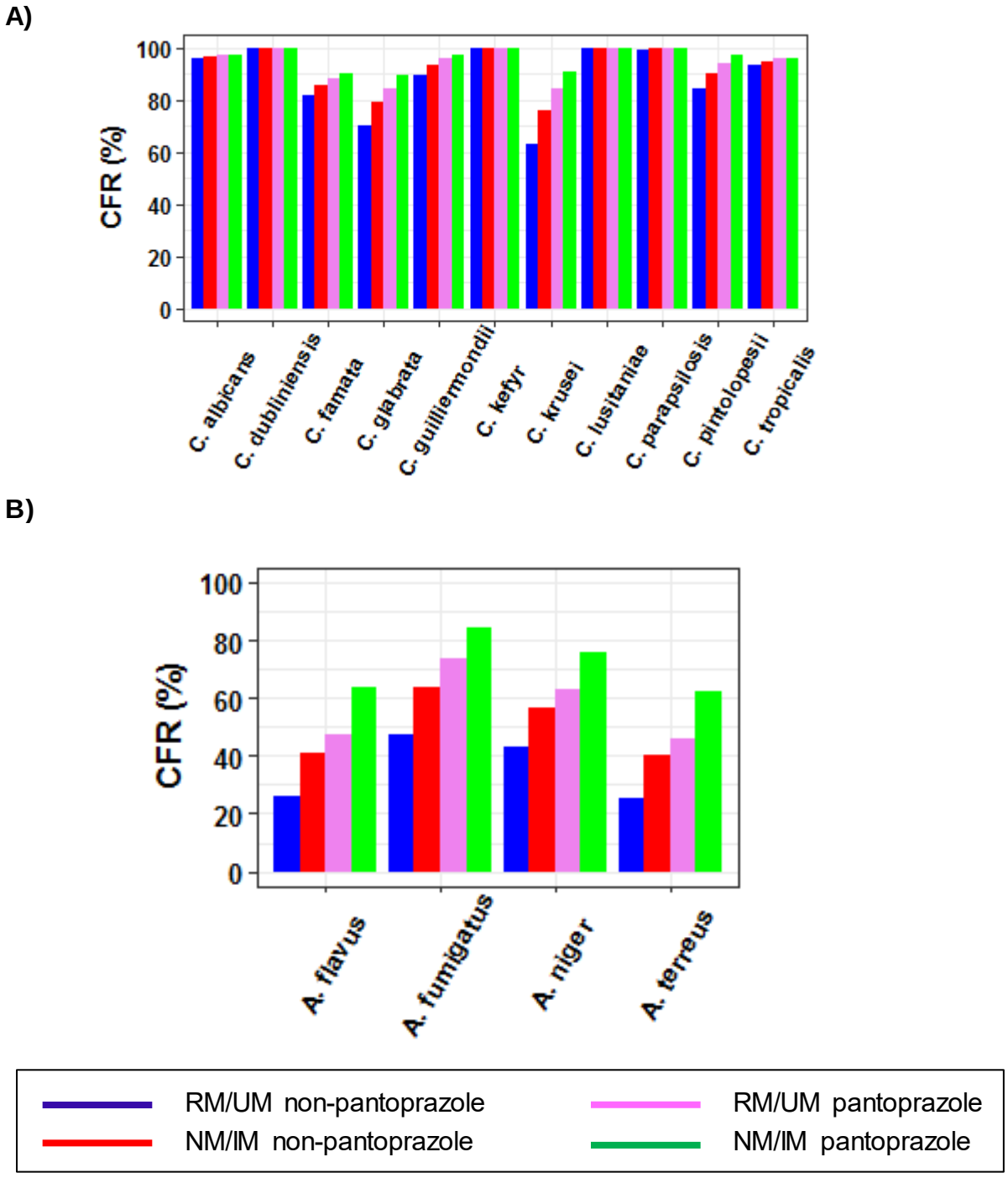

Figure 4-5. Cumulative fraction of response (CFR) following label-recommended dosing regimen of voriconazole (200 mg BID) against A) *Candida* spp. B) *Aspergillus* spp.

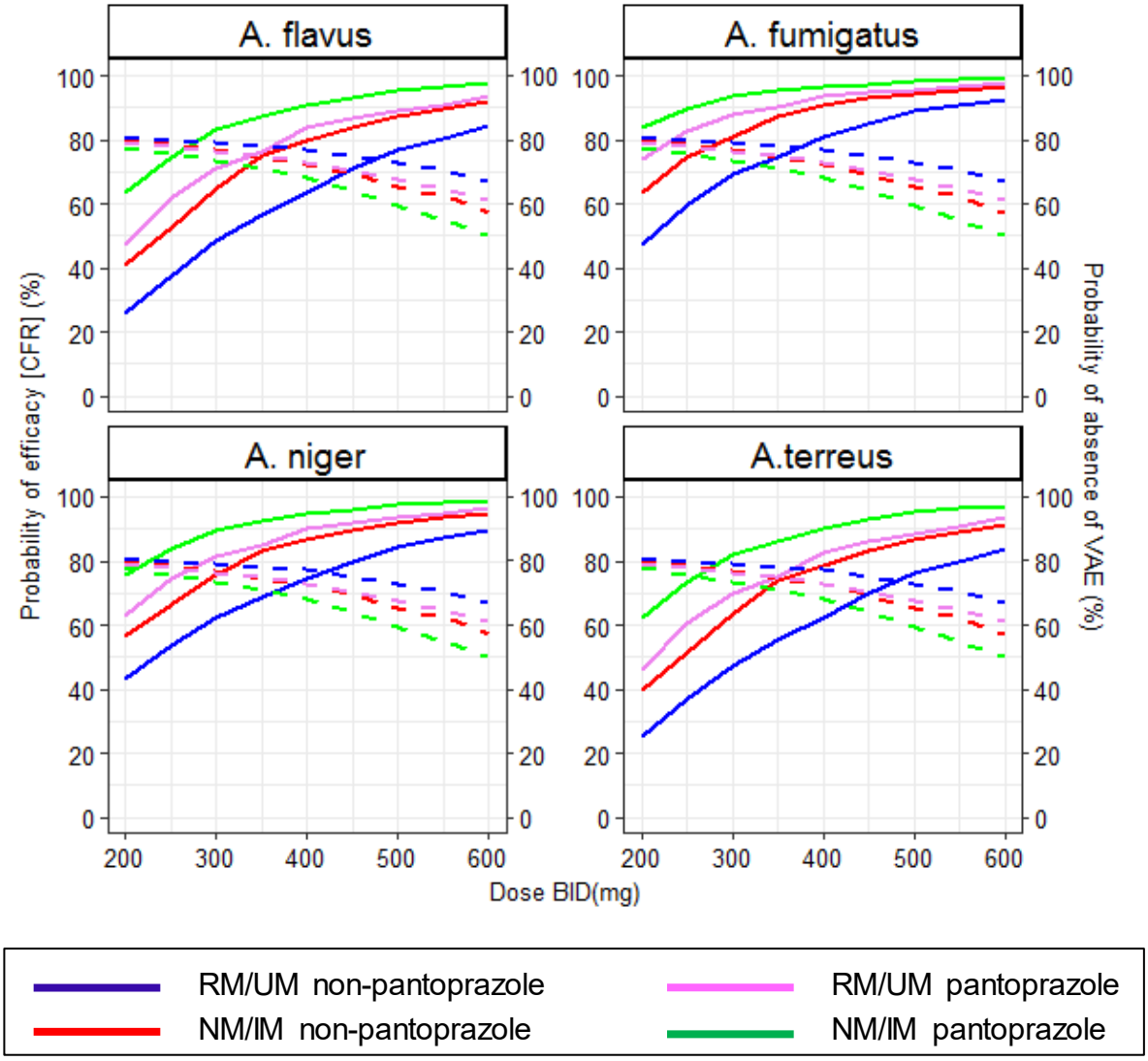

Figure 4-6. Benefit-risk analysis1: Probability of efficacy (CFR %) and probability of safety (absence of visual adverse events (VAE)) with increasing BID dose of voriconazole against *Aspergillus* spp. infections. Different colored solid lines represent efficacy while dashed lines represent safety for respective phenotypes

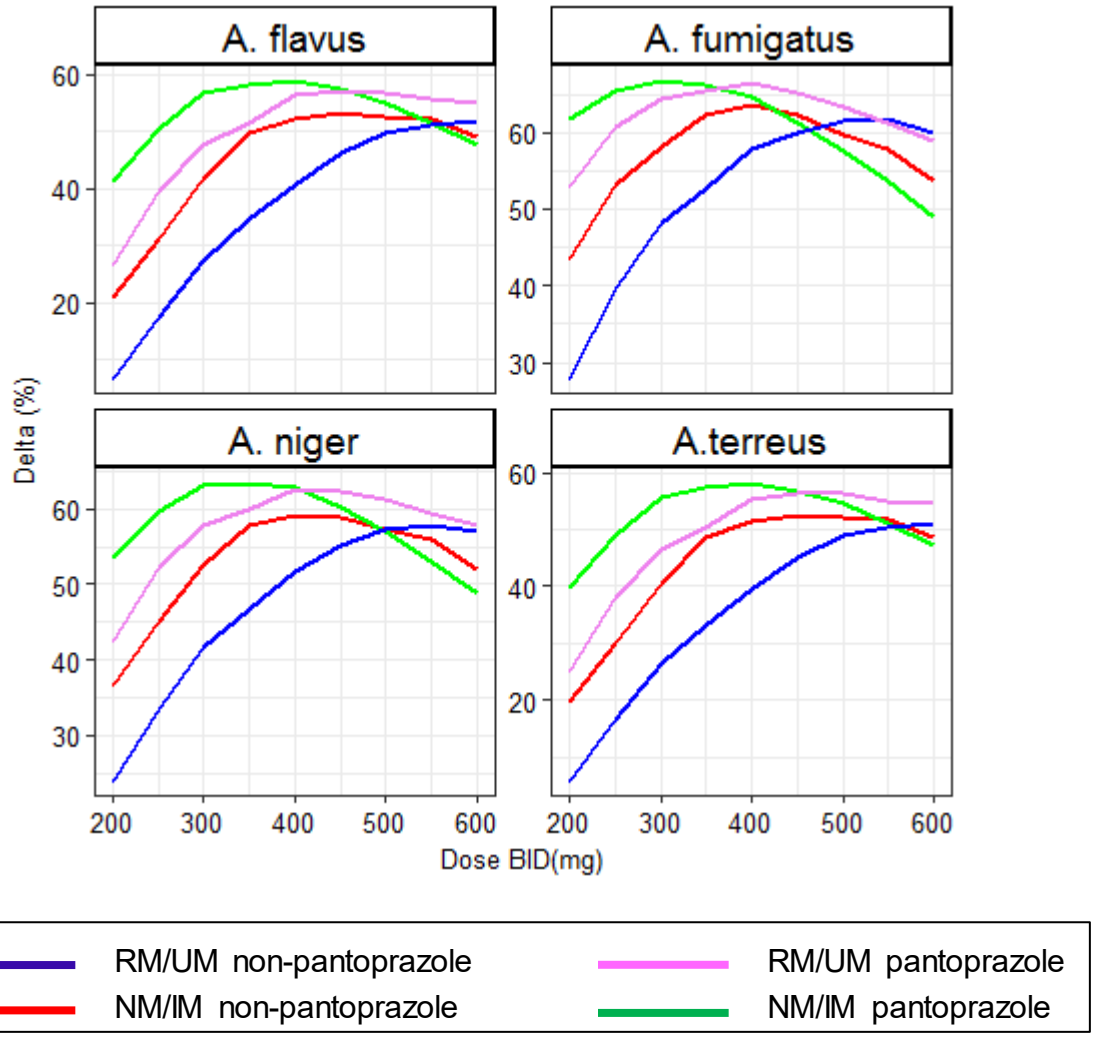

Figure 4-7. Delta* values by phenotype and Aspergillus spp

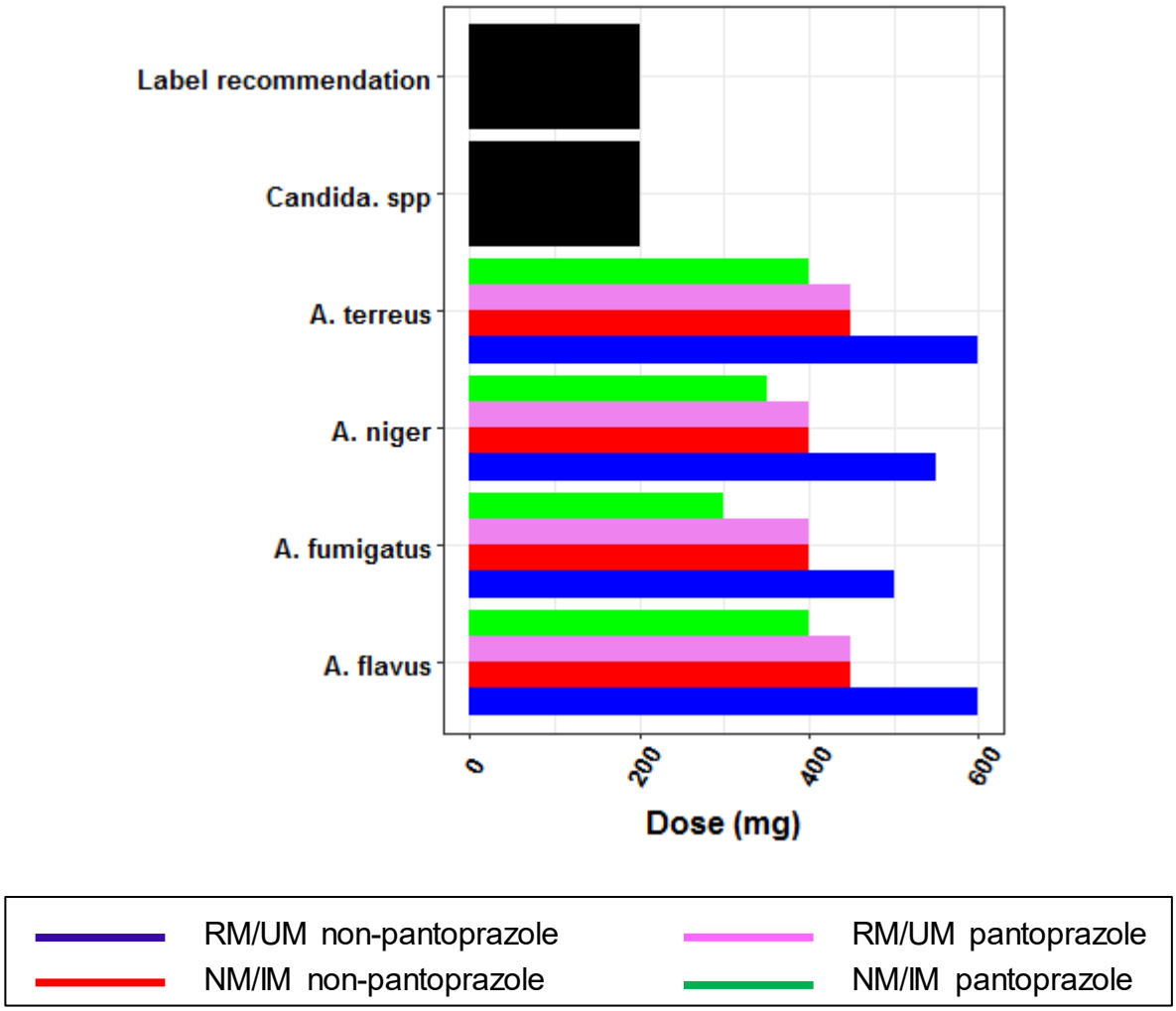

Figure 4-8. Dosing nomogram for voriconazole: Label-recommended and proposed BID maintenance doses of voriconazole for the treatment of invasive fungal infections caused by *Aspergillus* spp. and *Candida* spp. in adults by *CPY2C19* phenotype, pantoprazole use and type of infection

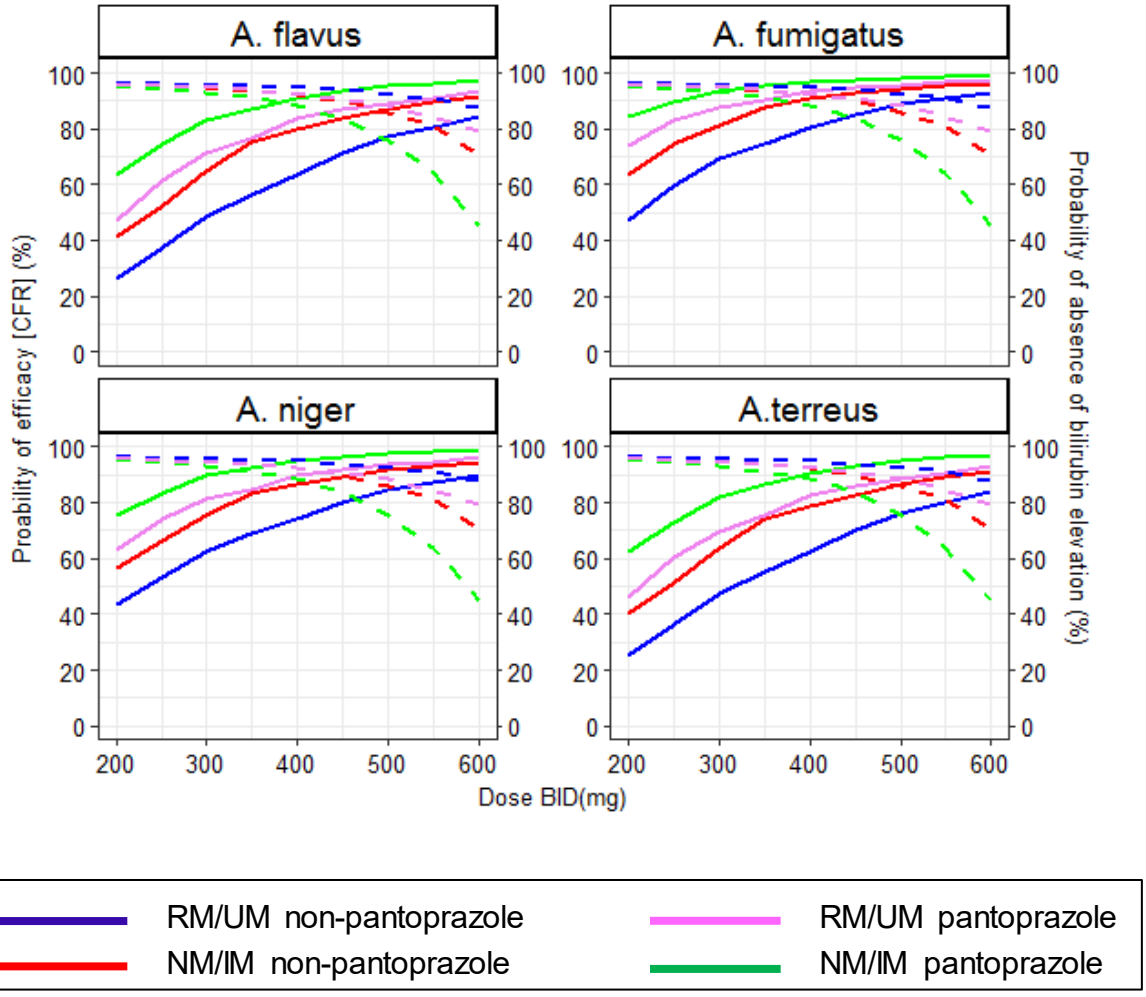

Figure 4-9. Benefit-risk analysis 2: Probability of efficacy (CFR %) and probability of safety (absence of bilirubin elevation) with increasing BID dose of voriconazole against *Aspergillus spp.* infections. Different colored solid lines represent efficacy while dashed lines represent safety for respective phenotypes

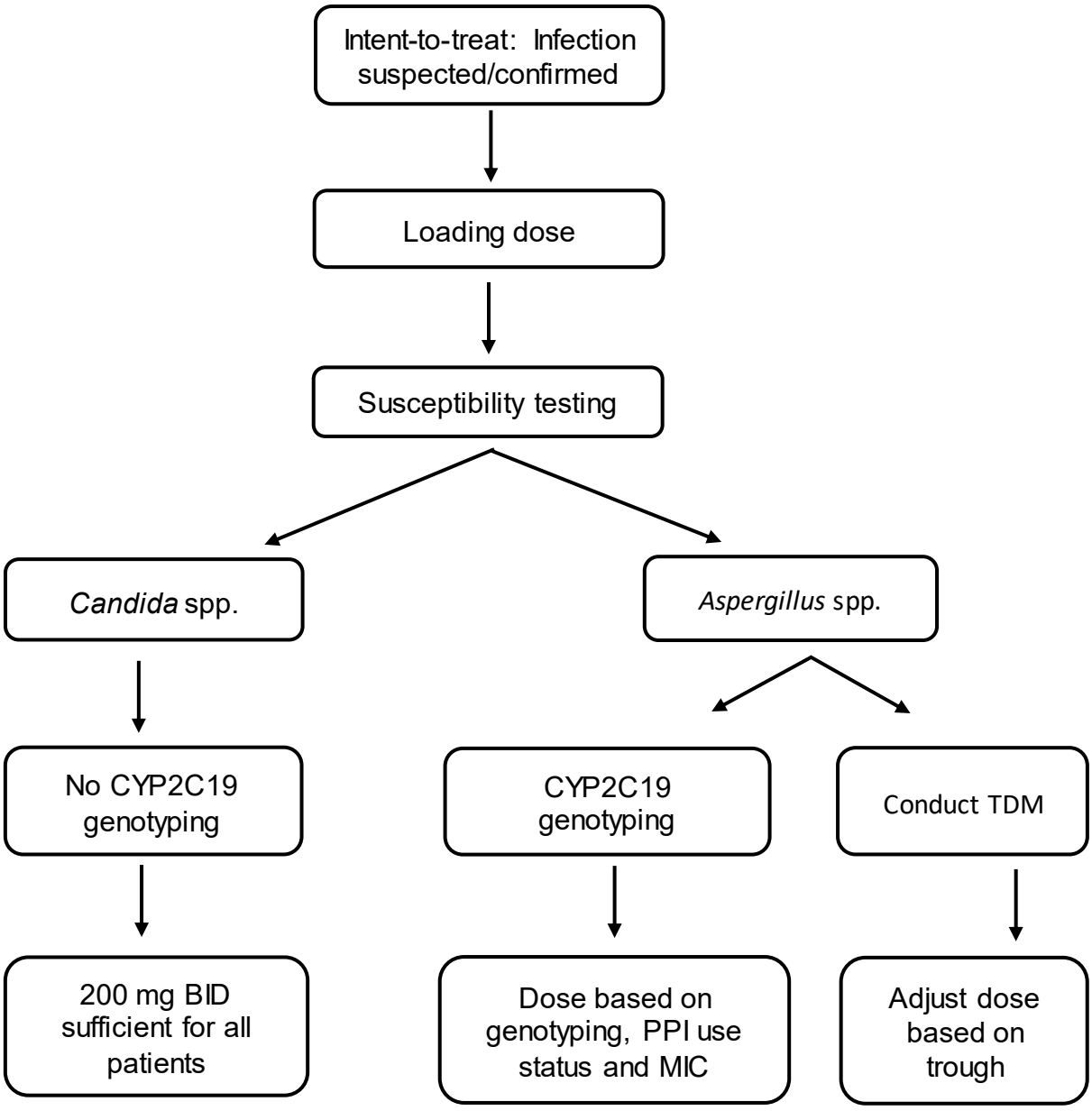

Figure 4-10. Clinical recommendations for dosing voriconazole in adults with suspected/confirmed infections

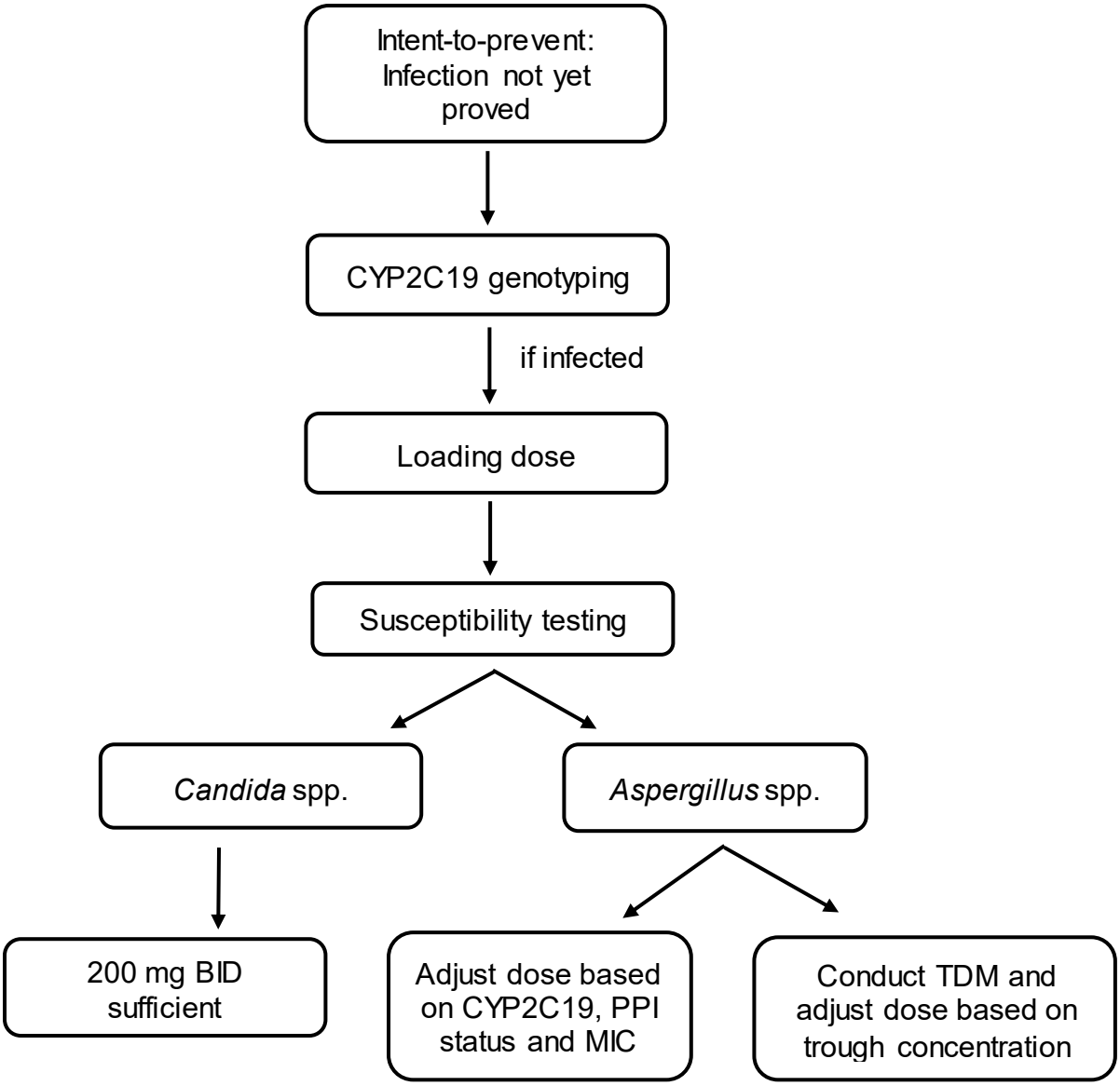

Figure 4-11. Clinical recommendations for dosing voriconazole in adults, at risk for infections

CHAPTER 5
OPTIMIZATION OF OXYCODONE THERAPY FOR CHRONIC PAIN MANAGEMENT

Introduction

Chronic pain is defined as pain without apparent biological value that has persisted beyond the normal healing time of 3-6 months[142]. Chronic pain is a major public health concern because it affects one in four adults in the United States[143]. Among primary care appointments, 22% focus on chronic pain management (CPM)[144]. Both the American College of Occupational Environmental Medicine (ACOEM) Guidelines[145] for the chronic use of opioids and the American Society of Interventional Pain Physicians[146] recommend combination medication therapy including opioids, anti-depressants, nonsteroidal anti-inflammatory drugs, and anticonvulsants. The volume of prescribed opioids in the US increased 1177% between 1997 and 2006 [147]. Examples of the most commonly prescribed opioids used in chronic pain are oxycodone, hydrocodone, codeine, tramadol morphine, hydromorphone, methadone and fentanyl.

Oxycodone accounts for approximately 60% of opioid use for CPM - and there has been widespread use of oxycodone since a controlled-release dosage form of it became available. Oxycodone prescriptions increased 720% during the same 1997-2006 time frame [147]. Unfortunately, there are sparse data on the metabolism of oxycodone in CPM patients, and no data on phenoconversion in oxycodone users. The primary metabolic pathways of opioids depend on hepatic enzymes such as CYP2D6 (applicable for oxycodone, hydrocodone, codeine, tramadol), UGT (for oxycodone, morphine and hydromorphone), and CYP3A4 (for fentanyl and methadone). The specific pathway by which each of these drugs is mediated varies. For oxycodone, 47% of its metabolism is mediated by CYP3A4 N-demethylation to noroxycodone (which has

only weak activity), and 11% by CYP2D6 to its major active metabolite, oxymorphone (Figure 5-1). Oxymorphone is further converted to oxymorphone-3-glucuronide by UDPGT, while noroxycodone is converted to noroxymorphone by CYP3A4 [148]. Although oxymorphone is the responsible for pharmacological activity, Oxycodone has in important role on pharmacological because it is actively transported to the brain, with subsequent conversion to Oxymorphone through brain CYP2D6.

The CYP2D6 pathway is a critically important one because there are four clinical phenotypes related to clearance of CYP2D6 substrates: poor metabolizer (PM), intermediate metabolizer (IM), extensive or normal metabolizer (EM or NM), and ultrarapid metabolizer (UM). PMs with homozygous germline mutations encoded by the CYP2D6 gene have little or no metabolic function. The highest prevalence of germline (inherited from parents) PMs is 6-10% in Caucasians, as compared 2-7% in African-Americans and 1-5% in Asians [149]. Similarly, UM can have increased oxymorphone formation, potentially resulting in dose-related toxicity in clinic.

In contrast to germline mutations, IMs, EMs and UMs can be converted to PM/UM status by co-medications that inhibit/induce hepatic CYP2D6 through competition for available enzyme, a process called phenoconversion. Importantly, patients with chronic pain commonly receive polypharmacy, increasing the chances of drug-drug interactions. Although, the exact rate of phenoconversion for opioids is unknown, it could result in unfavourable benefit-risk profile for the oxycodone therapy.

The objective of our research was to study the influence of germ-line mutations and phenoconversion on the plasma and urine pharmacokinetics of oxycodone and its different metabolites. To do so, a PBPK model was developed and qualified for

oxycodone and its metabolites based on data from literature as well as in-house clinical data. Developed model was then applied to predict the effect of *CY2D6* polymorphisms and drug-drug interactions with strong CYP2D6 inhibitors (e.g. paroxetine, quinidine), CYP3A4 inhibitors (e.g. ketoconazole) and CYP3A4 inducers (e.g. Rifampin) on the plasma PK of oxycodone and its metabolites. Model was also applied to predict cumulative urinary excretion of oxycodone and its metabolites following oral administration of oxycodone. The feasibility of using steady state cumulative urinary excretion data as a surrogate for plasma concentrations was also investigated.

Materials and Methods

Data Sources

Human clinical PK data for PBPK model development and external qualification were obtained from a combination of published literature sources (Table 5-1) and in-house drug-drug interaction (DDI) study, conducted at University of Montreal (unpublished data). In the DDI study, 12 healthy volunteers with CYP2D6 EM (*1/*1, *1/*3, *1/*4) status were administered a single oral dose of 15 mg oxycodone without or with 100 mg quindine (2h before oxycodone, 6h and 12 h after oxycodone administration) in a cross-over design. Plasma was sampled before and 0.5, 1, 1.5, 2, 3, 4, 6, 8, 12 and 24 h following administration of oxycodone. Urine was also collected for 24 h post oxycodone administration. Concentrations of oxycodone, oxymorphone, noroxycodone and noroxymorphone were determined in plasma and urine.

PBPK Model Development and Qualification

The PBPK model was developed and externally qualified to characterize the plasma concentrations of oxycodone and its major metabolites such as oxymorphone, noroxymorphone and noroxycodone, following intravenous (i.v.) and oral administration

of oxycodone using GastroPlus v.9.0 (Simulations Plus, CA). Drug-specific parameters such as molecular weight, Log P, PK_a, $f_{u,p}$, B/P ratio, V_{max} and K_m were obtained from published literature sources or *in silico* predictions (ADMET predictor 7.0 , Simulations Plus), as shown in Table 5-2. Parameters were also optimized, if necessary during the model building step. PBPK model was developed in a step-wise fashion (Figure 5-2) to gain more confidence in a specific metabolic pathway before addition of other metabolic pathways. Main steps are listed below.

Development and external qualification of PBPK model following i.v. administration of oxycodone

Oxycodone PK was characterized following i.v. administration to characterize systemic clearance and avoid complications due to first pass metabolism and absorption-related issues. Different specific and non-specific metabolic pathways of oxycodone were mapped in a step procedure.

Contribution of CYP3A4-mediated metabolism. Oxycodone is metabolized into oxymorphone via CYP2D6 enzyme and noroxycodone via CYP3A4 enzyme. Other pathways of elimination include conversion of oxycodone into oxycodols by non-specific enzymes and elimination of unchanged drug in urine[150]. A DDI study[151] showed that Paroxetine knocks down the CYP2D6 pathway completely, inhibiting the formation of oxymorphone. Therefore, we first developed a PBPK model characterizing the conversion of oxycodone into noroxycodone (formed by CYP3A4-mediated pathway) using data from study ID-1, Table 5-1. Drug-specific parameters for this conversion are shown in Table 5-2.

Contribution of CYP2D6-mediated metabolism. After successfully mapping out the CYP3A4-mediated metabolism of oxycodone to oxymorphone, contribution of CYP2D6-mediated metabolism of oxycodone-oxymoprhone was characterized using data from Study ID-2, Table 5-1. Secondary metabolism of oxymorphone to noroxymorphone via CYPA4 enzyme was also quantified. It is also known that oxymorphone undergoes glucuronidation via UGT2B7 enzyme and gets eliminated in urine in glucuronidated form along with unchanged oxymorphone. Elimination of noroxymorphone is through unknown pathways, so a non-specific clearance was used to characterize it. Drug-specific parameters for this conversion are shown in Table 5-2.

The developed model was externally qualified by simulating out the median and 90% prediction interval for the observations obtained from an external data sets which were not used for model building (Table 5-1, Study ID-3,4) .

Development and external qualification of PBPK model following oral administration of oxycodone

Once developed and qualified for i.v. administration, the model was extended to characterize the effect of pre-systemic absorption on the pharmacokinetics of oxycodone and its metabolites following oral administration of oxycodone using data from Study ID-6, Table 5-1. To do so, following assumptions were made:

- Immediate release formulations were assumed to have similar dissolution and solubilization profile.
- Only CYP3A enzyme was assumed to be present in enterocytes.
- CYP2D6 extensive metabolizers were assumed to represent the pooled population for model development and qualification.

Qualification in plasma. The performance of the developed oral PBPK model was evaluated by conducting visual predictive checks. Briefly, a virtual population of 50 subjects was simulated and model-predicted median plasma concentrations as well as 90% prediction interval (PI) were superimposed with the observed concentrations obtained from an external data set, not used for model building (Table 5-1, Study ID-9).

Qualification in urine. The model was also qualified by overlaying model-predicted steady state excreted amount of oxycodone, oxymorphone and noroxycodone with observed excreted amount (Table 5-1, Study ID-9,10), following oral administration of oxycodone. A comparison of observed and predicted % dose of oxycodone, oxymorphone and noroxycodone, recovered in urine was also performed.

Applications of the Developed PBPK Model

The developed and qualified oral PBPK model was applied to predict the effect of following factors on the PK of oxycodone and its metabolites (Figure 5-2):

Gene-drug interactions (GDI)

The effect of CYP2D6 and UGT2B7 polymorphisms on the PK of oxycodone and its metabolite was evaluated using data from Study ID-7, 8, Table 5-1. While fine-tuning the model for its application, following assumptions were made:

- CYP2D6 poor metabolizers can be depicted as phenotypically devoid of any CYP2D6 enzyme activity[152]
- In the absence of any *in vitro* enzyme kinetic data for CYP2D6 ultra-rapid metabolizer genotype, it was assumed that CYP2D6 enzyme activity in UM genotype would be 150% of the observed enzyme activity in extensive metabolizers.

Drug-drug interactions (DDI)

Drug-drug interactions of oxycodone with strong CYP2D6 inhibitors (e.g. , quinidine), CYP3A4 inhibitors (e.g. ketoconazole) and CYP3A4 inducers (e.g. rifampin) were also evaluated in different CYP2D6/UGT2B7 clinical phenotypes, using data from Study ID-5-8, Table 1. Model-predicted steady state AUC/AUC ratios were calculated and compared with observed AUC/AUC ratios, depending on the availability of data.

$$AUC\ ratio = \frac{AUC\ of\ oxycodone, oxymorphone\ in\ presence\ of\ perpetrator}{AUC\ of\ oxycodne,\ oxymorphone\ in\ absence\ of\ perpetrator}$$

According to the FDA guidelines[153] on DDIs, we categorized an interaction with an inhibitor drug strong if AUC increases by ≥5-fold, moderate if AUC increases by ≥2-fold to <5-fold and weak if AUC increases by ≥1.25-fold to <2-fold.

Relationship between plasma exposure and cumulative urinary excretion

The developed PBPK model was applied to predict steady state plasma AUC and cumulative urinary excretion of unconjugated oxymorphone at different oxycodone doses, ranging from 5-30 mg, administered every 6 hours. A linear regression analysis was performed to investigate if there is any relationship between plasma AUC and cumulative urinary excretion.

Results

PBPK Model Development and Qualification

Development and external qualification of PBPK model following i.v. administration of oxycodone

CYP2D6, CYP3A4 and other non-specific metabolic pathways of oxycodone were successfully mapped in a 2-step procedure.

Contribution of CYP3A4-mediated metabolism. Contribution of CYP3A4-mediated metabolism of oxycodone to noroxycodone was successfully characterized following intravenous administration of oxycodone. Fitted concentration-time profiles of oxycodone and noroxycodone are shown in Figure 5-3. Model was able to capture the mean and variability around the observation concentrations reasonably well.

Contribution of CYP2D6-mediated metabolism. Contribution of CYP2D6-mediated metabolism of oxycodone to oxymorphone was successfully added to step (i). Fitted plasma concentration-time profiles of oxycodone, oxymorphone, nooxycodone and noroxymorphone are shown in Figure 5-4.

The developed PBPK model for oxycodone, oxymorphone, noroxymorphone, and noroxycodone was successfully validated using an external dataset. The model was able to predict the central tendency (median) as well as the variability of observed concentration-time profile reasonably well. All observations were contained within the 95 % prediction interval of the predicted mean as shown in Figure 5-5.

Development and qualification of PBPK model following oral administration of oxycodone

The developed PBPK model for oxycodone, oxymorphone, noroxymorphone, and noroxycodone (Figure 5-6) after oral administration of immediate release formulations could predict the observed concentration-time profile reasonably well.

Qualification in plasma. The developed PBPK model was successfully qualified as it was able to predict concentrations for an external data set, which was not used for training the model (Figure 5-7).

Qualification in urine. The model was able to predict 24-hour cumulative urinary excretion of oxycodone, oxymorphone and noroxycodone following a single dose of oxycodone as shown in Figure 5-8. Model-predicted % of recovered dose were in close agreement with observed % recovered dose for all compounds for both Lalovic *et. al.* and an in-house unpublished study (Table 5-3 and Table 5-4).

Applications of the Developed PBPK Model

The developed and qualified oral PBPK model was applied to predict the effect of following factors on the PK of oxycodone and its metabolites:

Gene-drug interactions

Figures 5-9 and Figure 5-10 show that there is a good overlay between model-predicted and observed concentration-time profiles for oxycodone, noroxycodone, oxymorphone and noroxymorphone concentrations in CYP2D6 PM and CYP2D6 UM, respectively. It is important to note that CYP2D6 enzyme does not have activity in PM so, there is no formation of oxymorphone or noroxymorphone in these subjects. Overall, it can be noticed that the model-predicted steady state AUCs are in agreement with observed AUCs for oxycodone, oxymorphone and noroxycodone in different CYP2D6 phenotypes (EM, PM and UM) (Figure 5-11). Also, it seems that there is no statistically significant difference in AUCs amongst CYP2D6 EM, PM and UM (Figure 5-11). However, our analysis is limited by low sample size for CYP2D6 UM/PM (n=2). Additionally, when polymorphism in UGT2B7 are considered along with those in CYP2D6, the AUC of oxymorphone was 3-fold higher in subjects with CYP2D6 UM and UGT2B7 PM status and 2-fold higher in subjects with CYP2D6 EM and UGT2B7 PM status compared to those with CYP2D6 EM/UM and UGT2B7 EM status (Figure 5-12 B).

Interestingly, the AUC of oxycodone was not statistically different amongst CYP2D6/UGT2B7 clinical phenotypes (Figure 5-12 A). These findings in plasma AUC were in agreement with cumulative urinary excretion data as shown in Figure 5-13 A and Figure 5-13 B.

Drug-drug interactions

Figure 5-14 and Figure 5-15 show the comparison of observed and model-predicted AUC ratios for oxycodone and oxymorphone, respectively, when different perpetrator drugs were concomitantly administered with oxycodone. It can be observed that model-predicted AUC ratio were in very good agreement with observed AUC ratios for most of the DDIs. Furthermore, there were no statistically significant differences amongst different CYP2D6 phenotypes. Amongst all the DDIs tested, the effect of concomitant administration of rifampin (CYP3A4 inducer) was most significant (strong), with 5-7 fold lower steady state plasma AUC of oxycodone for different CYP2D6 phenotypes, in the presence of rifampin (Figure 5-14). Similarly, steady state AUC of oxymorphone was 6-12 fold lower in the presence of rifampin (Figure 5-15). For ketoconazole (CYP3A4 inhibitor), AUC ratios were approximately near 2 for both oxycodone and oxymorphone (Figure 5-14 and Figure 5-15), categorized as moderate inhibition. Similarly, for quinidine (CYP3A4 and CYP2D6 inhibitor), AUC ratios were near 2 for oxycodone, and about 0.5 for oxymorphone (Figure 5-14 and Figure 5-15) (moderate inhibition). We also evaluated DDIs in different CYP2D6/UGT2B7 clinical phenotypes. There were no differences in AUC ratios for oxycodone and oxymorphone, amongst different CYP2D6/UGT2B7 clinical phenotypes, in the presence of different perpetrator drugs as evident in Figure 5-16 A. However, steady state AUC of

oxymorphone was 7-fold higher for CYP2D6 UM and UGT2B7 PM and 5-fold higher for CYP2D6 EM and UGT2B7 PM subjects on ketoconazole, compared to those with CYP2D6 EM and UGT2B7 EM status and not on ketoconazole (Figure 5-16 B).

Relationship between plasma exposure and cumulative urinary excretion

Linear regression analysis indicated that there is a good correlation (R^2=0.98) between steady state cumulative urinary excretion and plasma AUC of unconjugated oxymorphone when corrected by oxycodone dose, as shown in Figure 5-17.

Discussion

PBPK models allow integration of available *in vitro* and *in vivo* information in to mathematical relationships which can characterize the concentration-time profiles of drugs[154]. The main structure of PBPK models constitutes of 3 different types of parameters: system-specific parameters, drug-specific parameters and trial-design specific parameters[23]. Such a structure offers a unique advantage over conventional pharmacometrics-based modeling approaches in the sense that a developed PBPK model for a drug can be adopted to a similar drug by changing the drug-specific and trial-design specific parameters. In this case, a PBPK model was successfully developed for oxycodone and its metabolites by systematically characterizing the metabolic pathways involved. Effect of germ-line mutations in metabolizing enzymes (CYP2D6 and UGT2B7) and drug-drug interactions on the PK of oxycodone and its metabolites was successfully evaluated. There is a published PBPK model[155] for oxycodone and its metabolites, however, the model did not evaluate the impact of polymorphisms in CYP2D6 and UGT2B7 on the PK of oxycodone and its metabolites. To our knowledge, this is the first PBPK model for oxycodone which has been

developed and applied to predict the effect of gene-drug interactions (e.g. CYP2D6, UGT2B7) and drug-drug interactions (quinidine, rifampin, ketoconazole) on the PK of oxycodone and its major metabolites.

Oxycodone undergoes O-demethylation to form oxymorphone via CYP2D6 and N-demethylation to form noroxycodone via CYP3A4-mediated metabolism[156]. Furthermore, oxymorphone can also undergo glucuronidation by UGT2B7 and get excreted as a glucuronide in urine. Both processes i.e. the formation of oxymorphone via CYP2D6 and elimination of oxymorphone via UGT2B7 are prone to polymorphisms, potentially resulting in clinically distinct phenotypes. In our analysis, we found that polymorphism in CYP2D6 did not result in statistically significant differences in steady state plasma exposure (AUC) of oxycodone and oxymorphone. Interestingly, when polymorphisms in UGT2B7 were considered along with those in CYP2D6, the differences in AUCs were significant amongst different clinical phenotypes. Steady state AUC of oxymorphone was significantly higher in subjects with CYP2D6 UM and UGT2B7 PM status (3-fold) and subjects with CYP2D6 EM and UGT2B7 PM status (2-fold) compared to those with CYP2D6 EM/UM and UGT2B7 EM status. Higher exposure of oxymorphone in CYP2D6 UM and UGT2B7 PM is explainable as these subjects have increased formation and reduced elimination rate of oxymorphone because of their CYP2D6 and UGT2B7 genetic composition. The significance of CYP2D6 polymorphisms in oxycodone analgesia is not very clear in the literature. In experimental pain, variation in CYP2D6 activity has been found to affect analgesia[157,158], however, in different pain settings, CYP2D6 activity does not seem to affect analgesic effect of oxycodone[159-161]. Unfortunately, there are no published *in vitro*

studies or clinical studies evaluating the combined impact of polymorphisms in both CYP2D6 and UGT2B7. This could be due to the fact the frequency of such a clinical phenotype could be <1% in Caucasian population. Nevertheless, these results could be significant, given that the total number of oxycodone users could be in millions in US alone. Based on these results, we can stratify patients into 3 bins according to the toxicity risk- Green bin: (CYP2D6 EM/UM and UGT2B7 EM), no dose adjustment is necessary; Yellow bin: (CYP2D6 EM and UGT2B7 PM), caution needed while dosing, dose adjustment may be considered; Red bin: (CYP2D6 UM and UGT2B7 PM), dose adjustment needed in clinic. These findings in plasma AUC were in agreement with urine data as evident by a strong correlation (R^2=0.98) between plasma AUC and cumulative urinary excretion of unconjugated oxymorphone, for different CYP2D6 and UGTB7 clinical phenotypes. The developed relationship can be used to predict plasma AUC of unconjugated oxymorphone based on a urine test, eliminating the need for taking a blood sample. Moreover, CYP2D6 or UGTB7 genotyping may not be necessary as the concentration of unconjugated oxymorphone in urine will be reflective of CYP2D6 and UGTB7 activity in a particular patient. Based on urinary measurement of unconjugated oxymorphone, optimal oxycodone dose can be selected to target a pre-defined therapeutic range.

For DDIs, rifampin, a CYP3A4 inducer was predicted to have most significant impact on the AUC of oxycodone and oxymorphone. For instance, plasma AUC of oxymorphone in subjects, who were taking rifampin as a concomitant medication was predicted to be 6-12-fold lower compared to the subjects on oxycodone alone, when polymorphisms in both CYP2D6 and UGT2B7 were considered. Induction of CYP3A4

pathway shifts the metabolic equilibrium of oxycodone towards formation of noroxycodone via CYP3A4, leading to decreased formation of oxymorphone via CYP2D6. Given that oxymorphone concentrations could be the main drivers of pharmacodynamics effect, dose adjustment of oxycodone is recommended when rifampin is used concomitantly. Ketoconazole (CYP3A4 inhibitor) and quindine (CYP2D6/CYP3A4 inhibitor) were predicted to have a mild-moderate DDI effect (AUC ratio=0.5-2) on AUC of oxymorphone when only polymorphisms in CYP2D6 were considered. However, when both CYP2D6/UGT2B7 polymorphisms are considered, magnitude of DDI with ketoconazole becomes larger, especially in subjects with CYP2D6 EM/UM and UGT2B7 PM status. These results indicate that the DDIs should be evaluated in light of both CYP2D6 and UGT2B7 polymorphisms.

In conclusion, we developed a PBPK model for oxycodone and its major metabolites following intravenous and oral administration of oxycodone. The model allows for the prediction of gene-drug as well as drug-drug interactions of oxycodone in a quantitative manner. We also found that the urinary measurements of unconjugated oxymorphone can be used for therapeutic drug monitoring and inform dosing decisions in clinic. Given that there can be lot of similarity amongst semi-synthetic opioids, the model can be extended to other opioids by changing the drug-specific and trial-design specific parameters. In future, the PBPK model can be linked to pharmacodynamic data to develop a dose-exposure-response relationship for oxycodone.

Table 5-1. Characteristics of studies used for PBPK model development and qualification

Study ID	Age (years)	Dose	Weight (kg)	Cohort used	CYP2D6 status	Route	Reference
1	24	0.1 mg/kg	67.5	Oxycodone + Paroxetine	10 EM/1 UM/1PM	IV	[151]
2	24	0.1 mg/kg	67.5	Oxycodone	10 EM/1 UM/1PM	IV	[151]
3	30.5	0.1 mg/kg	64.2	Oxycodone	7 EM/1 UM/3 IM/ 1 PM	IV	[162]
4	25.5	0.1 mg/kg	81.5	Oxycodone	11 EM/1 PM	IV	[163]
5	25.5	15 mg	81.5	Oxycodone+ Rifampin	11 EM/1 PM	Oral	[163]
6	25	0.2 mg/kg	76.4	Oxycodone+ Placebo/ Ketoconazole/ Quinidine	6 EM	Oral	[164]
7	25	0.2 mg/kg	76.4	Oxycodone+ Placebo/ Ketoconazole/ Quinidine	2 PM	Oral	[164]
8	25	0.2 mg/kg	76.4	Oxycodone+ Placebo/ Ketoconazole/ Quinidine	2 UM	Oral	[164]
9	26	15 mg	86.9	Oxycodone	12 EM	Oral	unpublished data
10	25.5	15 mg	73	Oxycodone	unknown	Oral	[150]

Table 5-2. Compound-specific parameters used for PBPK model development

Parameters	Oxycodone	Noroxycodone	Oxymorphone	Noroxymorphone
Molecular weight (g/mol)[165]	315.37	302.32	301.34	287.32
Log P	1.64[a166]	0.61[b]	0.61[b]	0.0779[b]
Compound type	Base	Base	Base/Acid	Base/Acid
pK_a	8.894(28)	8.69[b]	7.98/9.47[b]	8.43/9.54[b]
B/P ratio[b]	0.9	0.93	0.93	1.27
$f_{u,\ p}$ (plasma)	0.55[167]	0.6546[b]	0.89[b]	1.27[b]
Cl_{Renal} (L/h)	4.8(30)	20.4(30)	Fu*GFR	Fu*GFR
Distribution model	Perfusion Limited	Perfusion Limited	Perfusion Limited	Perfusion Limited
CYP2D6 metabolism (13)				
Vmax (pmol/min/pmol)	0.0016 [0.0019]*	0.00315 [0.000227]*		
K_m(μM)	41	6.32		
CYP3A4 metabolism (13)				
Vmax (pmol/min/pmol)	0.00544 [0.00275]*			
K_m(μM)	189.2			
UGT metabolism (8)				
Vmax (pmol/min/pmol)			0.01 [0.03]*	
K_m(μM)			262.2	

Notes:

a. Log D.

b. ADMET predictor 7.0 GastroPlus v.9.0

*values in the brackets are model-optimized values

Table 5-3. Comparison of observed and model-predicted cumulative urinary excretion of oxycodone and noroxycodone

study	% recovered dose in urine			
	Oxycodone		Noroxycodone	
	Observed (mean±SD)	Predicted	Observed (mean±SD)	Predicted
in house unpublished data	5.75 ± 1.95	4.99	21.5 ± 4.08	17.2
Lalovic *et al*., 2006[150]	8.0 ± 2.6	5.191	23.1 ± 7.6	20.88

Table 5-4. Comparison of observed and model-predicted cumulative urinary excretion of total oxymorphone and unconjugated oxymorphone

	% recovered dose in urine			
study	Total oxymorphone		Unconjugated oxymorphone	
	Observed (mean±SD)	Predicted	Observed (mean±SD)	Predicted
in house unpublished data	5.42 ± 3.62	3.62	-	-
Lalovic *et al*., 2006[150]	10.7 ± 5.5	4.77	0.33 ± 0.4	0.15

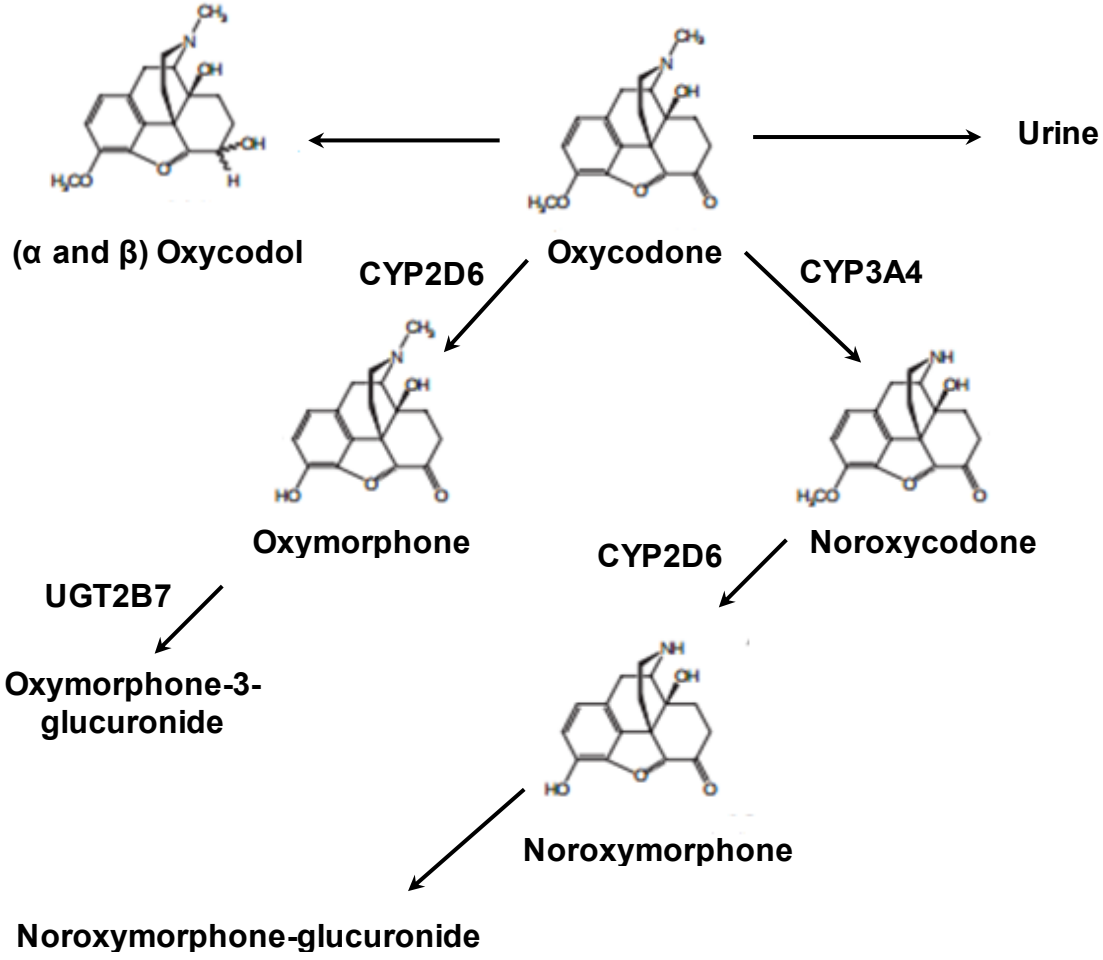

Figure 5-1. Schematic representation of oxycodone metabolism into oxymorphone, noroxycodone and noroxymorphone[168]

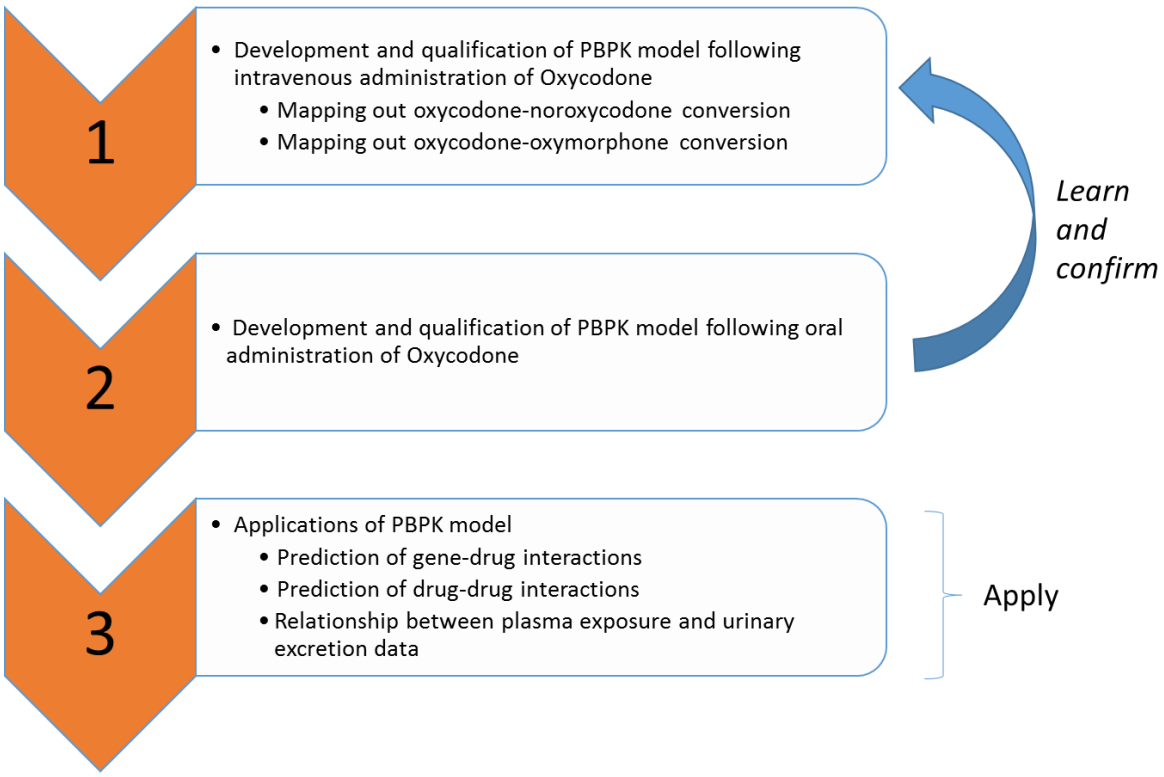

Figure 5-2. Schematic workflow of PBPK model development, qualification and application.

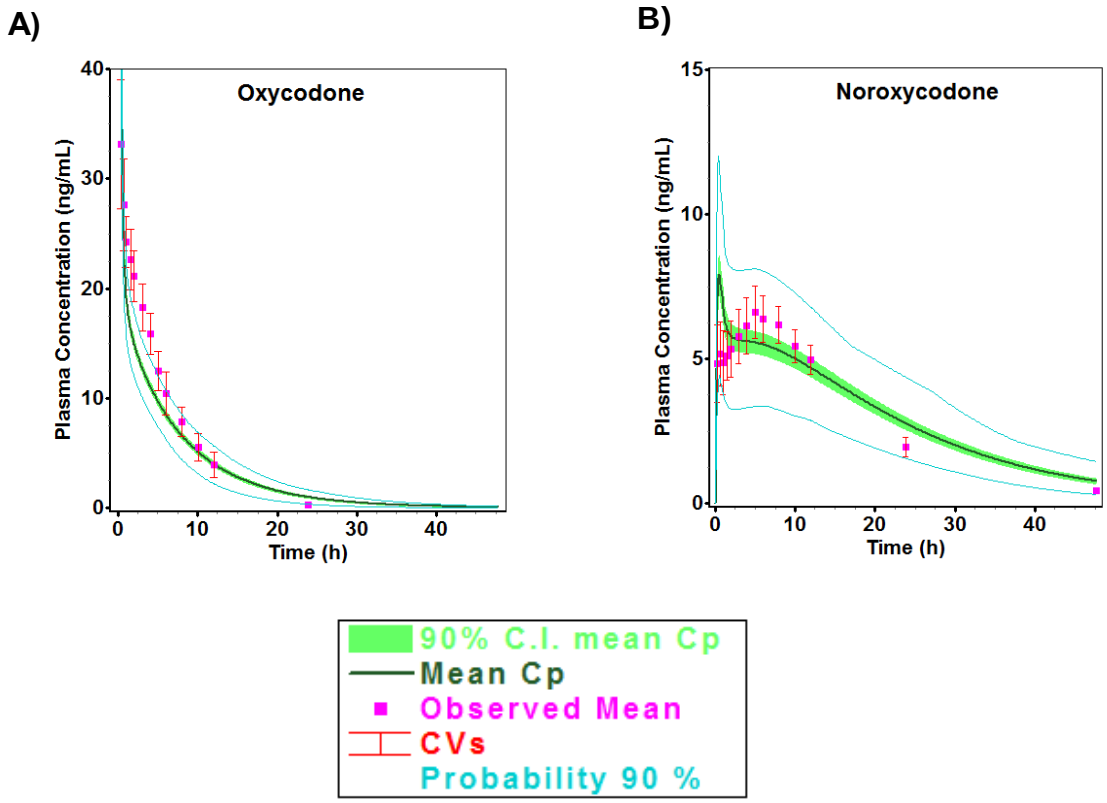

Figure 5-3. Fitted concentration-time profiles characterizing the CYP3A4-mediated oxycodone-noroxycodone conversion. A) Oxycodone. B) Noroxycodone.

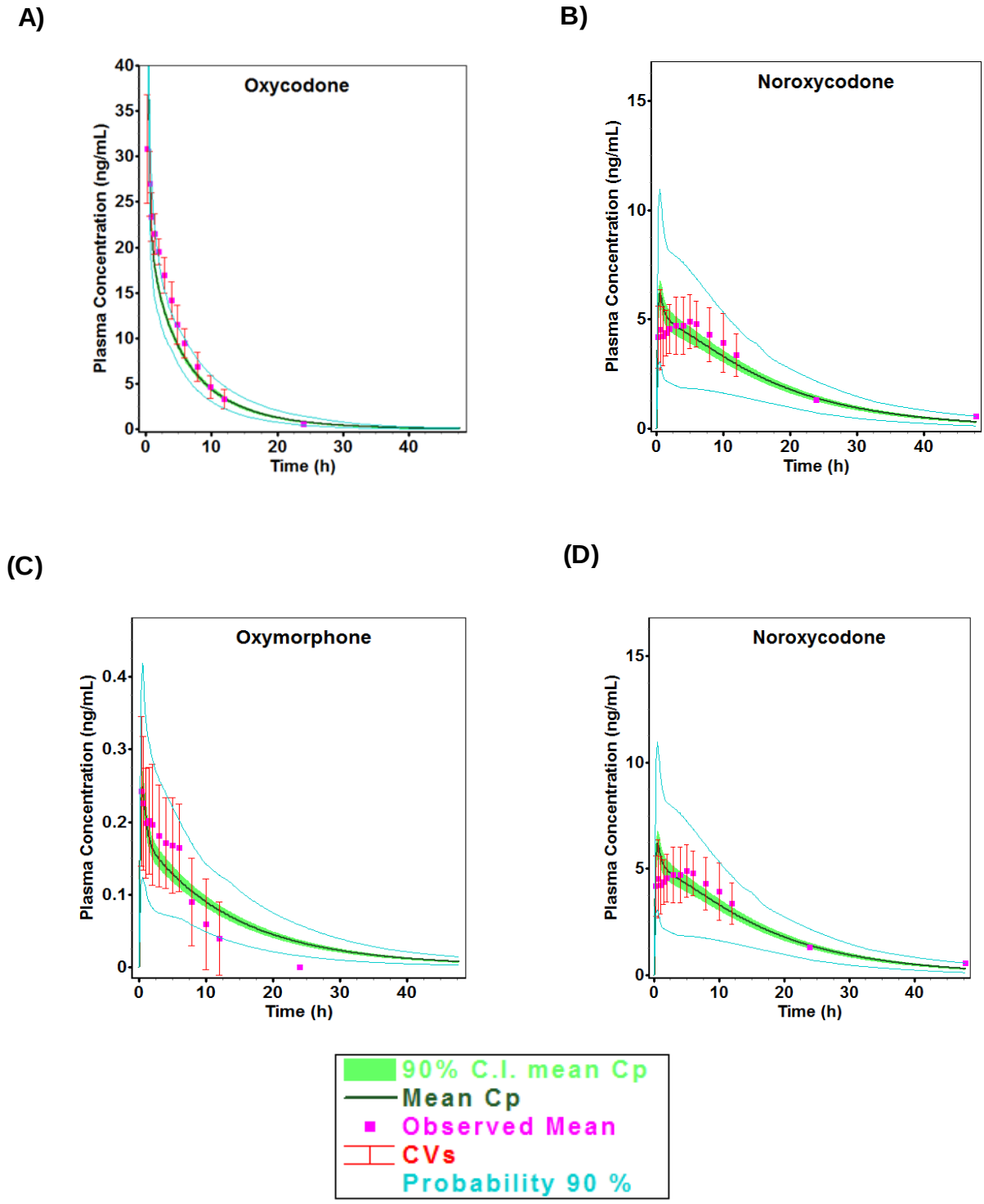

Figure 5-4. Model-fitted plasma concentration-time profiles following intravenous administration of oxycodone (0.1 mg/kg mg). A) Oxycodone. B) Noroxycodone. C) Oxymorphone. D) Noroxymorphone

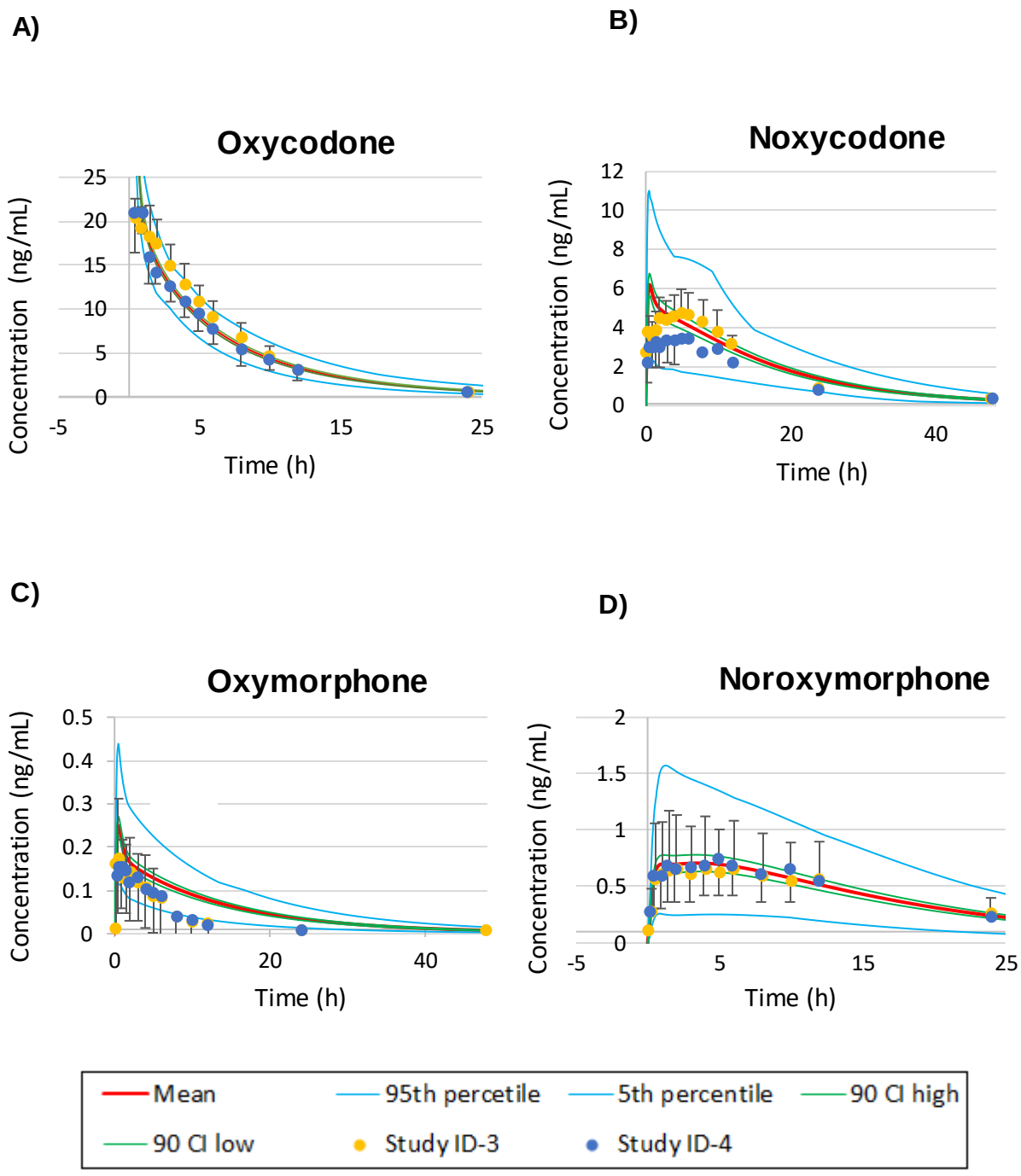

Figure 5-5. External model qualification of the intravenous PBPK model: Concentration-time profiles for A) Oxycodone. B) Noroxycodone. C) Oxymorphone. D) Noroxymorphone. Error bars represent the CV% of observations

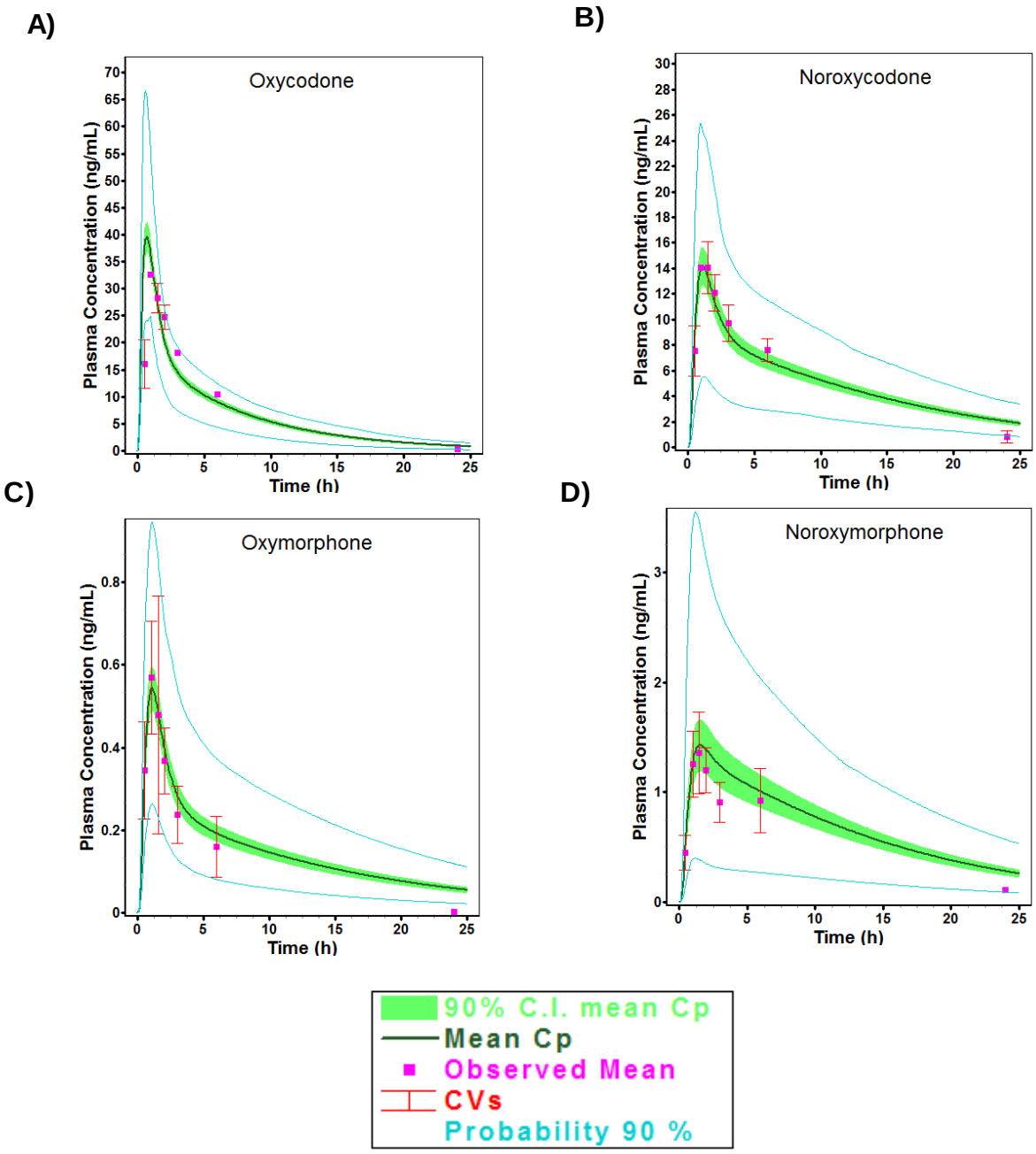

Figure 5-6. Model-fitted concentration-time profiles following oral administration of oxycodone. A) Oxycodone. B) Noroxycodone. C) Oxymorphone. D) Noroxymorphone

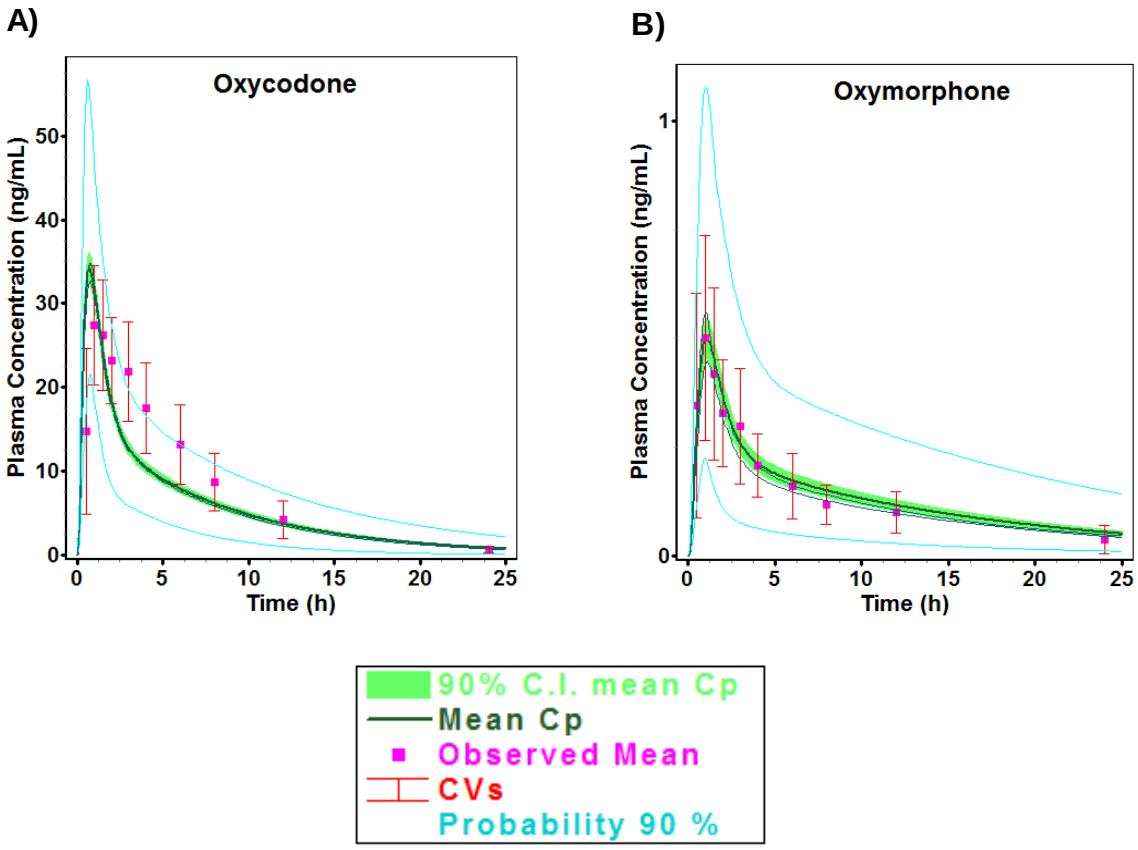

Figure 5-7. External qualification of the oral PBPK model in plasma: Comparison of observed and model-predicted concentration-time profiles for A) Oxycodone. B) Oxymorphone.

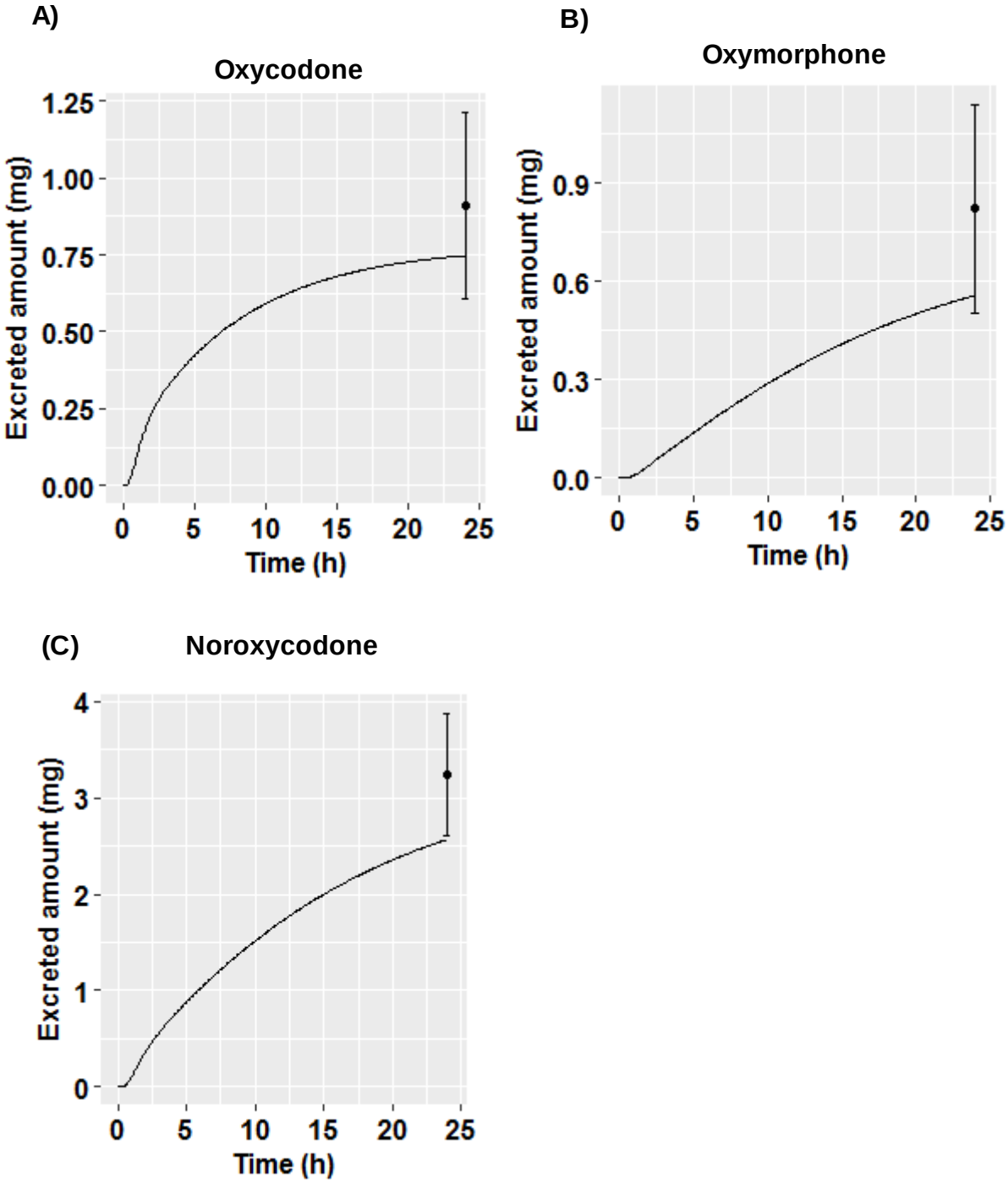

Figure 5-8. External model qualification of oral PBPK model in urine: Comparison of observed and model-predicted cumulative urinary excretion for A) Oxycodone. B) Oxymorphone. C) Noroxycodone

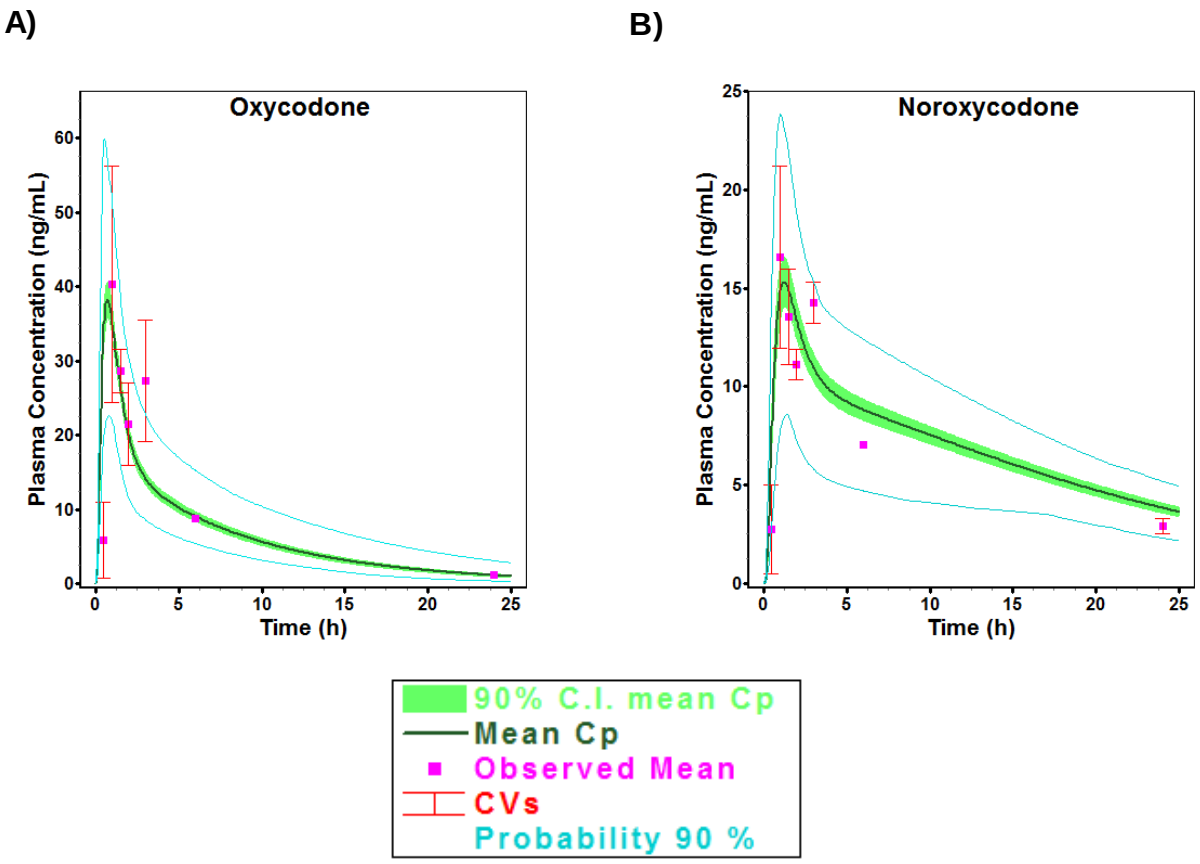

Figure 5-9. Overlay of model-predicted concentrations over observed concentrations in CYP2D6 poor metabolizers following oral administration of oxycodone for A) Oxycodone. B) Noroxycodone

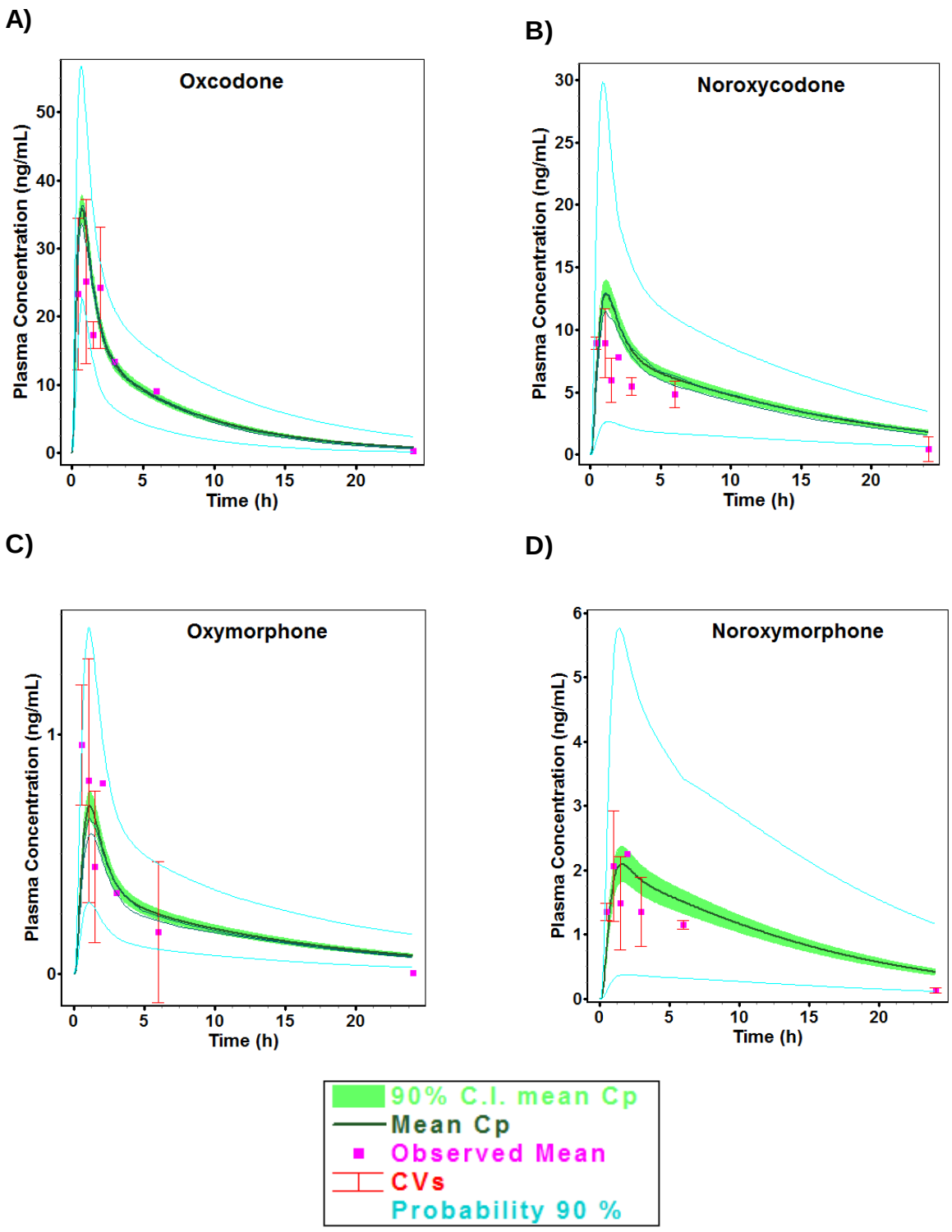

Figure 5-10. Overlay of model-predicted concentrations over observed concentrations in CYP2D6 ultra-rapid metabolizers following oral administration of oxycodone. A) Oxycodone. B) Noroxycodone. C) Oxymorphone. D) Noroxymorphone

(A)

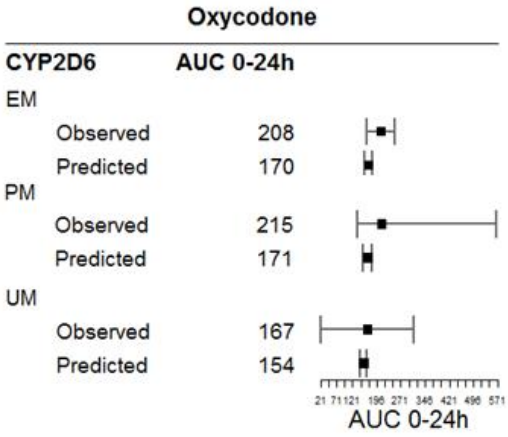

(B)

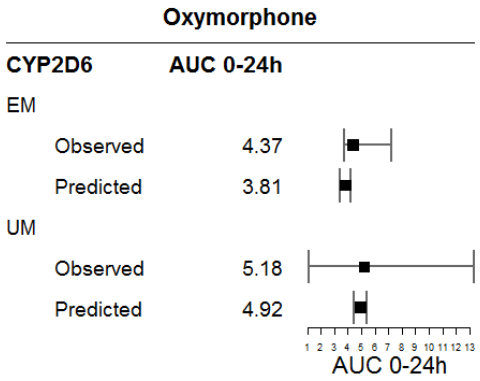

(C)

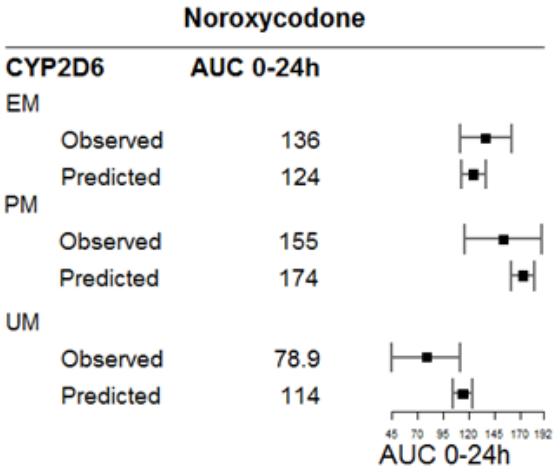

Figure 5-11. Model-predicted steady state AUC for different CYP2D6 phenotypes. (A) Oxycodone. (B) Oxymorphone. (C) Noroxycodone

(A)

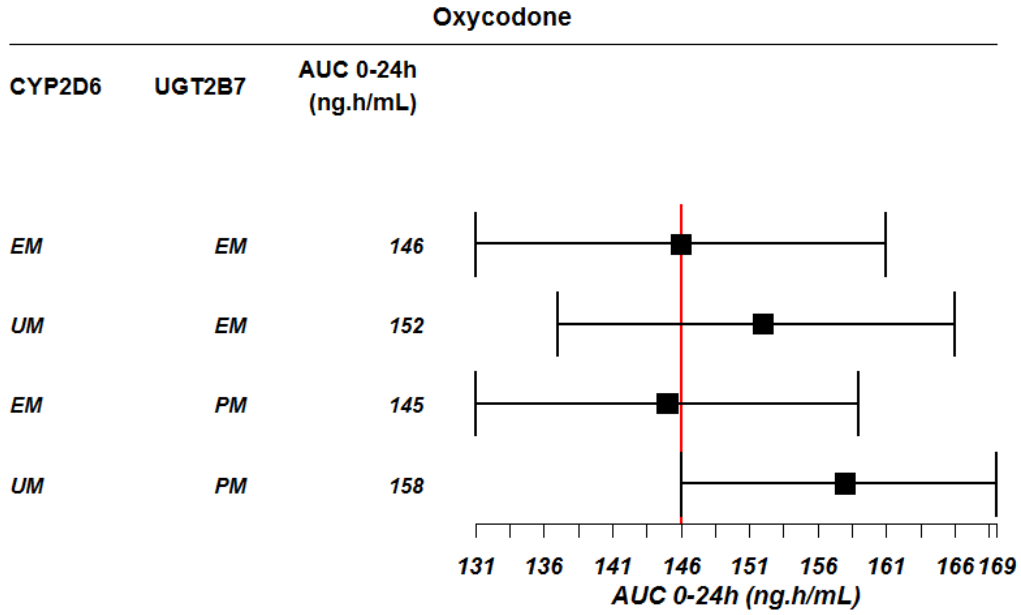

(B)

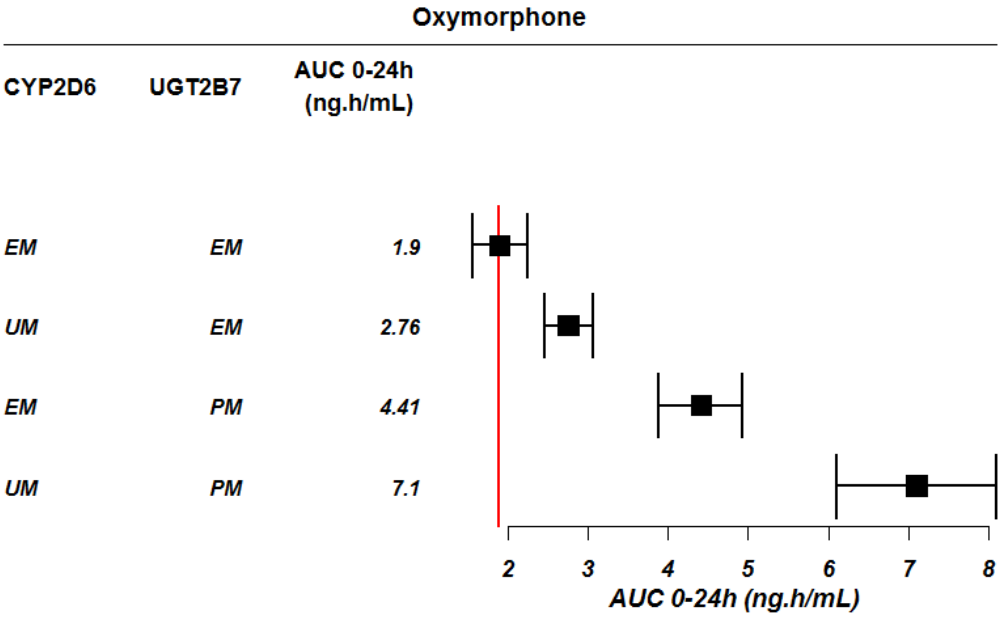

Figure 5-12. Model-predicted steady state AUC for different CYP2D6/UGT2B7 phenotypes. (A) Oxycodone. (B) Oxymorphone

(A)

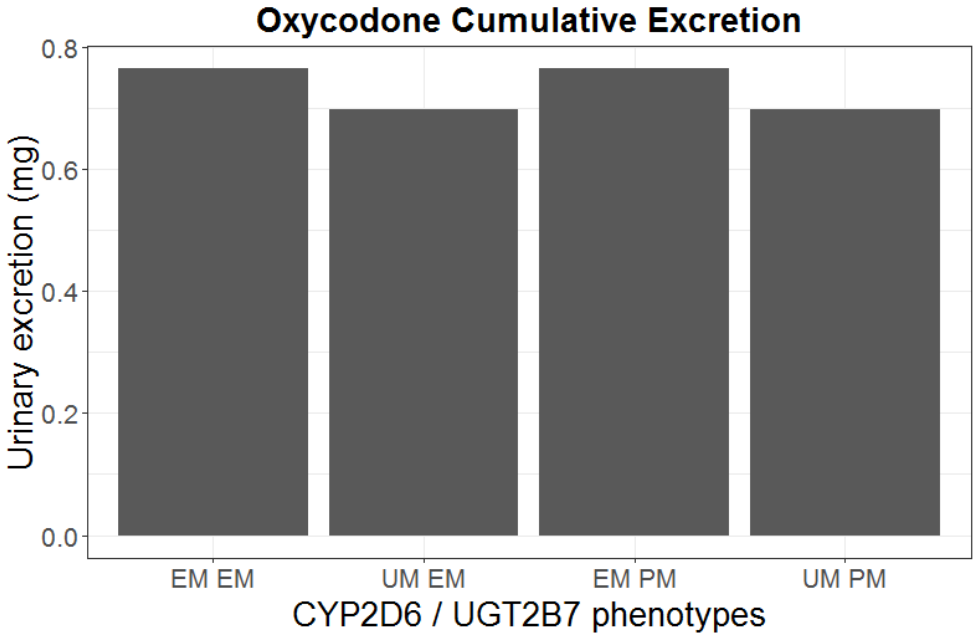

(B)

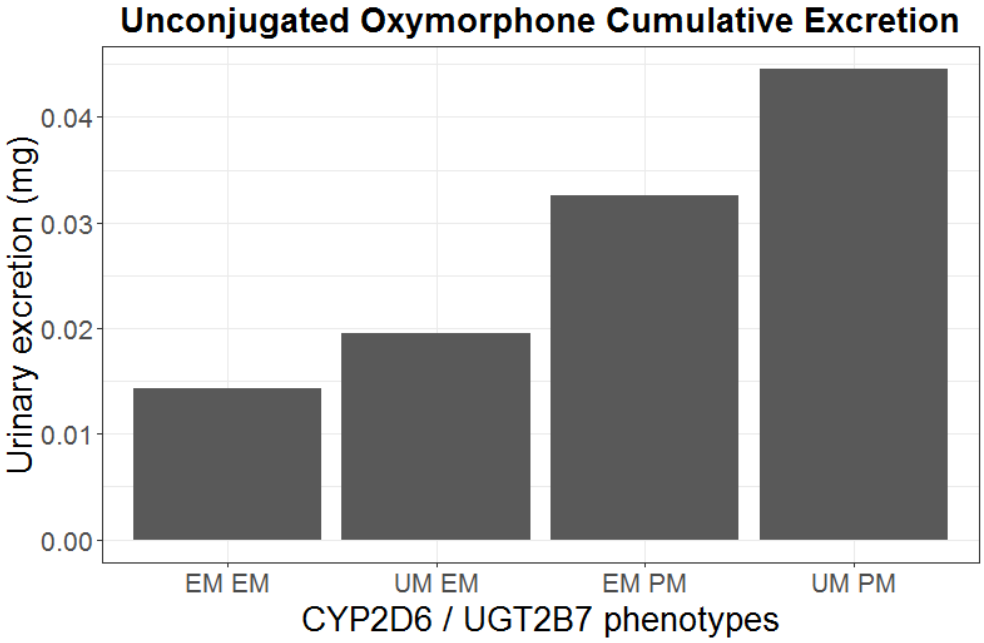

Figure 5-13. Model-predicted steady state cumulative urinary excretion for different CYP2D6/UGT2B7 phenotypes. (A) Oxycodone. (B) Unconjugated oxymorphone

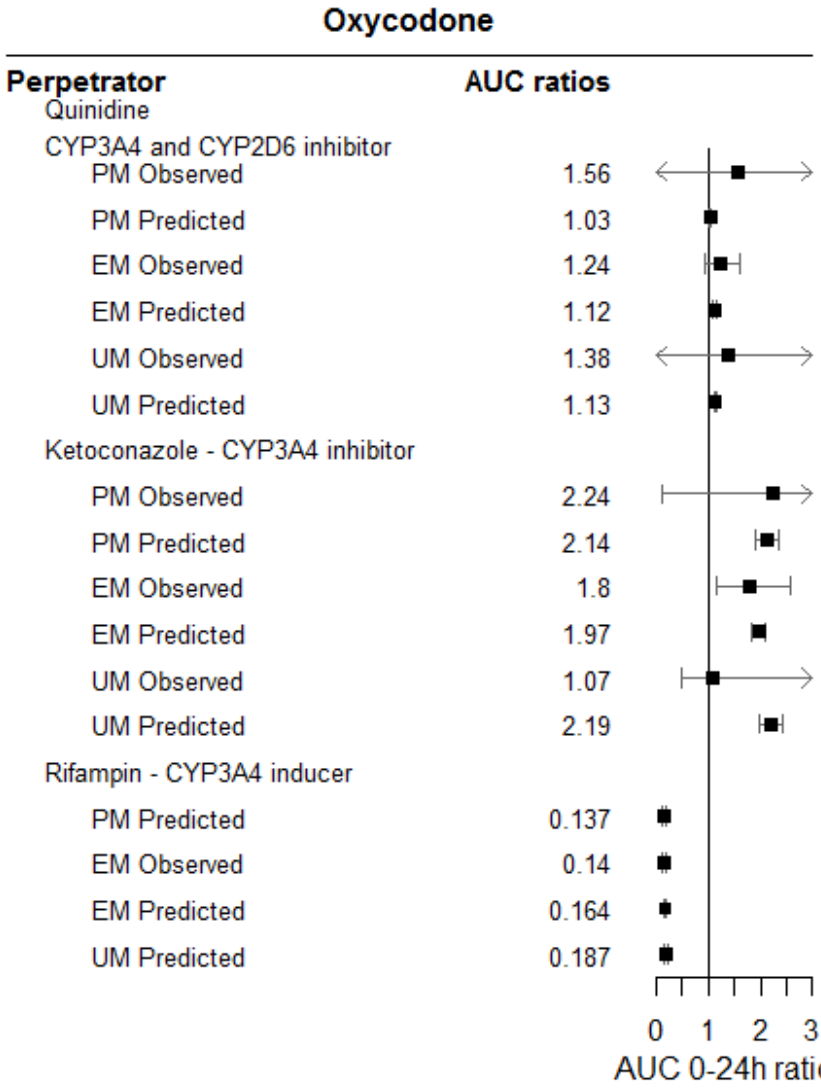

Figure 5-14. Comparison of model-predicted and observed AUC ratios of oxycodone for different perpetrator drugs

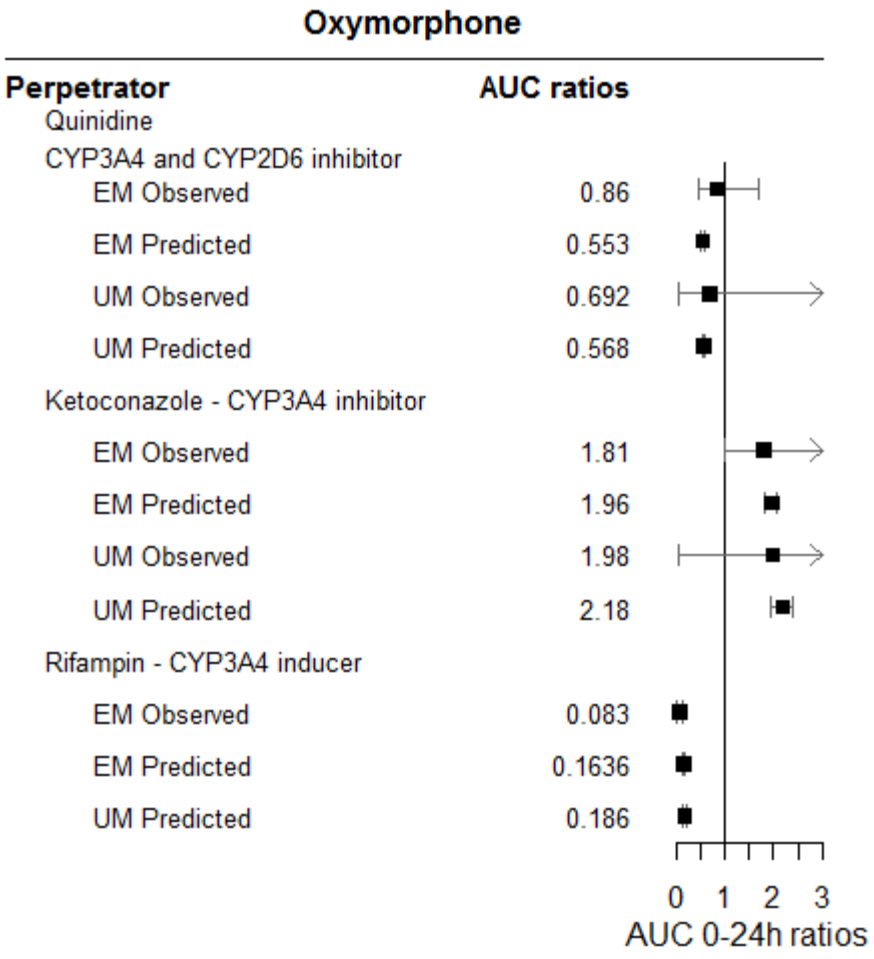

Figure 5-15. Comparison of model-predicted and observed AUC ratios of oxymorphone for different perpetrator drugs

(A)

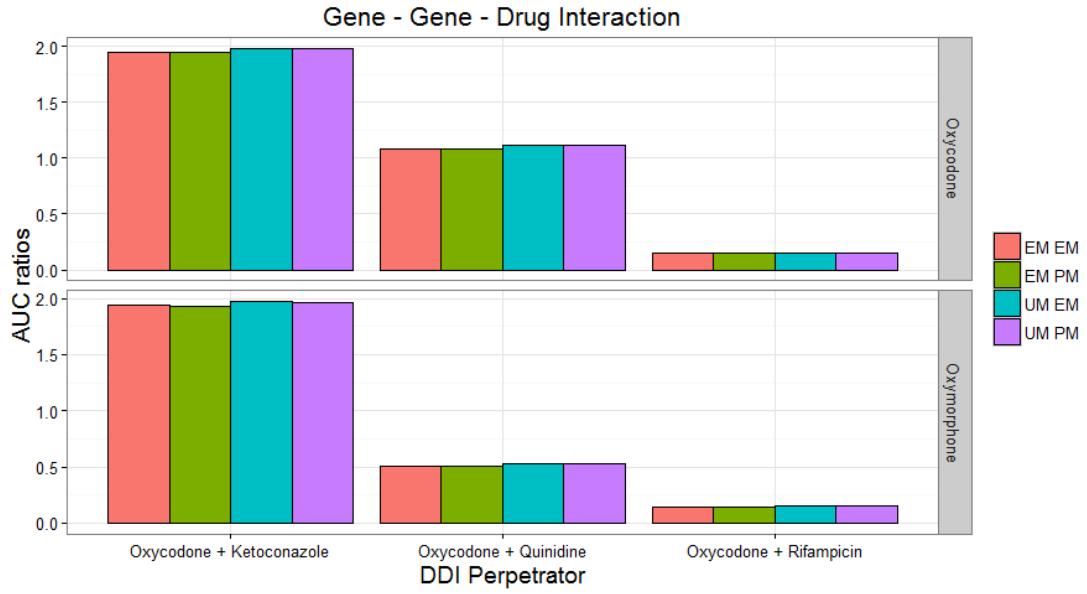

(B)

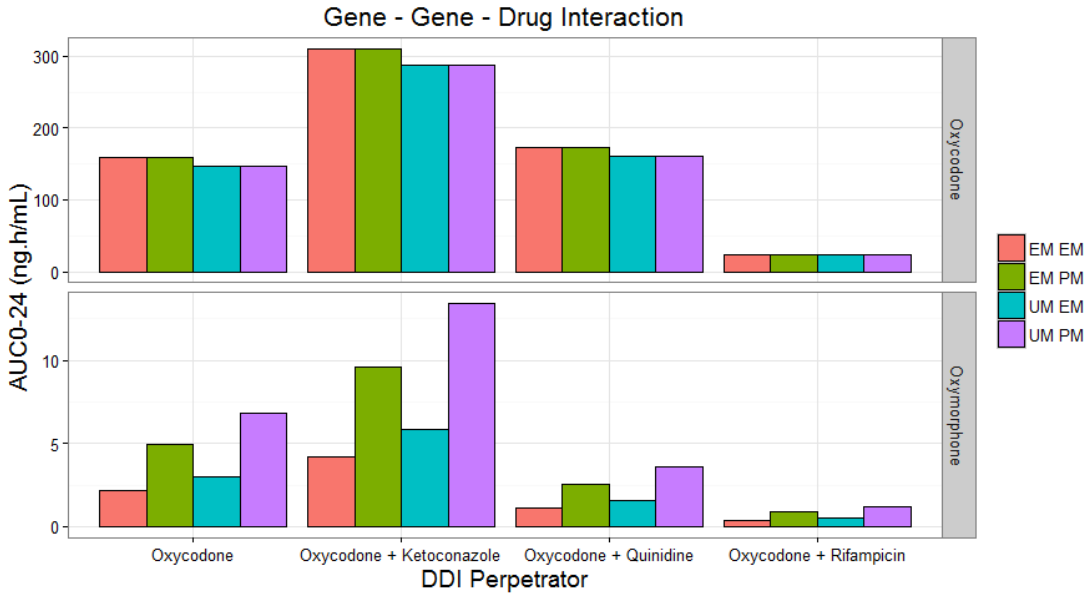

Figure 5-16. Model-predicted (A) AUC ratios and (B) AUCs for different CYP2D6/UGT2B7 clinical phenotypes in presence of various perpetrator drugs

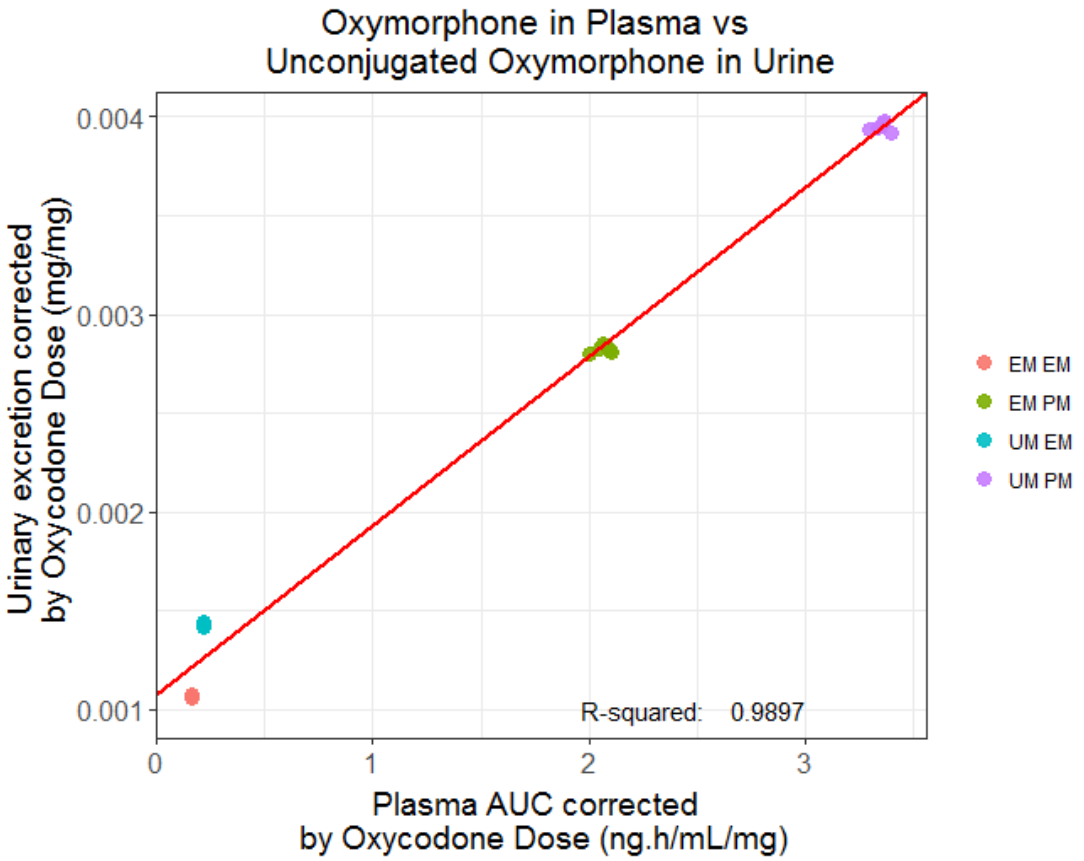

Figure 5-17. Correlation between steady state plasma AUC and cumulative urinary excretion of unconjugated oxymorphone

CHAPTER 6
CONCLUSIONS

Quantitative clinical pharmacology (QCP)-based decision support tools have already impacted the drug development process and continues to do so. In pharmaceutical industry, these tools are increasingly being used to integrate data from various research disciplines such as pre-clinical, formulation, pharmacokinetics, pharmacodynamics, toxicokinetics, and outcomes research to develop unifying models. Such model-based approaches can allow companies to make timely decisions in the drug development process, saving time and money. Regulatory agencies such as US Food and Drug Administration (FDA) and European Medical Agency (EMA) are also increasingly recommending sponsors to conduct pharmacometrics analysis as a part of new drug applications. However, the wider acceptability of M&S approaches still faces some challenges. One of the biggest challenge is that there can be a significant communication gap between modeling scientists and other stakeholders mainly, the clinicians. Along with technical skills, soft skills (e.g. communication) and business skills (e.g. drug development) are increasingly necessary for an aspiring clinical pharmacologist/pharmacometrician[169]. Nevertheless, QCP tools are proving to be of immense value in drug development and bringing value to the patient, the ultimate consumer of health care system.

In our research, we highlighted 3 different case studies where quantitative clinical decision support tools can bring value to the patient: 1) Dose prediction in children- A case study of dicloroacetate for the treatment of congenital lactic acidosis in children; 2) Dose optimization of voriconazole for the treatment of invasive fungal infections in adults); 3) Optimization of oxycodone therapy for chronic pain management. In all these

areas, there were some knowledge gaps which were not appreciated earlier or very costly and difficult to fill using laboratory-based studies or clinical studies. For example, in case of DCA, conducting clinical studies in children is very difficult, mainly due to the difficulties associated with enrollment of these young children, suffering from the rare CLA disease in study. As such, there was limited information on exposure-response relationship of DCA in Children. In our modeling work, along with the *in vitro, in vivo* literature-based evidences, we leveraged the information from adults and used the "full extrapolation" approach, as recommended by FDA, to inform dosing decisions in children. Furthermore, we used our model to come up with various possibilities to explain the differences seen in DCA PK following its repeated administration in adults or children and tested them methodically. In case of voriconazole, there were no prior clinical studies which prospectively evaluated the effect of CYP2C19 genotype or drug-drug interaction on the steady state PK. We conducted the clinical study to first identify the clinical phenotypes that may need dose adjustment from standard dose of voriconazole. Also, traditionally, dose adjustments were made empirically, mainly based on clinical experience of the caregivers. We have provided a scientific rationale for dose adjustment based on a benefit-risk analysis and provided probabilities of successful clinical response at a given dose of voriconazole. In case of oxycodone, tolerance development, abuse and addiction-related deaths has been a major problem associated with its use. Polymorphisms in CYP2D6 and drug-drug interactions are thought to contribute to these problems at least partially. However, there are very limited studies, directly observing the impact of CYP2D6 polymorphisms on the PK of oxycodone and its metabolites. Conducting studies to evaluate the impact of both CYP2D6 and

UGT2B7 polymorphisms in the same population is a greater challenge due to difficulties associated with enrollment of these subjects. However, it is also known that drug-drug interactions can phenoconvert subjects into different CYP2D6 phenotypes - Poor metabolizers (PM), Intermediate metabolizers (IM) or Ultra-rapid metabolizers (UM). Through modeling and simulation, we were able to leverage the PK information obtained in drug-drug interactions studies conducted in extensive metabolizers (EM) to predict the PK in subjects with germ-line mutations in CYP2D6 and/or UGT2B7. Our conclusions for three different case studies utilizing quantitative clinical pharmacology-based tools to solve critical problems are summarized below.

Dose Prediction in Children- A Case Study of Dichloroacetate (DCA) for the Treatment of Congenital Lactic Acidosis

Response to DCA therapy in young children may be sub-optimal following body weight-based dosing. This is due to auto-inhibition of its metabolism, age dependent changes in pharmacokinetics and polymorphisms in glutathione transferase zeta1 (GSTZ1), its primary metabolizing enzyme. Using PK data obtained in adults, we successfully developed a semi-mechanistic PK model for DCA which was scaled to pediatrics using allometry and physiology-based scaling approaches. DCA-induced inactivation was found to be an important covariate in the model which resulted in phenoconversion of all subjects into slow metabolizers after repeated dosing. However, rate and extent of inactivation was 2-fold higher in subjects without the wild type EGT allelic variant of *GSTZ1* resulting in further phenoconversion into ultra-slow metabolizers after repeated DCA administration. Furthermore, DCA-induced GSTZ1 inactivation rate and extent was found to be 25-30-fold lower in children than in adults, potentially accounting for the observed age-dependent changes in PK. In a previous clinical study

in children, it was shown that steady state trough concentrations of 5-25 mg/L are correlated with the efficacy of DCA. Clinical trial simulations were performed to attain targeted trough concentrations of 5-25 mg/L and optimal DCA doses were proposed. It was noticed that the relationship of steady state clearance clearance and dose of DCA is highly non-linear at doses ~>12.5 mg/kg and ~>10.6 mg/kg for EGT carriers and EGT noncarriers, respectively. Hence, a 12.5 mg/kg and 10.6 mg/kg twice daily DCA dose was proposed for the treatment of EGT carriers and EGT noncarrier children for the treatment of congenital lactic acidosis.

Dose Optimization of Voriconazole for the Treatment of Invasive Fungal Infections

PK modeling of the steady state trough and peak concentration data obtained from the clinical study revealed that the *CYP2C19* polymorphisms and pantoprazole-use are significant factors affecting the clearance of voriconazole. These results were consistent with the previous exploratory analysis of the data where it was shown that the steady state trough concentrations in RM/UM group are 2.5-fold lower as compared to EM/IM group. Similarly, steady state trough concentrations were 2.5-fold higher in patients taking pantoprazole as a concomitant medication compared to those who were not. Differences in clearance of voriconazole due to *CYP2C19* polymorphisms and pantoprazole use were reflected in probability of target attainment (PTA). PTA was found to be lowest for RM/UM non-pantoprazole, followed by EM/IM non-pantoprazole, RM/UM pantoprazole and EM/IM pantoprazole group patients at a given voriconazole dose. Subsequently, these PTA were linked with MIC distribution data for *Candida spp.* and *Aspergillus spp.* (PD) to analyze these results in a PK/PD context rather than just PK. For Candida spp. infections, it was shown that a label-recommended oral dose of

200 mg voriconazole is sufficient for all patients, irrespective of *CYP2C19* genotype status or pantoprazole-use status. Moreover, therapeutic drug monitoring in case of Candida spp. infections can be avoided. For Aspergillus spp. infections, voriconazole oral doses ranging from 300-600 mg BID were required for successful treatment depending on the type of *Aspergillus* infection, *CYP2C19* genotype and pantoprazole-use status. A benefit-risk analysis revealed that the proposed escalated doses improved the probability of target attainment significantly for all phenotypes of voriconazole, without causing a significant increase in probability of voriconazole-related adverse events. The proposed dosing recommendations can be very helpful in optimizing voriconazole therapy, especially when information on susceptibility of fungal infection and *CYP2C19* genotype information is available.

Optimization of Oxycodone Therapy for Chronic Pain Management

A PBPK model for oxycodone and its metabolites was successfully developed using prior knowledge of the relevant metabolic pathways and formation of noroxycodone, oxymorphone and noroxymorphone. The model was informed using intravenous and oral data from the literature as well as the individual patient level data from collaborators at the University of Montreal. The model was developed by mapping out the different metabolic pathways of oxycodone (i.e. CYP2D6, CYP3A4 and UGT2B7) in a stepwise manner. Once developed, the model was successfully qualified by overlaying model-based predictions (median and 95% prediction intervals) with respective sets of observations, which were not used for model building. The developed model was applied to predict the effect of germ-line mutations in CYP2D6 and UGT2B7 on the plasma and urine PK of oxycodone and its metabolites. Effect of drug-drug interactions with strong CYP2D6 inhibitors (e.g. paroxetine, quinidine), CYP3A4

inhibitors (e.g. ketoconazole) and CYP3A4 inducers (e.g. Rifampin) were evaluated. The feasibility of using steady state cumulative urinary excretion data as predictor of plasma concentrations was also investigated.

Our results indicated that CYP2D6 polymorphisms may not be clinically relevant when analyzed in isolation, however, in conjunction with UGT2B7 polymorphisms, the clinical impact can be very significant, necessitating dose adjustment. For instance, the plasma exposure in subjects with CYP2D6 UM and UGT2B7 PM status was 3-fold higher than subjects with CYP2D6 EM and UGT2B7 EM status. Although the frequency of such a clinical phenotype is predicted to be <1% in Caucasian population, nonetheless the impact could be significant considering the fact that oxycodone users could be in millions in US alone. Amongst all the DDIs tested, the effect of concomitant administration of rifampin (CYP3A4 inducer) was most significant, with 10-fold lower steady state plasma AUC of oxymorphone, in the presence of rifampin. A good correlation (R^2=0.98) between steady state cumulative urinary excretion and plasma AUC for unconjugated oxymorphone was observed. Using the developed relationship, plasma AUC of unconjugated oxmorphone can be predicted using measurement of cumulative excretion in urine, without having to do plasma measurements or CYP2D6/UGT2B7 genotyping. Developed PBPK model can then be used to back calculate the oxycodone dose required to achieve the target steady state AUC of oxymorphone or oxycodone. The developed model can be applied in clinical settings to optimize oxycodone therapy for chronic pain management.

LIST OF REFERENCES

1. Umscheid CA, Margolis DJ, Grossman CE. Key concepts of clinical trials: a narrative review. *Postgraduate medicine.* 2011;123(5):194-204.

2. Senn S, Rolfe K, Julious SA. Investigating variability in patient response to treatment–a case study from a replicate cross-over study. *Statistical methods in medical research.* 2011;20(6):657-666.

3. Hughes JP, Rees S, Kalindjian SB, Philpott KL. Principles of early drug discovery. *British journal of pharmacology.* 2011;162(6):1239-1249.

4. Burman CF, Wiklund SJ. Modelling and simulation in the pharmaceutical industry—some reflections. *Pharmaceutical statistics.* 2011;10(6):508-516.

5. Manolis E, Rohou S, Hemmings R, Salmonson T, Karlsson M, Milligan P. The role of modeling and simulation in development and registration of medicinal products: output from the EFPIA/EMA modeling and simulation workshop. *CPT: pharmacometrics & systems pharmacology.* 2013;2(2):1-4.

6. Kimko H, Pinheiro J. Model-based clinical drug development in the past, present and future: a commentary. *British journal of clinical pharmacology.* 2015;79(1):108-116.

7. Lee JY, Garnett CE, Gobburu JV, et al. Impact of pharmacometric analyses on new drug approval and labelling decisions. *Clinical pharmacokinetics.* 2011;50(10):627-635.

8. Standing JF. Understanding and applying pharmacometric modelling and simulation in clinical practice and research. *British journal of clinical pharmacology.* 2016.

9. Lin S-J, Schranz J, Teutsch SM. Aspergillosis case-fatality rate: systematic review of the literature. *Clinical Infectious Diseases.* 2001;32(3):358-366.

10. Singh N, Paterson DL. Aspergillus infections in transplant recipients. *Clinical microbiology reviews.* 2005;18(1):44-69.

11. Liu C, Bayer A, Cosgrove SE, et al. Clinical practice guidelines by the Infectious Diseases Society of America for the treatment of methicillin-resistant Staphylococcus aureus infections in adults and children. *Clinical infectious diseases.* 2011:ciq146.

12. Hyland R, Jones B, Smith D. Identification of the cytochrome P450 enzymes involved in the N-oxidation of voriconazole. *Drug Metabolism and Disposition.* 2003;31(5):540-547.

13. Walsh TJ, Karlsson MO, Driscoll T, et al. Pharmacokinetics and safety of intravenous voriconazole in children after single-or multiple-dose administration. *Antimicrobial agents and chemotherapy.* 2004;48(6):2166-2172.

14. Pascual A, Calandra T, Bolay S, Buclin T, Bille J, Marchetti O. Voriconazole therapeutic drug monitoring in patients with invasive mycoses improves efficacy and safety outcomes. *Clinical infectious diseases.* 2008;46(2):201-211.

15. Wang G, Lei H-P, Li Z, et al. The CYP2C19 ultra-rapid metabolizer genotype influences the pharmacokinetics of voriconazole in healthy male volunteers. *European journal of clinical pharmacology.* 2009;65(3):281-285.

16. Berge M, Guillemain R, Trégouet DA, et al. Effect of cytochrome P450 2C19 genotype on voriconazole exposure in cystic fibrosis lung transplant patients. *European journal of clinical pharmacology.* 2011;67(3):253-260.

17. Verhaak PF, Kerssens JJ, Dekker J, Sorbi MJ, Bensing JM. Prevalence of chronic benign pain disorder among adults: a review of the literature. *Pain.* 1998;77(3):231-239.

18. Gureje O, Simon GE, Von Korff M. A cross-national study of the course of persistent pain in primary care. *Pain.* 2001;92(1):195-200.

19. Dowell D, Haegerich TM, Chou R. CDC guideline for prescribing opioids for chronic pain—United States, 2016. *Jama.* 2016;315(15):1624-1645.

20. Barrett J. Pharmacometrics in Pediatrics. *Applied Pharmacometrics*: Springer; 2014:83-108.

21. Coté CJ, Kauffman RE, Troendle GJ, Lambert GH. Is the" therapeutic orphan" about to be adopted? *Pediatrics.* 1996;98(1):118-123.

22. Wang J. Pediatric Global Regulatory Overview- Status, Challenges and Opportunities with Focus on the US and European Union; Presented at Annual American College of Clinical Pharmacology Meeting; 14-16 September 2014; Atlanta, GA, USA.

23. Zhao P, Zhang L, Grillo J, et al. Applications of physiologically based pharmacokinetic (PBPK) modeling and simulation during regulatory review. *Clinical Pharmacology & Therapeutics.* 2011;89(2):259-267.

24. Zisowsky J, Krause A, Dingemanse J. Drug development for pediatric populations: regulatory aspects. *Pharmaceutics.* 2010;2(4):364-388.

25. Simmons J. Application of physiologically based pharmacokinetic modelling to combination toxicology. *Food and Chemical Toxicology.* 1996;34(11):1067-1073.

26. Cojutti P, Candoni A, Forghieri F, et al. Variability of voriconazole trough levels in haematological patients: influence of comedications with cytochrome P450 (CYP) inhibitors and/or with CYP inhibitors plus CYP Inducers. *Basic & clinical pharmacology & toxicology.* 2016;118(6):474-479.

27. Roberts R, Rodriguez W, Murphy D, Crescenzi T. Pediatric drug labeling: improving the safety and efficacy of pediatric therapies. *JAMA.* 2003;290(7):905-911.

28. Laughon MM, Benjamin DK, Jr., Capparelli EV, et al. Innovative clinical trial design for pediatric therapeutics. *Expert review of clinical pharmacology.* 2011;4(5):643-652.

29. Clark A. *Handbuch der experimentellen Pharmakologie.* Julius Springer Berlin; 1937.

30. Johnson TN. The problems in scaling adult drug doses to children. *Archives of Disease in Childhood.* 2008;93(3):207-211.

31. Christensen ML, Helms RA, Chesney RW. Is pediatric labeling really necessary? *Pediatrics.* 1999;104(Supplement 3):593-597.

32. Weiss CF, Glazko AJ, Weston JK. Chloramphenicol in the newborn infant: a physiologic explanation of its toxicity when given in excessive doses. *New England Journal of Medicine.* 1960;262(16):787-794.

33. Silverman WA, Andersen DH, Blanc WA, Crozier DN. A difference in mortality rate and incidence of kernicterus among premature infants allotted to two prophylactic antibacterial regimens. *Pediatrics.* 1956;18(4):614-625.

34. Moore B. The relationship of dosage of a drug to the size of the animal treated, especially in regard to the cause of the failures to cure trypanosomiasis, and other protozoan diseases in man and in large animals. *Biochemical Journal.* 1909;4(5-7):323.

35. Shirkey HC. Drug dosage for infants and children. *JAMA.* 1965;193(6):443-446.

36. Pinkel D. Body surface and dosage: a pragmatic view. *Quarterly Review of Pediatrics.* 1958;14:187-189.

37. Lack J, Stuart-Taylor M. Calculation of drug dosage and body surface area of children. *British Journal of Anaesthesia.* 1997;78(5):601-605.

38. Butler AM, Richie RH. Simplification and improvement in estimating drug dosage and fluid and dietary allowances for patients of varying sizes. *New England Journal of Medicine.* 1960;262(18):903-908.

39. Du Bois D, Du Bois E. A formula to estimate the approximate surface area if height and weight be known. 1916. *Nutrition (Burbank, Los Angeles County, Calif).* 1989;5(5):303.

40. Kleiber M. Body size and metabolism. *Hilgardia.* 1932;6:315-351.

41. Schmidt-Nielsen K. *Scaling: why is animal size so important?* : Cambridge University Press; 1984.

42. Barrett JS. Modeling and simulation in pediatric research and development. *Clinical Trial Simulations*: Springer; 2011:397-429.

43. Turner DC, Navid F, Daw NC, et al. Population pharmacokinetics of bevacizumab in children with osteosarcoma: implications for dosing. *Clinical Cancer Research.* 2014;20(10):2783-2792.

44. Bai S, Jorga K, Xin Y, et al. A guide to rational dosing of monoclonal antibodies. *Clinical Pharmacokinetics.* 2012;51(2):119-135.

45. Zheng S, Gaitonde P, Andrew M, Gibbs M, Lesko L, Schmidt S. Model-Based Assessment of Dosing Strategies in Children for Monoclonal Antibodies Exhibiting Target-Mediated Drug Disposition. *CPT: Pharmacometrics & Systems Pharmacology.* 2014;3(10):e138.

46. Daniel WA, Wöjcikowski J. Contribution of lysosomal trapping to the total tissue uptake of psychotropic drugs. *Pharmacology & Toxicology.* 1997;80(2):62-68.

47. Bartelink IH, Rademaker CM, Schobben AF, van den Anker JN. Guidelines on paediatric dosing on the basis of developmental physiology and pharmacokinetic considerations. *Clinical Pharmacokinetics.* 2006;45(11):1077-1097.

48. Friis-Hansen B. Body composition during growth. In vivo measurements and biochemical data correlated to differential anatomical growth. *Pediatrics.* 1971;47(1):Suppl 2:264+.

49. McLeod H, Relling M, Crom W, et al. Disposition of antineoplastic agents in the very young child. *The British Journal of Cancer Supplement.* 1992;18:S23.

50. Hayani KC, Hatzopoulos FK, Frank AL, et al. Pharmacokinetics of once-daily dosing of gentamicin in neonates. *The Journal of Pediatrics.* 1997;131(1):76-80.

51. Watterberg KL, Kelly HW, Angelus P, Backstrom C. The need for a loading dose of gentamicin in neonates. *Therapeutic Drug Monitoring.* 1989;11(1):16-20.

52. Kimura T, Sunakawa K, Matsuura N, Kubo H, Shimada S, Yago K. Population pharmacokinetics of arbekacin, vancomycin, and panipenem in neonates. *Antimicrobial Agents and Chemotherapy.* 2004;48(4):1159-1167.

53. Gu Y, Wang J, Li K, et al. Preclinical pharmacokinetics and disposition of a novel selective VEGFR inhibitor fruquintinib (HMPL-013) and the prediction of its human pharmacokinetics. *Cancer chemotherapy and pharmacology.* 2014;74(1):95-115.

54. Vozmediano V, Ortega I, Lukas JC, Gonzalo A, Rodriguez M, Lucero ML. Integration of preclinical and clinical knowledge to predict intravenous PK in human: Bilastine case study. *European Journal of Drug Metabolism and Pharmacokinetics.* 2014;39(1):33-41.

55. Ahlawat P, Srinivas N. Interspecies scaling of a camptothecin analogue: human predictions for intravenous topotecan using animal data. *Xenobiotica.* 2008;38(11):1377-1385.

56. Kumar VVP, Srinivas NR. Application of allometry principles for the prediction of human pharmacokinetic parameters for irbesartan, a AT1 receptor antagonist, from animal data. *European Journal of Drug Metabolism and Pharmacokinetics.* 2008;33(4):247-252.

57. Momper JD, Mulugeta Y, Green DJ, et al. Adolescent dosing and labeling since the Food and Drug Administration Amendments Act of 2007. *JAMA Pediatrics.* 2013;167(10):926-932.

58. Hamberg A-K, Friberg LE, Hanséus K, et al. Warfarin dose prediction in children using pharmacometric bridging—comparison with published pharmacogenetic dosing algorithms. *European Journal of Clinical Pharmacology.* 2013;69(6):1275-1283.

59. Mahmood I. Interspecies Scaling for the Prediction of Drug Clearance in Children. *Clinical Pharmacokinetics.* 2010;49(7):479-492.

60. Iftekhar M. Prediction of drug clearance in children from adult clearance: allometric scaling versus exponent 0.75. *Pharmacokinetic Allometric Scaling in Pediatric Drug Development.* Rockville: Pine House Publishers; 2013.

61. Edginton AN, Willmann S. Physiology-based versus allometric scaling of clearance in children; an eliminating process based comparison. *Paediatric and Perinatal Drug Therapy.* 2006;7(3):146-153.

62. Johnson TN, Rostami-Hodjegan A. Resurgence in the use of physiologically based pharmacokinetic models in pediatric clinical pharmacology: parallel shift in incorporating the knowledge of biological elements and increased applicability to drug development and clinical practice. *Paediatric anaesthesia.* 2011;21(3):291-301.

63. Andersen ME. A physiologically based toxicokinetic description of the metabolism of inhaled gases and vapors: Analysis at steady state. *Toxicology and Applied Pharmacology.* 1981;60(3):509-526.

64. Pelekis M, Gephart L, Lerman S. Physiological-model-based derivation of the adult and child pharmacokinetic intraspecies uncertainty factors for volatile organic compounds. *Regulatory Toxicology and Pharmacology.* 2001;33(1):12-20.

65. Price K, Haddad S, Krishnan K. Physiological modeling of age-specific changes in the pharmacokinetics of organic chemicals in children. *Journal of Toxicology and Environmental Health Part A.* 2003;66(5):417-433.

66. Ginsberg G, Hattis D, Russ A, Sonawane B. Physiologically based pharmacokinetic (PBPK) modeling of caffeine and theophylline in neonates and adults: implications for assessing children's risks from environmental agents. *Journal of toxicology and environmental health Part A.* 2004;67(4):297-329.

67. Parrott MN, Davies B, Hoffmann G, et al. Development of a physiologically based model for oseltamivir and simulation of pharmacokinetics in neonates and infants. *Clinical Pharmacokinetics.* 2011;50(9):613-623.

68. Jiang X, Zhao P, Barrett J, Lesko L, Schmidt S. Application of physiologically based pharmacokinetic modeling to predict acetaminophen metabolism and pharmacokinetics in children. *CPT: Pharmacometrics & Systems Pharmacology.* 2013;2(10):e80.

69. Johnson TN, Rostami-Hodjegan A, Tucker GT. Prediction of the clearance of eleven drugs and associated variability in neonates, infants and children. *Clinical Pharmacokinetics.* 2006;45(9):931-956.

70. Björkman S. Prediction of drug disposition in infants and children by means of physiologically based pharmacokinetic (PBPK) modelling: theophylline and midazolam as model drugs. *British Journal of Clinical Pharmacology.* 2005;59(6):691-704.

71. Heiskanen T, Heiskanen T, Kairemo K. Development of a PBPK model for monoclonal antibodies and simulation of human and mice PBPK of a radiolabelled monoclonal antibody. *Current Pharmaceutical Design.* 2009;15(9):988-1007.

72. Davda JP, Jain M, Batra SK, Gwilt PR, Robinson DH. A physiologically based pharmacokinetic (PBPK) model to characterize and predict the disposition of monoclonal antibody CC49 and its single chain Fv constructs. *International Immunopharmacology.* 2008;8(3):401-413.

73. Shah DK, Betts AM. Towards a platform PBPK model to characterize the plasma and tissue disposition of monoclonal antibodies in preclinical species and human. *Journal of Pharmacokinetics and Pharmacodynamics.* 2012;39(1):67-86.

74. Walsh TJ, Anaissie EJ, Denning DW, et al. Treatment of aspergillosis: clinical practice guidelines of the Infectious Diseases Society of America. *Clinical infectious diseases.* 2008;46(3):327-360.

75. Zhang X, Zheng N, Lionberger RA, Yu LX. Innovative approaches for demonstration of bioequivalence: the US FDA perspective. *Therapeutic Delivery.* 2013;4(6):725-740.

76. Nestorov I. Whole-body physiologically based pharmacokinetic models. *Expert opinion on drug metabolism & toxicology.* 2007;3(2):235-249.

77. Barton HA, Chiu WA, Setzer RW, et al. Characterizing uncertainty and variability in physiologically based pharmacokinetic models: state of the science and needs for research and implementation. *Toxicological Sciences.* 2007;99(2):395-402.

78. Robinson B, MacKay N, Chun K, Ling M. Disorders of pyruvate carboxylase and the pyruvate dehydrogenase complex. *Journal of inherited metabolic disease.* 1996;19(4):452-462.

79. Disorders NOfR. https://rarediseases.org/rare-diseases/congenital-lactic-acidosis/. Accessed Nov 22, 2016.

80. Stacpoole PW, Barnes CL, Hurbanis MD, Cannon SL, Kerr DS. Treatment of congenital lactic acidosis with dichloroacetate. *Archives of disease in childhood.* 1997;77(6):535-541.

81. Barshop BA, Naviaux RK, McGowan KA, et al. Chronic treatment of mitochondrial disease patients with dichloroacetate. *Molecular genetics and metabolism.* 2004;83(1):138-149.

82. Aynsley-Green A, Weindling A, Soltesz G, Ross B, Jenkins P. Dichloroacetate in the treatment of congenital lactic acidosis. *Journal of inherited metabolic disease.* 1984;7(1):26-26.

83. Li W, James MO, McKenzie SC, Calcutt NA, Liu C, Stacpoole PW. Mitochondrion as a novel site of dichloroacetate biotransformation by glutathione transferase ζ1. *Journal of Pharmacology and Experimental Therapeutics.* 2011;336(1):87-94.

84. Stacpoole PW, Henderson GN, Yan Z, Cornett R, James MO. Pharmacokinetics, metabolism, and toxicology of dichloroacetate. *Drug metabolism reviews.* 1998;30(3):499-539.

85. Stacpoole PW, Wright EC, Baumgartner TG, et al. A controlled clinical trial of dichloroacetate for treatment of lactic acidosis in adults. *New England Journal of Medicine.* 1992;327(22):1564-1569.

86. Stacpoole PW, Kerr DS, Barnes C, et al. Controlled clinical trial of dichloroacetate for treatment of congenital lactic acidosis in children. *Pediatrics.* 2006;117(5):1519-1531.

87. Shroads AL, Guo X, Dixit V, Liu H-P, James MO, Stacpoole PW. Age-dependent kinetics and metabolism of dichloroacetate: possible relevance to toxicity. *Journal of Pharmacology and Experimental Therapeutics.* 2008;324(3):1163-1171.

88. Blackburn AC, Tzeng H-F, Anders M, Board PG. Discovery of a functional polymorphism in human glutathione transferase zeta by expressed sequence tag database analysis. *Pharmacogenetics and Genomics.* 2000;10(1):49-57.

89. Board P, Blackburn A, Jermiin LS, Chelvanayagam G. Polymorphism of phase II enzymes: identification of new enzymes and polymorphic variants by database analysis. *Toxicology letters.* 1998;102:149-154.

90. James MO, Stacpoole PW. Pharmacogenetic considerations with dichloroacetate dosing. *Pharmacogenomics.* 2016;17(7):743-753.

91. Shroads AL, Langaee T, Coats BS, et al. Human polymorphisms in the glutathione transferase zeta 1/maleylacetoacetate isomerase gene influence the toxicokinetics of dichloroacetate. *The Journal of Clinical Pharmacology.* 2012;52(6):837-849.

92. Shroads A, Coats B, McDonough C, Langaee T, Stacpoole P. Haplotype variations in glutathione transferase zeta 1 influence the kinetics and dynamics of chronic dichloroacetate in children. *The Journal of Clinical Pharmacology.* 2015;55(1):50-55.

93. Curry SH, Lorenz A, Limacher M, Stacpoole PW. Disposition and pharmacodynamics of dichloroacetate (DCA) and oxalate following oral DCA doses. *Biopharmaceutics & drug disposition.* 1991;12(5):375-390.

94. Wells P, Moore G, Rabin D, Wilkinson G, Oates Ja, Stacpoole P. Metabolic effects and pharmacokinetics of intravenously administered dichloroacetate in humans. *Diabetologia.* 1980;19(2):109-113.

95. Berg JM, Tymoczko JL, Stryer L. The Michaelis-Menten model accounts for the kinetic properties of many enzymes. 2002.

96. Tong Z, Board PG, Anders M. Glutathione transferase zeta-catalyzed biotransformation of dichloroacetic acid and other α-haloacids. *Chemical research in toxicology.* 1998;11(11):1332-1338.

97. Li W, Gu Y, James MO, et al. Prenatal and postnatal expression of glutathione transferase ζ 1 in human liver and the roles of haplotype and subject age in determining activity with dichloroacetate. *Drug Metabolism and Disposition.* 2012;40(2):232-239.

98. Abdelmalak M, Lew A, Ramezani R, et al. Long-term safety of dichloroacetate in congenital lactic acidosis. *Molecular genetics and metabolism.* 2013;109(2):139-143.

99. Chu PI. *Pharmacokinetics of sodium dichloroacetate*, University of Florida; 1987.

100. Samant TS, Mangal N, Lukacova V, Schmidt S. Quantitative clinical pharmacology for size and age scaling in pediatric drug development: a systematic review. *The Journal of Clinical Pharmacology.* 2015;55(11):1207-1217.

101. Dunbar E, Coats B, Shroads A, et al. Phase 1 trial of dichloroacetate (DCA) in adults with recurrent malignant brain tumors. *Investigational new drugs.* 2014;32(3):452-464.

102. Brüggemann RJ, Donnelly JP, Aarnoutse RE, et al. Therapeutic drug monitoring of voriconazole. *Therapeutic drug monitoring.* 2008;30(4):403-411.

103. Zhong G, Li W, Gu Y, Langaee T, Stacpoole PW, James MO. Chloride and other anions inhibit dichloroacetate-induced inactivation of human liver GSTZ1 in a haplotype-dependent manner. *Chemico-biological interactions.* 2014;215:33-39.

104. Klieber M, Oberacher H, Hofstaetter S, et al. CYP2C19 phenoconversion by routinely prescribed proton pump inhibitors omeprazole and esomeprazole: clinical implications for personalized medicine. *Journal of Pharmacology and Experimental Therapeutics.* 2015;354(3):426-430.

105. Preskorn SH, Kane CP, Lobello K, et al. Cytochrome P450 2D6 phenoconversion is common in patients being treated for depression: implications for personalized medicine. *The Journal of clinical psychiatry.* 2013;74(6):614-621.

106. Shah RR, Smith RL. Inflammation-induced phenoconversion of polymorphic drug metabolizing enzymes: hypothesis with implications for personalized medicine. *Drug Metabolism and Disposition.* 2015;43(3):400-410.

107. Shah RR, Smith RL. Addressing phenoconversion: the Achilles' heel of personalized medicine. *British journal of clinical pharmacology.* 2015;79(2):222-240.

108. Anderson BJ, Meakin GH. Scaling for size: some implications for paediatric anaesthesia dosing. *Pediatric Anesthesia.* 2002;12(3):205-219.

109. Jahn SC, Rowland-Faux L, Stacpoole PW, James MO. Chloride concentrations in human hepatic cytosol and mitochondria are a function of age. *Biochemical and biophysical research communications.* 2015;459(3):463-468.

110. VFEND P. Package insert. *VFEND Tablets/VFEND IV (voriconazole).* 2002.

111. Theuretzbacher U, Ihle F, Derendorf H. Pharmacokinetic/pharmacodynamic profile of voriconazole. *Clinical pharmacokinetics.* 2006;45(7):649-663.

112. Shi H-Y, Yan J, Zhu W-H, et al. Effects of erythromycin on voriconazole pharmacokinetics and association with CYP2C19 polymorphism. *European journal of clinical pharmacology.* 2010;66(11):1131-1136.

113. Weiss J, Hoevel MM, Burhenne J, et al. CYP2C19 genotype is a major factor contributing to the highly variable pharmacokinetics of voriconazole. *The Journal of Clinical Pharmacology.* 2009;49(2):196-204.

114. Mikus G, Scholz IM, Weiss J. Pharmacogenomics of the triazole antifungal agent voriconazole. *Pharmacogenomics.* 2011;12(6):861-872.

115. Hamadeh IS, Klinker KP, Borgert SJ, et al. Impact of the CYP2C19 genotype on voriconazole exposure in adults with invasive fungal infections. *Pharmacogenetics and genomics.* 2017;27(5):190-196.

116. Committee FADA. Briefing document for voriconazole (oral and intravenous formulations). *Silver Spring MD: US Food and Drug Administration.* 2001.

117. Yanni SB, Annaert PP, Augustijns P, Ibrahim JG, Benjamin DK, Thakker DR. In vitro hepatic metabolism explains higher clearance of voriconazole in children versus adults: role of CYP2C19 and flavin-containing monooxygenase 3. *Drug Metabolism and Disposition.* 2010;38(1):25-31.

118. Dolton MJ, Mikus G, Weiss J, Ray JE, McLachlan AJ. Understanding variability with voriconazole using a population pharmacokinetic approach: implications for optimal dosing. *Journal of Antimicrobial Chemotherapy.* 2014;69(6):1633-1641.

119. Drusano G, Preston S, Hardalo C, et al. Use of preclinical data for selection of a phase II/III dose for evernimicin and identification of a preclinical MIC breakpoint. *Antimicrobial agents and chemotherapy.* 2001;45(1):13-22.

120. Andes D, Marchillo K, Stamstad T, Conklin R. In vivo pharmacokinetics and pharmacodynamics of a new triazole, voriconazole, in a murine candidiasis model. *Antimicrobial agents and chemotherapy.* 2003;47(10):3165-3169.

121. Troke PF, Hockey HP, Hope WW. Observational study of the clinical efficacy of voriconazole and its relationship to plasma concentrations in patients. *Antimicrobial agents and chemotherapy.* 2011;55(10):4782-4788.

122. Mouton JW, Dudley MN, Cars O, Derendorf H, Drusano GL. Standardization of pharmacokinetic/pharmacodynamic (PK/PD) terminology for anti-infective drugs. *International journal of antimicrobial agents.* 2002;19(4):355-358.

123. Tan K, Brayshaw N, Tomaszewski K, Troke P, Wood N. Investigation of the potential relationships between plasma voriconazole concentrations and visual adverse events or liver function test abnormalities. *The Journal of Clinical Pharmacology.* 2006;46(2):235-243.

124. Moriyama B, Obeng AO, Barbarino J, et al. Clinical Pharmacogenetics Implementation Consortium (CPIC) Guidelines for CYP2C19 and Voriconazole Therapy. *Clinical Pharmacology & Therapeutics.* 2017.

125. Park WB, Kim N-H, Kim K-H, et al. The effect of therapeutic drug monitoring on safety and efficacy of voriconazole in invasive fungal infections: a randomized controlled trial. *Clinical Infectious Diseases.* 2012;55(8):1080-1087.

126. Moriyama B, Kadri S, Henning SA, Danner RL, Walsh TJ, Penzak SR. Therapeutic drug monitoring and genotypic screening in the clinical use of voriconazole. *Current fungal infection reports.* 2015;9(2):74-87.

127. Wang T, Chen S, Sun J, et al. Identification of factors influencing the pharmacokinetics of voriconazole and the optimization of dosage regimens based on Monte Carlo simulation in patients with invasive fungal infections. *Journal of Antimicrobial Chemotherapy.* 2013;69(2):463-470.

128. Chen L, Wang T, Wang Y, et al. Optimization of voriconazole dosage regimen to improve the efficacy in patients with invasive fungal disease by pharmacokinetic/pharmacodynamic analysis. *Fundamental & clinical pharmacology.* 2016;30(5):459-465.

129. Xu G, Zhu L, Ge T, Liao S, Li N, Qi F. Pharmacokinetic/pharmacodynamic analysis of voriconazole against Candida spp. and Aspergillus spp. in children, adolescents and adults by Monte Carlo simulation. *International journal of antimicrobial agents.* 2016;47(6):439-445.

130. Lee S, Kim BH, Nam WS, et al. Effect of CYP2C19 polymorphism on the pharmacokinetics of voriconazole after single and multiple doses in healthy volunteers. *The Journal of Clinical Pharmacology.* 2012;52(2):195-203.

131. Kim S-H, Lee D-G, Kwon J-C, et al. Clinical impact of cytochrome P450 2C19 genotype on the treatment of invasive aspergillosis under routine therapeutic drug monitoring of voriconazole in a Korean population. *Infection & chemotherapy.* 2013;45(4):406-414.

132. Li X-Q, Andersson TB, Ahlström M, Weidolf L. Comparison of inhibitory effects of the proton pump-inhibiting drugs omeprazole, esomeprazole, lansoprazole, pantoprazole, and rabeprazole on human cytochrome P450 activities. *Drug metabolism and disposition.* 2004;32(8):821-827.

133. Dolton MJ, Ray JE, Chen SC-A, Ng K, Pont LG, McLachlan AJ. Multicenter study of voriconazole pharmacokinetics and therapeutic drug monitoring. *Antimicrobial agents and chemotherapy.* 2012;56(9):4793-4799.

134. Heinz W, Kloeser C, Helle A, et al. Comparison of plasma trough concentrations of voriconazole in patients with or without comedication of ranitidine or pantoprazole. *Clinical Microbiology & Infection.* 2007;13:S357.

135. Miyakis S, Van Hal SJ, Ray J, Marriott D. Voriconazole concentrations and outcome of invasive fungal infections. *Clinical Microbiology and Infection.* 2010;16(7):927-933.

136. Smith J, Safdar N, Knasinski V, et al. Voriconazole therapeutic drug monitoring. *Antimicrobial agents and chemotherapy.* 2006;50(4):1570-1572.

137. Ueda K, Nannya Y, Kumano K, et al. Monitoring trough concentration of voriconazole is important to ensure successful antifungal therapy and to avoid hepatic damage in patients with hematological disorders. *International journal of hematology.* 2009;89(5):592-599.

138. Walsh TJ, Pappas P, Winston DJ, et al. Voriconazole compared with liposomal amphotericin B for empirical antifungal therapy in patients with neutropenia and persistent fever. *New England Journal of Medicine.* 2002;346(4):225-234.

139. Laties AM, Fraunfelder FT, Tomaszewski K, et al. Long-term visual safety of voriconazole in adult patients with paracoccidioidomycosis. *Clinical therapeutics.* 2010;32(13):2207-2217.

140. Lamoureux F, Duflot T, Woillard J-B, et al. Impact of CYP2C19 genetic polymorphisms on voriconazole dosing and exposure in adult patients with invasive fungal infections. *International journal of antimicrobial agents.* 2016;47(2):124-131.

141. Owusu Obeng A, Egelund EF, Alsultan A, Peloquin CA, Johnson JA. CYP2C19 polymorphisms and therapeutic drug monitoring of voriconazole: are we ready for clinical implementation of pharmacogenomics? *Pharmacotherapy: The Journal of Human Pharmacology and Drug Therapy.* 2014;34(7):703-718.

142. Trescot AM, Boswell MV, Atluri SL, et al. Opioid guidelines in the management of chronic non-cancer pain. *Pain Physician.* 2006;9(1):1.

143. Medicine TAAoP. 2014; http://www.painmed.org/patientcenter/facts-on-pain/.

144. Rasu RS, Vouthy K, Crowl AN, et al. Cost of pain medication to treat adult patients with nonmalignant chronic pain in the United States. *Journal of Managed Care Pharmacy.* 2014;20(9):921-928.

145. ACOEM. Guidelines for the chronic use of opioids. 2011; http://www.acoem.org/Guidelines_Opioids.aspx.

146. Manchikanti L, Abdi S, Atluri S, et al. American Society of Interventional Pain Physicians (ASIPP) guidelines for responsible opioid prescribing in chronic non-cancer pain: Part 2--guidance. *Pain physician.* 2012;15(3 Suppl):S67-116.

147. Manchikanti L, Singh A. Therapeutic opioids: a ten-year perspective on the complexities and complications of the escalating use, abuse, and nonmedical use of opioids. *Pain physician.* 2008;11(2 Suppl):S63-S88.

148. Coller JK, Christrup LL, Somogyi AA. Role of active metabolites in the use of opioids. *European journal of clinical pharmacology.* 2009;65(2):121-139.

149. *Clinical Application of Pharmacogenetics.* InTech; 2012.

150. Lalovic B, Kharasch E, Hoffer C, Risler L, Liu-Chen LY, Shen DD. Pharmacokinetics and pharmacodynamics of oral oxycodone in healthy human subjects: role of circulating active metabolites. *Clinical pharmacology & therapeutics.* 2006;79(5):461-479.

151. Grönlund J, Saari TI, Hagelberg NM, Neuvonen PJ, Laine K, Olkkola KT. Effect of Inhibition of Cytochrome P450 Enzymes 2D6 and 3A4 on the Pharmacokinetics of Intravenous Oxycodone. *Clinical drug investigation.* 2011;31(3):143-153.

152. Lagishetty CV, Deng J, Lesko LJ, Rogers H, Pacanowski M, Schmidt S. How Informative Are Drug-Drug Interactions of Gene-Drug Interactions? *The Journal of Clinical Pharmacology.* 2016;56(10):1221-1231.

153. Huang SM, Temple R, Throckmorton D, Lesko L. Drug interaction studies: study design, data analysis, and implications for dosing and labeling. *Clinical Pharmacology & Therapeutics.* 2007;81(2):298-304.

154. Zhuang X, Lu C. PBPK modeling and simulation in drug research and development. *Acta Pharmaceutica Sinica B.* 2016;6(5):430-440.

155. Marsousi N, Daali Y, Rudaz S, et al. Prediction of metabolic interactions with oxycodone via CYP2D6 and CYP3A inhibition using a physiologically based pharmacokinetic model. *CPT: pharmacometrics & systems pharmacology.* 2014;3(12):1-8.

156. Smith HS. Opioid metabolism. Paper presented at: Mayo Clinic Proceedings2009.

157. Samer CF, Daali Y, Wagner M, et al. Genetic polymorphisms and drug interactions modulating CYP2D6 and CYP3A activities have a major effect on oxycodone analgesic efficacy and safety. *British journal of pharmacology.* 2010;160(4):919-930.

158. Heiskanen T, Olkkola KT, Kalso E. Effects of blocking CYP2D6 on the pharmacokinetics and pharmacodynamics of oxycodone. *Clinical Pharmacology & Therapeutics.* 1998;64(6):603-611.

159. Lemberg K, Heiskanen T, Neuvonen M, et al. Does co-administration of paroxetine change oxycodone analgesia: an interaction study in chronic pain patients. *Scandinavian Journal of Pain.* 2010;1(1):24-33.

160. Zwisler ST, Enggaard TP, Mikkelsen S, Brosen K, Sindrup SH. Impact of the CYP2D6 genotype on post-operative intravenous oxycodone analgesia. *Acta anaesthesiologica Scandinavica.* 2010;54(2):232-240.

161. Andreassen TN, Eftedal I, Klepstad P, et al. Do CYP2D6 genotypes reflect oxycodone requirements for cancer patients treated for cancer pain? A cross-sectional multicentre study. *European journal of clinical pharmacology.* 2012;68(1):55-64.

162. Saari TI, Grönlund J, Hagelberg NM, et al. Effects of itraconazole on the pharmacokinetics and pharmacodynamics of intravenously and orally administered oxycodone. *European journal of clinical pharmacology.* 2010;66(4):387-397.

163. Nieminen TH, Hagelberg NM, Saari TI, et al. Rifampin greatly reduces the plasma concentrations of intravenous and oral oxycodone. *The Journal of the American Society of Anesthesiologists.* 2009;110(6):1371-1378.

164. Samer CF, Daali Y, Wagner M, et al. The effects of CYP2D6 and CYP3A activities on the pharmacokinetics of immediate release oxycodone. *British journal of pharmacology.* 2010;160(4):907-918.

165. https://pubchem.ncbi.nlm.nih.gov/.

166. Plummer JL, Cmielewski PL, Reynolds GD, Gourlay GK, Cherry DA. Influence of polarity on dose-response relationships of intrathecal opioids in rats. *Pain.* 1990;40(3):339-347.

167. Leow KP, Smith MT, Williams B, Cramond T. Single-dose and steady-state pharmacokinetics and pharmacodynamics of oxycodone in patients with cancer. *Clinical Pharmacology & Therapeutics.* 1992;52(5):487-495.

168. Lalovic B, Phillips B, Risler LL, Howald W, Shen DD. Quantitative contribution of CYP2D6 and CYP3A to oxycodone metabolism in human liver and intestinal microsomes. *Drug Metabolism and Disposition.* 2004;32(4):447-454.

169. Mehrotra S, Gobburu J. Communicating to Influence Drug Development and Regulatory Decisions: A Tutorial. *CPT: pharmacometrics & systems pharmacology.* 2016;5(4):163-172.

BIOGRAPHICAL SKETCH

Naveen Mangal was born in 1989 in Bharatpur, Rajasthan, India. In 2010, he received his Bachelor of pharmacy from Guru Gobind Singh Indraprastha University, New Delhi, India. In 2010, Naveen moved to United States of America to pursue a Master of Science from State University of New York at Buffalo, NY. In 2014, he joined University of Florida for Doctor of Philosophy program at the Center for Pharmacometrics & Systems Pharmacology in the University of Florida, Lake Nona campus. During his training, Naveen pursued 2 summer internships in pharmaceutical industry (AbbVie and GlaxoSmithKline) to get hands-on experience in drug development. He got married in 2017. He received his Ph.D. in pharmaceutics in December 2017.